Microfluidic in vitro model to study cell mechanisms and drug efficacy

Nishanth Venugopal Menon

2015

Nishanth Venugopal Menon. (2015). Microfluidic in vitro model to study cell mechanisms and drug efficacy. Doctoral thesis, Nanyang Technological University, Singapore.

https://hdl.handle.net/10356/65723

https://doi.org/10.32657/10356/65723

NANYANG TECHNOLOGICAL UNIVERSITY

MICROFLUIDIC *IN VITRO* MODEL TO STUDY CELL MECHANISMS AND DRUG EFFICACY

NISHANTH VENUGOPAL MENON

SCHOOL OF CHEMICAL AND BIOMEDICAL ENGINEERING

2015

MICROFLUIDIC *IN VITRO* MODEL TO STUDY CELL MECHANISMS AND DRUG EFFICACY

NISHANTH VENUGOPAL MENON

School of Chemical and Biomedical Engineering

A thesis submitted to the Nanyang Technological University in partial fulfillment of the requirements for the degree of Doctor of Philosophy

2015

Acknowledgement

Foremostly I would like to take this opportunity to thank my supervisor, Asst. Prof. Kang Yuejun, for his advice, guidance, support, patience and also for creating a friendly atmosphere in the lab which has helped me learn a lot and develop lasting friendships throughout the course of my doctoral study programme.

I would like to thank my collaborators, Asst. Prof. Mayasari Lim, Asst. Prof. Cao Bin, Asst. Prof. Shang You Tee, Asst. Prof. Zhao Yanli and the members of their group, Dr. Manisha Mukherjee, Dr. Cao Xue, Zhang Yingdan, Jingjing and Ng Chun Kiat for their support and assistance during crucial times of my Ph.D program. A big thank you to my friend and collaborator Dr. Hou Han Wei and his team for their assistance and support.

I thank Dr. Sreejith Sivaramapanicker for the help and guidance he has offered me; besides being a good friend and colleague.

A special thanks to my group mates, Chuah Yon Jin, Xue Peng, Guo Jinhong, Zhang Ying, Liu Shiying, Tay Li Min, Dhiman Das, Dang Tran Chien, Dr. Wu Yingnan and Dr. Wu Yafeng for being good friends and for supporting and assisting me in carrying out my lab work. I would also like to thank all the FYP's and masters students I have had the good fortune of working with Limin, Razina, Joann, Lusandra, Hilda, Bryan, Subhashree, Gopal, Jingling, Sean, Tayzar, Leiyang, Arie, Samantha and Liza.

A huge thanks to my friends and support system during my docotral studies programme from Singapore and India: Abhishek Ambede, Kaushik Sundar, Divya Kumar, Prerna Tarika Diwaker, Sumedh Dabhu, Ravi kishore, Vikram Shenoy Handiru, Supriya Sathyanarayana, Rajagopalan Badrinarayanan, Nikitha Radhakrishnan, Sheetal Sinha, Areetha Dsouza, Saurabh Singh, Dhirendra Singh, Lavanya Sundararaman, Laxmi Iyer, Manish Muhuri, Vinay Warrier, Narendra Madhavan, Ishani Dasgupta, Alolika Chakraborti, Mukesh Mahajan, Shubhadhra Pillai, Mishra sir, Basu sir, Sangith Sasidhar, Jagadish, Sumit Darak, Roger, Rahul, Ellen, Malini Bhadra, Ghazal Malik, Anee Mohanty, Jithin John Verghese and Neeraj Jain.

Finally I would like to thank my parents and my family in India for their unconditional love and support throughout the course of my studies.

Table of contents

List of figures

List of tables

List of abbreviations

ELISA	Enzyme linked immunosorbent assay
PDMS	Polydimethylsiloxane
RBC	Red blood cells
EC	Endothelial cells
ATP	Adenosine Triphosphate
VEGF	Vascular endothelial growth factor
ANG1, ANG2	Angiopoetin
TGF β1	Transforming growth factor β1
FGF-2	Fibroblast growth factor 2
fMLP	N-formyl-methionyl-leucyl-phenylalanine
IL-1 , IL-8	Human interleukin
SMC	Smooth muscle cells
MSC	Mesenchymal stem cells
FDA	Food and drug administration
MTF	Muscular thin film
hiPSCs	Human induced pluripotent stem cells
bpm	Beats per minute
DEP	Di-electrophoresis
ASCs	Adipose derived stem cells
ALp	Alkaline phosphatase
HSCs	Hepatopoietic stem cell
eBM	Engineered bone marrow
EMT	Epithelial-mesenchymal transition
HMVEC	Human dermal microvascular endothelial cells
PK-PD	Pharmacokinetics-pharmacodynamics
PCR	Polymerase chain reaction

qRT-PCR	Quantitative real time polymerase chain reaction
mRNA	Messenger Ribonucleic acid
IC	Integrated circuits
UV	Ultraviolet
PBS	Phosphate buffer saline
DMEM	Dulbecco's modified eagle medium
FBS	Fetal bovine serum
PS	Penicillin-Streptomycin
EDTA	Ethylenediaminetetraacetic acid
LSM	Laser scanning microscope
ROS	Reactive oxygen species
CMH2DCFDA	5-(and-6)-chloromethyl-2′,7′-dichlorodihydrofluorescein diacetate
RNA	Ribonucleic acid
cDNA	Complementary DNA
GAPDH	Glyceraldehyde 3-phosphate dehydrogenase
C_T	Cycle threshold
BCA	Bicinchoninic acid
AFM	Atomic force microscope
STM	Scanning tunneling microscope
SP	Stylus profilometer
DAPI	4',6-diamidino-2-phenylindole
EthD-1	Ethidium homodimer
FDA	Fluorescein diacetate
ANOVA	Analysis of variance
TCP	Tissue culture plate
TNT's	Tunneling nanotubes
ECM	Extracellular matrix

hBMSCs	Human bone marrow mesenchymal stem cells
PDT	Photodynamic therapy
PS	Photosensitizer
NIR	Near infra red
EPR	Enhanced permeability and retention
FR	Folate receptor
FA	Folic acid
SQ	Squaraine dye
CDI	N,N′- Carbonyldiimidazole
DMF	Dimethylformamide
DIPEA	N-Diisopropylethylamine
TEM	Transmission electron microscope
DLS	Dynamic light scattering
APC	Allophycocyanin

Abstract

In vitro models are commonly used biological tools involving culture of cells so as to replicate complex human organs and organ systems in an *ex-vivo* manner. Researchers have created *in vitro* models for many years now focusing on different physiologically relevant studies. Non-invasiveness and simplicity are some of the major advantages of *in vitro* models unlike in the case of animal models where animals are sacrificed and moreover the complexity of the animal physiology introduces a large number of variables thereby complicating the entire study. An *in vitro* model reduces the number of variables and hence simplifies the study. One of the techniques for the creation of *in vitro* models is cell patterning. It involves the spatial orientation of the cells in a controlled manner so that a desired study can be performed. Microfluidics is a platform that can be used for the development of *in vitro* models with good physiological relevance. The ability to control the flow of fluids inside a microfluidic device makes it an extremely attractive technique for the creation cell patterns. Most of the cell patterning on a chip has been done by controlling liquid flow using an actuating system like a syringe pump. Such a system tends to be bulky and complex. In the present work, cell patterning has been done by controlling liquid flow within compartments by modifying the property of the surface within the chip. This ability to control liquids allows for the culture of different cell types inside different compartments on a chip. Our aim was to develop a simple, easy to use microfluidic device, which can be used for different cell-based applications. Our chip design is modified from a design available from literature and we have devised a surface treatment technique wherein we have used a fake channel to coat the surface with suitable chemicals to control the hydrophilic property of the channel surfaces. Cells were cultured in the hydrophilic compartments of the chip and different studies were performed to show the significance of such an on-chip model. Cell mechanism based studies performed on-chip included a cell-cell interaction study where the impact of tumor cells on stromal cells was studied while another work involved the study of substratum properties on mesenchymal stem cell migration which is a vital phenomenon in regenerative medicine. Apart from the study of cellular phenomena, such models can also be used for drug testing to see the efficacy of the drug on human cells. Though the sophistication of the model does not allow for its usage in the later phases of drug testing, they can still be used as a part of the phase I tests of drugs, to see the impact the drug might have on human cells. In this thesis we have performed a drug efficacy test

where the co-culture model developed using this device was used to test the targeted killing potential of a photosensitizer that was designed to perform targeted photodynamic therapy of cancer cells. Apart from performing cell culture, the microfluidic chip also allows for easier analysis using suitable fluorescent probes. In this thesis we have discussed about a simple, easy to use and highly reproducible microfluidic model that was developed to perform cell culture and cellular analysis on chip according to the study of interest. Apart from cell mechanism studies, the model can be modified to perform other studies like testing drug selectivity, drug efficacy as well as for performing preliminary tests during hypothesis testing.

List of publications

Book chapters

1. **N.V. Menon**, J. Guo, Y. Kang. "Optofluidic imaging techniques", ***Encyclopedia of Micro- and Nanofluidics 2nd ed., Springer (2013).***
2. **N.V. Menon**, P. Xue, Y. Kang. "Microfluidic Platforms for Human Diseases", ***Encyclopedia of Micro- and Nanofluidics 2nd ed., Springer (2013).***
3. J. Guo, **N.V. Menon**, Y. Kang. "Optofluidic manipulation of biological molecules" ***Encyclopedia of Micro- and Nanofluidics 2nd ed., Springer (2014).***
4. Y.J. Chuah, **N.V. Menon**, Y. Kang. "Cell migration in scaffolds based microfluidic platform", ***Encyclopedia of Micro- and Nanofluidics 2nd ed., Springer (2013)***

Journal papers

1. **N.V. Menon**, Y.J. Chuah, B. Cao, M. Lim, Y. Kang*. "A microfluidic co-culture system to monitor tumor-stromal interactions on a chip". ***Biomicrofluidics***. 8 (6), 064118 (2014).
2. J.J. Han[†], **N.V. Menon**[†], Y. Kang*, S.Y. Tee*. "An *in vitro* study on collective tumor cell migration on nanoroughened poly(dimethylsiloxane) surfaces**".** ***Journal of Materials Chemistry B***. 3 (8), 1565-1572 (2015).
3. **N.V. Menon**, Y.J. Chuah, S. Phey, Y. Zhang, Y.N. Wu, V. Chan, Y. Kang*. "Microfluidic assay to study the combinatorial impact of substrate properties on mesenchymal stem cell migration". ***ACS Applied Materials & Interfaces***. 7 (31), 17095–17103 (2015).
4. P. Xue, Y.F. Wu, **N.V. Menon**, Y. Kang*. "Microfluidic synthesis of monodispersed PEGDA microbeads for sustained release of 5-Fluorouracil". ***Microfluidics and Nanofluidics***. 18 (2), 333-342 (2015).
5. P. Borah, S. Sreejith, P. Anees, **N.V. Menon**, Y. Kang, A. Ajayaghosh, Y. Zhao*. "Near-IR Squaraine Dye-Loaded Gated Periodic Mesoporous Silica for Photo-Oxidation of Phenol in Continuous-Flow Device". ***Science Advances***. 1 (8),e1500390 (2015).
6. S. Sreejith[†], J. Joseph[†], M. Lin, **N.V. Menon**, P. Borah, H.J. Ng, Y.X. Loong, Y. Kang, S. Yu, Y. Zhao*. "Near-Infrared Squaraine Dye Encapsulated Micelles for

In Vivo Fluorescence and Photoacoustic Bimodal Imaging". ***ACS Nano***. 9 (6), 5695-5704 (2015)

7. Y.J. Chuah, Y. Zhang, Y. Wu, **N.V. Menon**, G.H. Goh, A.C. Lee, V. Chan, Y.L. Zhang*, Y. Kang*. "Combinatorial effect of substratum properties on mesenchymal stem cell sheet engineering and subsequent multi-lineage differentiation". ***Acta Biomaterialia***. 23, 52-62 (2015).
8. J. Guo, X. Ma, **N.V. Menon**, C.M. Li, Y. Zhao*, Y. Kang*. "Dual fluorescence-activated study of tumor cell apoptosis by an optofluidic system". ***IEEE Journal of Selected Topics in Quantum Electronics***. 21 (4), 7100107 (2015).
9. P. Xue, J. Bao, Y.J. Chuah, **N.V. Menon**, Y. Zhang, Y. Kang*. "Protein covalently conjugated SU-8 surface for the enhancement of mesenchymal stem cell adhesion and proliferation". ***Langmuir***. 30, 3110-3117 (2014).
10. S. Kuddannaya[†], Y.J. Chuah[†], M.H.A. Lee, **N.V. Menon**, Y. Kang*, Y. Zhang*. "Surface chemical modification of Poly(dimethylsiloxane) for the enhanced adhesion and proliferation of Mesenchymal Stem Cells". ***ACS Applied Materials & Interfaces***. 5, 9777-9784 (2013).
11. D. Das, Z. Yan, **N.V. Menon**, Y. Kang, V. Chan, C. Yang. "Continuous detection of trace level concentration of oil droplets in water using microfluidic AC electroosmosis (ACEO)". ***RSC Advances***. 5, 70197-70203 (2015).

[†] *Authors have contributed equally*

Chapter 1 Introduction

1.1 *In vitro* models

The human body is an extremely complex system comprising of different organ systems, each with its own functions and significance. Such organ systems are made up of numerous organs that comprise millions of cells which are the building blocks of the body. The cells from these different organs are different from each other in their morphology as well as in their functions. Researchers have been studying the functioning of these cells to understand the functioning of the body. Such studies help us in gaining insights into the mechanisms undertaken by the cells and will help in forming a better picture of the organs and their functioning. These studies also help in developing insights into infections and diseases and a better understanding of these conditions will help in the development of a suitable cure. The realization of the ability to maintain organs outside the organism's body in the early 19th century triggered the development of the present day cell culture techniques. The understanding of cellular growth requirements over the past century has led to the development of formulations of solutions known as cell growth medium containing different components like amino acids, vitamins, glucose, glutamine, etc, that are required by cells to survive and proliferate in *ex vivo* conditions. Advancement in *ex vivo* cell culture techniques has led to the development of the conventional *in vitro* models that have been widely used over decades to gain a better understanding of the cells and their mechanisms and functionalities. The significance and popularity of such a model arises from its non-invasiveness and simplicity unlike the animal models. Disease studies is one of the major applications of these devices as they assist in understanding the mechanism of the specific disease and thus in developing a suitable cure for the same. These models also assist in performing drug testing where the pharmacodynamics of the drugs can be understood apart from helping in hypothesis testing as well as in the optimization of the drug dosing regimens.[1] A large number of models that focus on studying various cellular mechanisms have also been developed. [2-7]

Cell culture is the most basic part of developing such models and it may be a 2-dimensional (2D) monolayer cell culture which involves culturing cells on a 2D surface (X-Y plane) like petri-dish, or specialized flasks or 3-dimensional (3D) cell culture which involves the use of a scaffold or matrices for supporting cell growth in a 3D space (X-Y-Z space). While 2D cell culture is an established technique and a large number of bio-analytical assays have been developed to obtain a better understanding of the cellular functioning, researchers have shown that culturing cells inside a scaffold in 3D better

mimics the *in vivo* cell environment. For example 2D cell culture induces an apical-basal polarity apart from bringing a difference in their behavior in comparison to its behavior in physiological conditions while cells cultured within a 3D space are not polarized and are free to use their apical, basal as well as lateral domains of the plasma membrane.[8] Moreover 3D cell culture is technique used for the development of tissue constructs *in vitro.* Figure 1.1 illustrates the basic differences between the cells in a 2D and 3D environment. But the ease of 2D culture has caused it to be a more widely used method for *in vitro* models.

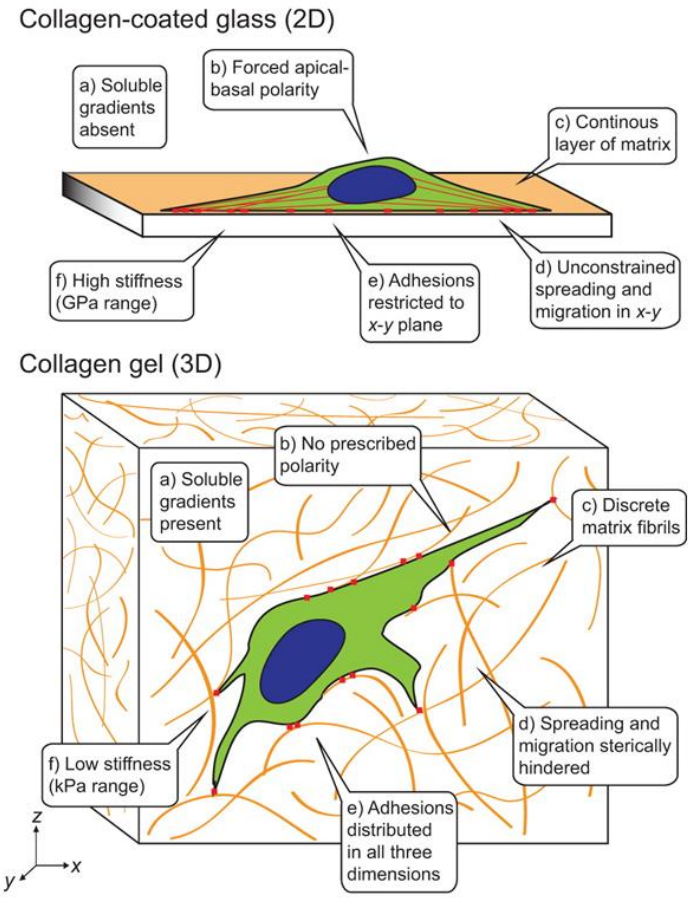

Figure 1.1: Cell in a 2D and 3D environment. Reprinted with permission from [9].

The simplicity of the *in vitro* models is often cited as its advantage because of the ability to breakdown the human body into smaller models which will help in easier studies and better understanding of different cell types. But this is often its biggest drawback, as the results from such a model might not always be relevant to an *in vivo* system. Moreover various physiological conditions like chemical gradient, shear stress, cellular co-culture are difficult to be recreated in the conventional *in vitro* models. Hence such *in vitro* models are widely used for preliminary analysis while for later stages of

studying a phenomenon or in testing a drug, *in vivo* models like animal models are used. But the inhumane sacrifice of animals and recent evidences point to the fact that the results in the mice models are different from those in humans primarily owing to the difference in the organism and its genetic makeup. [10-11]This has triggered the use of different techniques and methods to develop more physiologically relevant *in vitro* models making use of human cells. [12-13] Microfabrication is one such technique that has been used widely for the development of physiologically relevant models. [14-16]

1.2 Microfluidics

Microfluidics is a discipline of engineering that involves the development of systems in the micrometer scale which can be used to control and manipulate fluids to perform different applications. Such systems are generated using different microfabrication techniques, initially developed by the semiconductor industry. It is an application oriented field and the established microfabrication techniques allows for the development of microfluidic chips with designs to suit the application at hand. The fluid properties at the microscale are much different compared to that in macroscale. While gravity plays a significant role in macroscale, in microscale systems capillary and surface tension dominate. A variety of applications are possible using the capillary and the surface tension like creation of monodisperse droplets, [17-18] analyte filtering, [19-20] and substrate patterning. [21] The miniature size of these microfluidic devices and the advantage of microfabrication allows for the creation of high throughput devices by incorporating multiple chips into the same platform. Such a device is very useful for highly efficient chemical synthesis.[22-23] The maturity of microfabrication along with its miniature size has made microfluidic devices commonly called as micro total analysis systems (μTAS) to be of significance for biomedical applications, for the creation of biosensors, *in vitro* models as well as in point of care diagnostics. [24-25]

1.3 Microfluidics in biology

The increasing concern over the inhumane use of animals for biomedical studies as well as the growing realization that animal models are not good predictors for human *in vivo* phenomena has led to the development of advanced *in vitro* models that can mimic the physiological environment better. This has resulted in the use of microfluidics for the development of human cell-based *in vitro* models. With the development of such models, there also comes a necessity for the methods to carry out analysis within these

microfluidic models. This has led to the creation of bio-analytical devices which can be used integrated to these *in vitro* models for an array of functions like performing assays like ELISA (Enzyme linked immunosorbent assay), cell sorting, and cytometry amongst many others. This enhancement of microfluidic *in vitro* models is primarily due to the ability to easily integrate electrical or magnetic or mechanical systems with the existing microfluidic system according to the application at hand. Moreover the ability to perform fluid manipulation in the microfluidic chip allows the generation of chemical gradients and shear stress which are significant phenomena undergone by the cells *in-vivo*. Apart from the ability of microfluidic devices to create efficient and smart *in vitro* models and because of its miniature size the overall cost can be cut down on the usage of samples and solvents and also many studies can be performed simultaneously.

Microfluidic systems are fabricated by microfabrication techniques using different materials like polymers, glass, silicon and paper. Such materials are often surface treated to enhance their biocompatibility for cell culture. Recent advancements in material engineering have also allowed the creation of hydrogel based microfluidic chips [26-27] that have an innate quality of supporting cell growth. Among the different materials available for fabrication, the most commonly material used in laboratories is polydimethysiloxane (PDMS) due to its elasticity, durability, gas permeability, optical transparency, cost as well as its ease of fabrication. [28-30] In the following section I will briefly discuss about different PDMS based microfluidic *in vitro* models.

1.3.1 Microfluidic *in vitro* models

Microfluidic *in vitro* models can be created by performing a 2D cell culture or a 3D cell culture. As stated earlier in section 1.1, 3D cell culture allows the cells to maintain its physiological behavior in comparison to cell cultured in 2D. Microfluidics has been able to bridge this gap between 2D cell culture based models and 3D cell culture based models. With the help of microfabrication techniques, complex 3D microfluidic models can be created and the excellent fluid control allows for efficient cell patterning which allows for the creation of smart models that have been shown to have better physiological relevance in comaprison to 2D cell culture models created on a petri dish or flask. In this section, we have discussed such microfluidic models that have been created to perform different physiologically relevant studies.

Blood vessel models

a) Cell deformation studies

Microfluidics has been used for the creation of different models mimicking the *in-vivo* microenvironment with good temporal and spatial resolution. Models with different designs have been developed to study different aspects of cells in the vascular environment. In a study by Shevkoplyas et.al. [Figure 1.2 A] the size of the microchannels was tuned to match the size of capillaries *in-vivo* and the deformation of red blood cells (RBCs) was observed. [31] Such a system mimics the RBC deformation process which is often observed *in-vivo* during the exchange of gases between the RBCs and the endothelial cell wall of the blood capillaries. Apart from RBC deformation, a similar model has been used for the study of leukocyte deformation. It is known that the neutrophils *in-vivo* undergo deformation while in pulmonary circulation. The mechanism of the deformation of the neutrophils could be studied using a narrow channel microfluidic model. [32] Blood cell deformation may also have other pathophysiological significances. Changes in the cell deformability and complications in microvascular perfusion is a common sight in sickle cell diseases. A microfluidic model to study the sickle cell condition of the RBCs was developed and process of vaso-occlusion was studied. [33] The primary advantage of such a system over the existing conventional assay is that it allows for the visualization of the process helping in better understanding. Apart from the channel dimension, such cell deformability models can be brought about using optical forces, [34] [Figure 1.2 B] or electric fields [35] Microfluidic models can also be used to study the impact of shear on the endothelial cells (EC). The pressure that the blood exerts on the cell walls can be recreated in the microfluidic models to understand the impact of shear on EC.[36-38] Apart from the endothelial cells, blood cells like RBC are also influenced by the shear. Extracellular adenosine triphosphate (ATP) acts as a vasodilator [39] and an understanding of such a process is important as any impairment in the release of ATP could lead to a variety of diseases like pulmonary hypertension [40] and diabetes. [41] This has been achieved using microfluidic models which have been used to recreate similar conditions [42-43] [Figure 1.2 (C-D)] and to study the rate of release of ATP as well as the impact of conditions like cell stiffness on ATP release. [44]

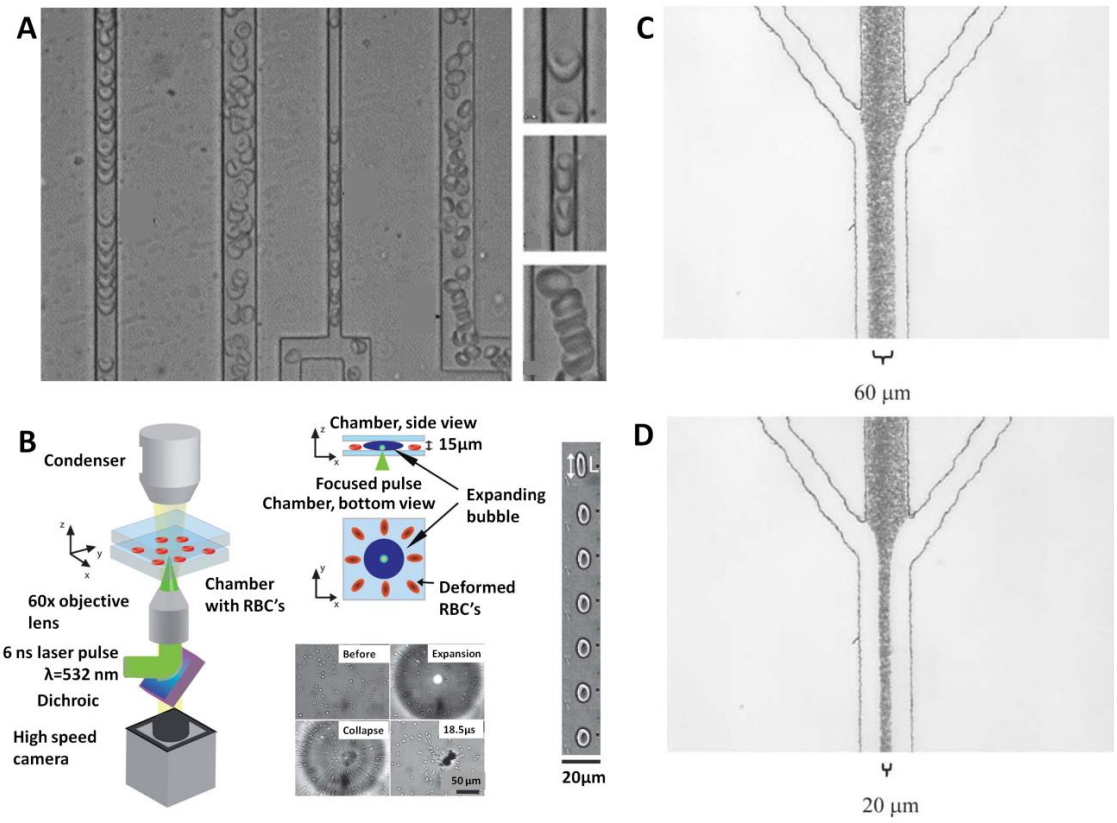

Figure 1.2: Microfluidics for hemodynamics. (A) Narrow channels for RBC deformation. Reprinted with permission from [31] , (B) Cell defromation in a microfluidic device using optical energy. Reprinted with permission from [34], (C-D) Hydrodynamic focusing for applying shear stress on RBCs. Reprinted with permission from [42]

Apart from the impact of mechanical stimuli on the cells, the cells *in-vivo* are under the influence of growth factors either as uniform distribution or as gradient. Growth factor based signaling stimulates different cellular processes *in-vivo* like cell migration, angiogenesis etc. An array of different growth factors may be involved in a particular process as in the case of angiogenesis vascular endothelial growth factor (VEGF) along with a multitude of other chemokines like platelet derived growth factor B, transforming growth factor beta 1 (TGF β1), fibroblast growth factor 2 (FGF 2), angiopoietins (ANG 1 and ANG 2) amongst many others are involved. These chemokines assist in the migration, proliferation and formation of the vasculature during the process of angiogenesis.

b) Wound healing and immune response

Cell migration forms an integral part in a large number of *in-vivo* processes. Wound healing and immune response would be examples of cell migration. The process of wound healing has been studied for decades and there are different conventional *in vitro* assays like the wound healing, scratch assay, Teflon assay to perform wound healing

studies. [5-7, 45]. It primarily involves the migration of healthy cells and replacing the dead or damaged cells in the area of the wound. Conventionally scratch assays involve a 2D culture of cells on a petri dish followed by the creation of a wound. Most common methods for wound generation involve either the physical scratching out of cells or by the removal of a physical barrier. [46] The wounded cells induce the migration of the surrounding cells causing the closure of the wound. To determine the growth factors involved in the cell migration, conventionally a Boyden's chamber was used. It has the ability to create a gradient which is normally the case *in-vivo* which cannot be replicated using a scratch assay. But the Boyden's chamber suffers from a major disadvantage where it does not allow for real time monitoring and hence cell migration cannot be observed. The transparency of the PDMS chip and the ability to control fluid flow inside the chip to create precise gradients make microfluidic wound healing assays a better substitute for the conventional *in vitro* models. Here the cells are cultured in a monolayer inside a microfluidic channel following which a wound is introduced by making use of the diffusion-less laminar flow of two or more liquids while flowing inside a microfluidic channel. Migration of endothelial cells to close down the wound [Figure 1.3 A and 1.3 B] could be observed indicating the effectiveness of using this model for wound healing studies. [47-48] Another study involved the recreation of the immune response to an infection by the migration of neutrophil inside a microfluidic chip. In this model [Figure 1.3 C], a 3D migration of the neutrophil was studied under the influence of growth factors like N-formyl-methionyl-leucyl-phenylalanine (fMLP) and human interleukin (IL-1 and IL-8). [49-50].

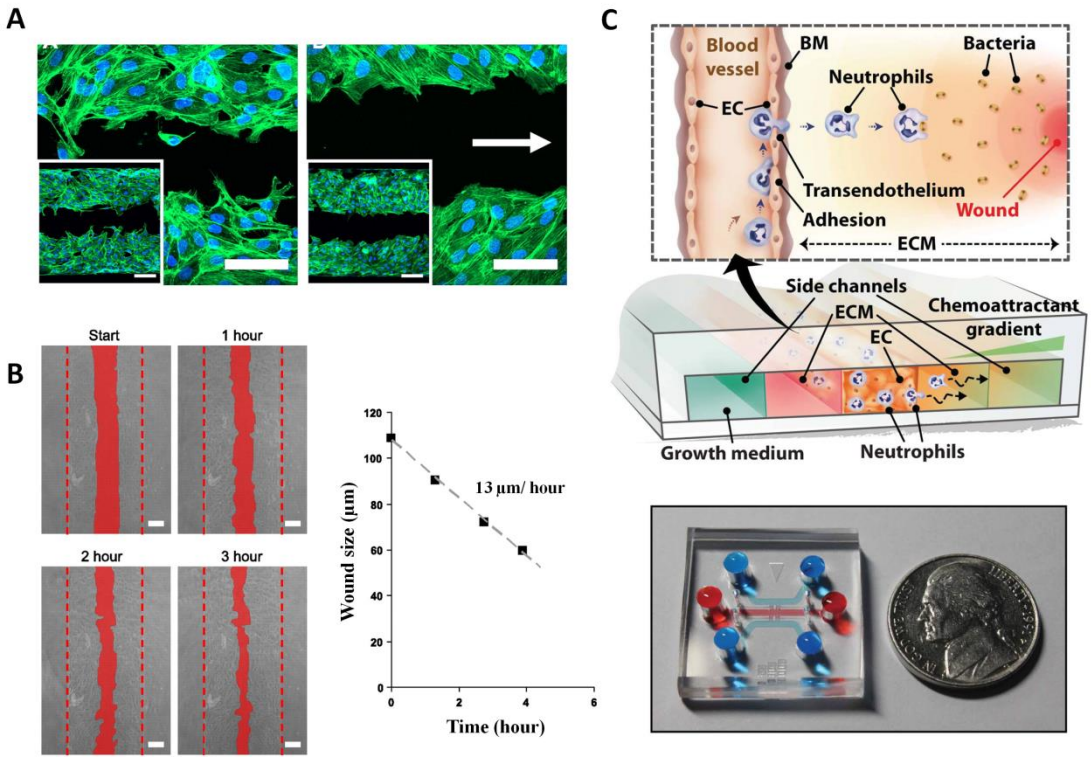

Figure 1.3:Wound healing and neutrophil extravasation. (A) and (B) show the creation of a wound using trypsin inside the chip and subsequent healing. Reprinted with permission from [48], (C) A schematic of the neutrophil extravastion model. Reprinted with permission from [50].

c) Angiogenesis

Angiogenesis is a physiological process that occurs *in-vivo* resulting in the formation of new blood vessels. Apart from blood vessel formation in healthy tissue, angiogenesis is also one of the key processes which occurs during the presence of a tumor. As stated earlier, a large number of growth factors are involved in the formation of these blood vessels. These growth factors are often secreted by the surrounding cells. Hence it is important that the *in vitro* model developed is able to accommodate the co-culture of cells. For such models to be physiologically relevant, they should be cultured on a matrix or scaffold that can support 3D cell migration and growth. Previously, Boyden's chamber [51] was used to study the transmigration of the endothelial cells under the influence of a growth factor gradient. But as stated above, the Boyden's chamber lacks the ability to support real time monitoring of the ECs. These issues can be alleviated using microfluidic devices and different chips have been designed to perform different angiogenesis studies. Primarily angiogenesis studies on-chip can be classified into two: 1) Mono-culture system (only EC) with growth factor gradient, and 2) Co-culture system with EC and other cells like smooth muscle cells (SMCs) and mesenchymal stem cells (MSCs).

Microfluidic models with mono-culture of endothelial cells have been used to understand the impact of different chemokines on cell sprouting and migration through a scaffold like collagen which is representative of the extracellular matrix (ECM) [Figure 1.4 (A-B)]. The impact of VEGF and ANG-1 in 3D sprouting angiogenesis of EC was observed within a microfluidic device. [52-54] Unlike the conventional cell culture systems, microfluidic systems allow the patterning of cells within confined spaces. They also allow one cell type to be embedded within the scaffold or hydrogel while culturing the EC on it. [55] In an alternative study, rat hepatocyte was cultured along with rat/human endothelial cells within a microfluidic device in two separate chambers connected by a collagen layer between them. The impact of the 2 cell types on the morphogenesis and migration through the scaffold was observed and studied. [56] Such models are also vital in the study of tumor progression and we will be covering these applications in a later section. The co-culture of ECs along with pericytes allowed for the physiological morphogenesis of ECs resulting in the interconnection of the ECs to form functional microvascular networks. [57] The vasculature also showed long term stability and strong barrier function [Figure 1.4 (C-D)]. The use of hydrogel, instead of PDMS as the material for chip fabrication has also resulted in the formation of a functional vasculature [Figure 1.4E]. [58-59]

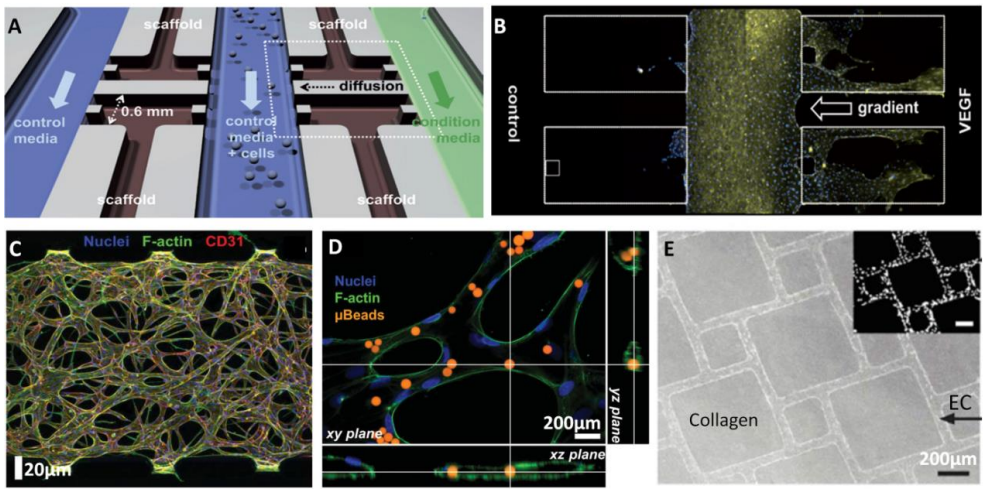

Figure 1.4: Microfluidics for angiogenesis. (A) and (B) Microfluidics model that can be used as a mono-culture or co-culture system. Reprinted with permission from [55], (C) Functional microvascular system on chip. (D) Orthogonal image using confocal demostrating the flow of micro-beads. Reprinted with permission from [57], (E) A functional vasculature in microfluidic hydrogels. Reprinted with permission from [58].

Disease models and organ on a chip

The most important goal of biomedical research is to study diseases so that a better understanding of its mechanism can be established to enable diagnosis and therapy become easier and effective. A recent survey [60] showed that only 10 to 15 % of the drugs

manage to get approval and the major reason for the suspension of a particular drug by the Food and Drug Administration (FDA) is due to its failure in drug efficacy study during phase 3 clinical trials. The reason for this failure has been attributed to a difference in the molecular mechanism of the diseases in animal models [10-11] signifying that though the drugs work effectively for the animal model, their activity fails in a human system. This increases the emphasis of performing disease studies on models containing human cells and microfluidics can be used to fill this role. In this section we will discuss some of the developed microfluidic models that have been shown to produce results comparable to animal models indicating that these models can be used as substitutes to animal models to perform studies to understand the molecular basis of the diseases as well as to perform drug testing.

Microfluidics allows for the creation of models involving 2D cell culture as well as 3D cell culture. 3D cell culture result in the formation of tissue microenvironment and these microfluidic models are termed as organ on a chip. These tissues are representatives of the respective organs and their potential to mimic the organ and some of its functions have been studied and compared to the data from animal models to show its significance as an effective substitute for animal models. The idea of such organ on chip model is to incorporate different organ systems into one microfluidic device, interconnected by microchannels such that they can form different parts of a human and eventually a human on-a- chip model can be created.

a) Heart

A 2D model to mimic the maladaptive remodeling of failing myocardium on chip has been developed by culturing cardiomyocytes on stretchable muscular thin film (MTF) substrates. The cells were then subjected to stimuli like cyclic stretching which triggered pathological gene expression [Figure 1.5 (A-D)] The results from this study was compared to the existing results from animal models and they were observed to be comparable, indicating that such model can be used to mimic abnormal contractile responses of a failing myocardium. [61]

Mathur et al. created a cardiac microphysiological system which can assist in drug screening. [62] In this work, they have used human induced pluripotent cells (hiPSCs) which was patient specific and obtained from the somatic cells. These cells were allowed to differentiate towards cardiomyocytes and the microfluidic chamber allowed the cells to

be aligned and arranged in a 3D tissue structure [Figure 1.5 (E-H)]. Within 24 hours of the culture on chip, the microtissue started beating spontaneously (without any stimulation) at rates of 55-80 beats per minute (bpm) which is comparable to physiological beating of the heart. The cardiac response of the system was tested using four established drugs. Moreover long term culture of cells was possible which is vital for drug studies. Such an organ on a chip model can be used to produce patient specific models to study cardiac disorders as well as drug efficacy.

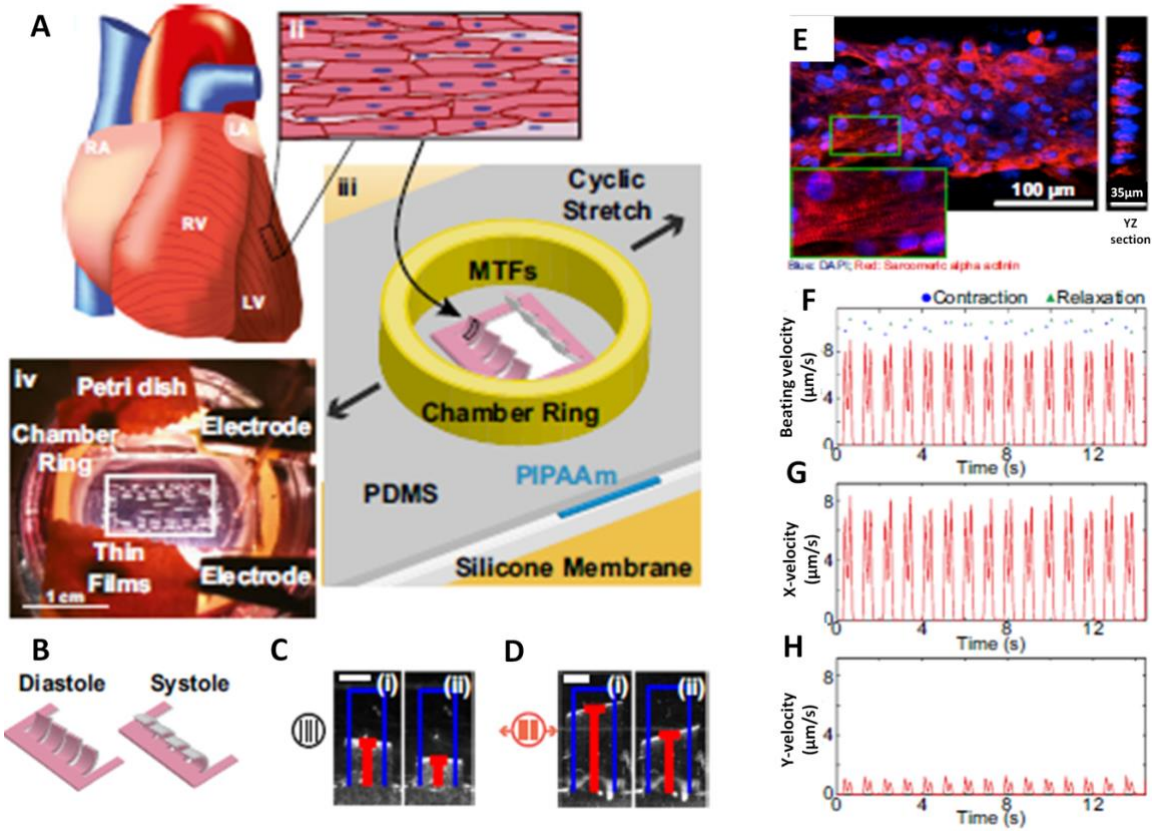

Figure 1.5: Microfluidic heart models. (A-D) Failing myocardium on chip using a muscular thin film for stretching the cardiomyocytes. Reprinted with permission from [61], (E-H) Beating heart on a chip. Reprinted with permission from [62].

b) Lungs

The alveolar-capillary interface of the human lungs was recreated in a lung on a chip model with human alveolar epithelial cells and pulmonary microvascular endothelial cells on either side of a stretchable porous membrane. [Figure 1.6 (A-C)] This was used to recreate the effect of tissue stretching that occurs *in*-vivo during breathing. The model was used to recreate conditions like pulmonary oedema. [63] It was also used to observe

inflammatory response to the presence of pathogenic bacteria in the alveolar compartment. [64]

Tavana et.al created a lung on a chip model with a multilayered PDMS chip to recreate the human distal airway. It primarily involved the culture of human pulmonary epithelial cells in the top chamber, which is separated from the bottom layer by a porous membrane. Air was constantly passed through the cell chamber and a liquid plug generator was integrated to the chip to bring about the closure of on chip airway [Figure 1.6 (D-G)]. Such a model was used to study the impact of surfactant dysfunction in the distal airway of the lungs. [65]

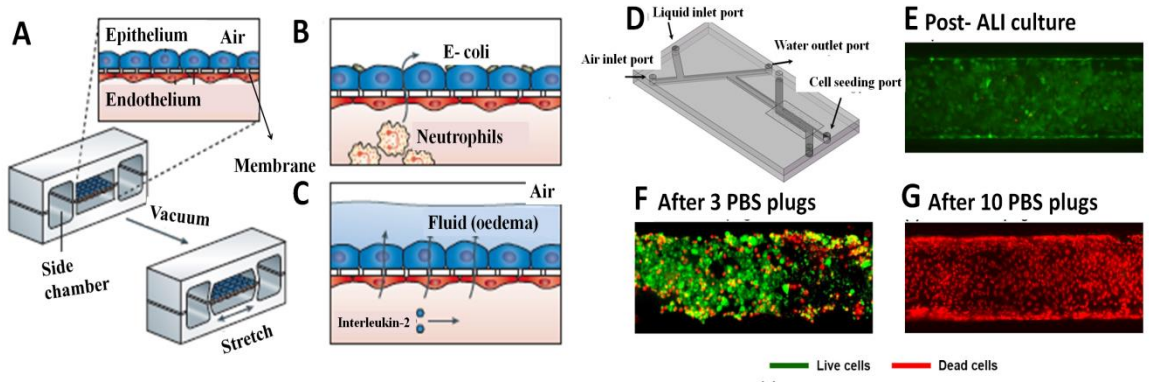

Figure 1.6: Microfluidic lung models. (A) Lung on a chip to study (B) Inflammatory response and (C) pulmonary oedema. Reprinted with permission from [66]. (D-G) Lung model to study surfactant dysfunction. Reprinted with permission from [65].

c) Liver

Chen et.al used the concept of dielectrophoresis (DEP) to bring about the patterning of hepatocytes and endothelial cells on a chip. [67] The patterns formed depended on the shape of the electrodes and hence such a method of cell patterning could be used to pattern different physiologically relevant arrangements. In this study DEP was used to selectively position one cell at a time and create a lobule like arrangement of the liver which is the natural arrangement of the liver cells. [67]

Different researchers have created liver on a chip model. Primarily, the hepatocytes are cultured either in 3D scaffolds that support their growth [68] or within grooves in concave shape. [69] Since liver is a vital organ, such models can be used for the study of pharmacodynamics of the drugs. They have also been used for cell-cell interaction studies by observing its interaction with the hepatic cells.

d) Intestine

Gut-on-a chip was developed using a microfluidic design which was similar to the one used for the creation of the lung-on- a-chip. [70] Human intestinal epithelial cells (Caco-2) were cultured on a flexible porous membrane. The existing models have not been able to recreate the *in-vivo* mechanically active microenvironment that involves the peristaltic motion and flow of intralumenal fluid. Also, the existing cultures fail to allow the co-culture of microbes, over extended periods of time, on the luminal surface of the epithelial cells like in a living intestine. The gut on a chip was subjected to flowing fluid and the peristaltic motion of the living intestine was mimicked by cyclic stretching of the flexible membrane. [Figure 1.7 (A-C)] These mechanical stimuli helped in the formation of cellular patterns that recapitulated microvilli of the intestine and also led to the formation of high integrity barrier to small molecules which is an important property of the intestine [Figure 1.7 (D-F)]. A common intestinal bacterium, *Lactobacillus rhamnosus*, was co-cultured along with the epithelium without compromising the epithelial cell viability and moreover, the bacterium was noted to improve the barrier function of the epithelium, which is the case *in-vivo*. The histological analysis of the villi formed and under the influence of the mechanical stimuli, the epithelial cells differentiate into different cell types which are normally found *in-vivo*. This gut on a chip model thus provides good recreation of the human intestine. [71]

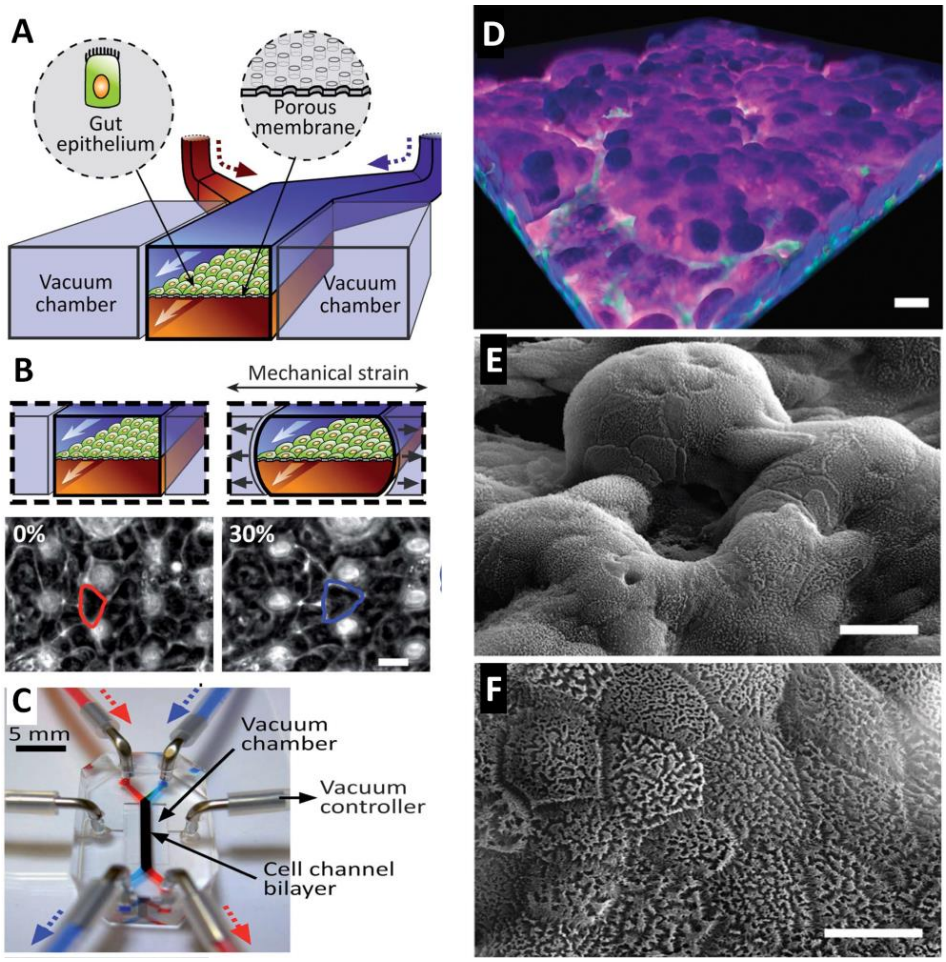

Figure 1.7: Microfluidic model of an intestine. (A-C) Gut-on-a-chip chip schematic and setup. Reprinted with permission from [70] (D-F) The mechanical conditions on chip stimulate the formation and differentiation of villi as in an *in-vivo* case. Reprinted with permission from [71]

e) Kidney

Kidney is a vital organ, especially during drug metabolism due to its part in controlling body fluids and homeostasis thereby controlling the elimination of drugs and chemicals from the human system. Microfluidic biochips have been designed and developed to study the functioning of the kidney cells. Different groups have focused on different aspects of kidney functions. Snouber et.al created a renal microfluidic biochip to analyse the transcriptmic and protemic profiles of the cells in a microfluidic chip. They used this chip to understand the cell functions and also to check its role as a potential model for drug studies [72]. Huang et.al developed a renal microfluidic chip to facilitate the development and maturation of the epithelial cells using its co-culture with adipose-derived stem cells (ASCs). The model was successfully able to analyse the impact of low values of shear on the epithelial cells and also enhanced the formation of cilia on these

cells which matches with cellular morphology *in-vivo*. [73] A multilayer microfluidic device was used to culture renal tubule cells such that an *in-vivo* like environment was created for the cells. This enviroment was created by the application of a very low shear stress which resulted in cell polarization and cell rearrangement. Such a modification allowed the cells to perform its inherent task of regulating water and ion balance. [74] But in all the above mentioned kidney models, rat cells are used. In another work by Jang et.al, a similar chip was used while using primary kidney epithelial cells from human. Here like previous results, application of shear stress resulted in enhanced cell polarization and cilia formation. Moreover during drug studies, the results from these models matched with those obtained *in-vivo* indicating the use of this kidney-on-a chip model drug for toxicity studies [Figure 1.8]. [75]

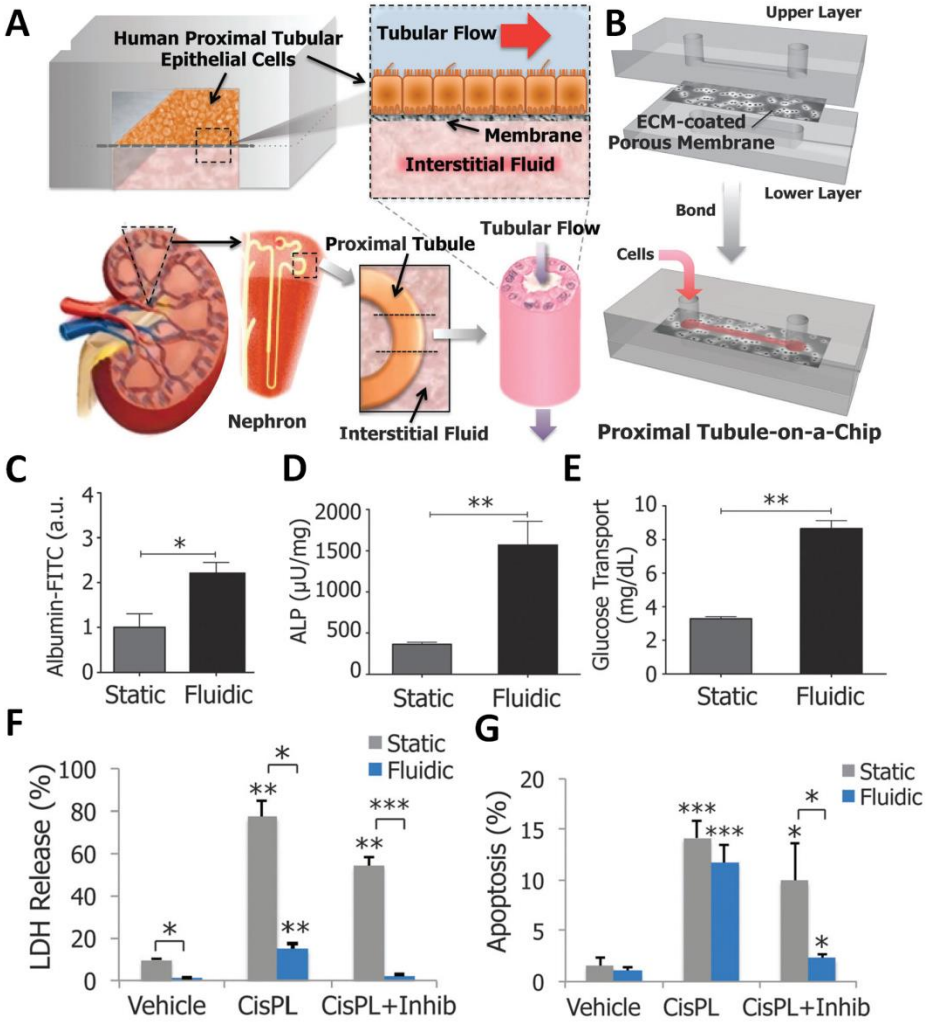

Figure 1.8: Microfluidic model of a kidney. (A) Schematic of kidney-on-a chip. (B) Microfluidic chip assembly (C-E) molecular transport across the epithelial cell layer of albumin, alkaline phosphatase (ALP) and glucose respectively. (F-G) Cytotoxicity studies in response to a known cancer chemotherapeutic drug, cisplatin. Reprinted with permission from [75].

f) Bone marrow

Bone marrow is a complex environment containing chemical, physical, cellular as well as structural cues which help in maintaining the hematopoietic system. Hematopoietic niche of the bone marrow regulates the hepatopoietic stem cells (HSCs). Recreation of this niche is very difficult and though numerous models have been previously created for maintaining the HSCs, the models have not been able to recreate the bone marrow environment and hence it results in the HSCs losing its pluripotency fast. In order to overcome such issues Torisawa et.al engineered the bone marrow *in-vivo* within a mouse [Figure 1.9]. Histological analysis of such a bone marrow developed seemed to match with that of the actual bone marrow. At the end of 8 weeks, the engineered bone marrow is implanted into the microfluidic chip. The bone marrow on chip was able to maintain its functionality for over a week. Such a model provides an alternative to the animal studies for bone marrow based research especially to understand drug responses and also hematologic diseases. [76]

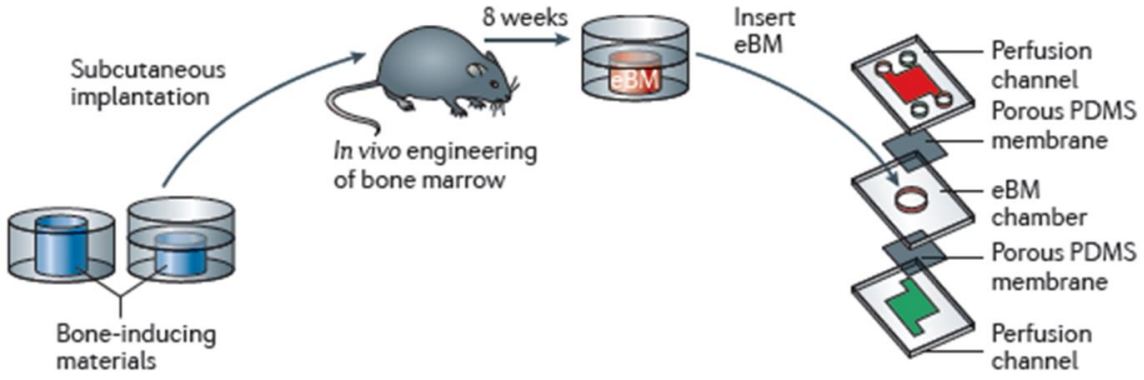

Figure 1.9: Schematic of *in-vivo* engineering of bone marrow. PDMS with bone inducing material is implanted into a mouse and at the end of 8 weeks the engineered bone marrow (eBM) tissue can be obtained, which is implanted into the microfluidic device for further studies. Reprinted with permission from [66].

g) Cancer models

Cancer is one of the widely studied diseases using microfluidics. Microfluidic models have helped in forming a better understanding of the processes involved in the progression of tumor. Tumor angiogenesis, [52-53, 77] tumor-stroma interactions in complex co-culture systems, [55] role of macrophages in tumor intravasation by increasing the permeability of the endothelial barrier (blood vessel walls) [78] and also to understand the

mechanism and cues that lead to the transition of non-invasive breast cancer into an invasive cancer [79] have been studied using microfluidic models.

The inherent ability to model flow system in microfluidics allows for the recreation of physiological conditions that the tumor cells will undergo while in the blood vessels. Moreover tumor metastasis can be studied. A 3D culture of bone tissue was performed on chip and the metastasis of breast cancer cells towards the bone tissue was studied. [80] In this system it was observed that the presence of multiple cells in the model increased the tumor migration and metastasis compared to system without any co-culture. This system highlights the significance of co-culture and the importance of tumor-stroma interaction in cancer progression. Another advantage of such a study is that the metastasis can be observed in real time and its mechanisms can be studied, which cannot be done in an *in-vivo* environment.

Apart from performing studies to understand cancer mechanism, such models also help in drug testing. One of the advantages of using microfluidics is the ability to modify the designs and the ease with which complex *in-vivo* arrangements can be reproduced. An example of this is the use of microfluidics to study drug diffusion in a tumor. One of the reasons for the ineffectiveness of drugs against cancer has been suggested to be because of the inability of the drugs to penetrate through the different layers of thick cancer tissue. This can be explained by that the cancer tissue is made up of many layers of cells. The layers closer to the blood vessels are classified as proliferating and layers farther away from the blood vessels are quiescent, which has good resistance to drugs. This multi-layered configuration of the cancer tissue makes it difficult for the drug to diffuse through to the quiescent zone. Walsh et al. created a microfluidic model to mimic this condition and to assist in drug testing. Such models help gain insight into the properties of tumor mass which can be exploited and can be used for developing suitable drugs. [81] A disease on a chip model was designed where normal breast luminal epithelium was cultured on semicircular acrylic supports that mimic portions of the mammary duct. [82] Cancer-on-a-chip model was developed incorporating 3D tumor spheroids along with endothelial cell lining, which mimicked the blood vessel. Such models can be used to study phenomena like epithelial to mesenchymal transition (EMT) and metastasis. [83] Some of the microfluidic models for cancer studies is shown in figure 1.10.

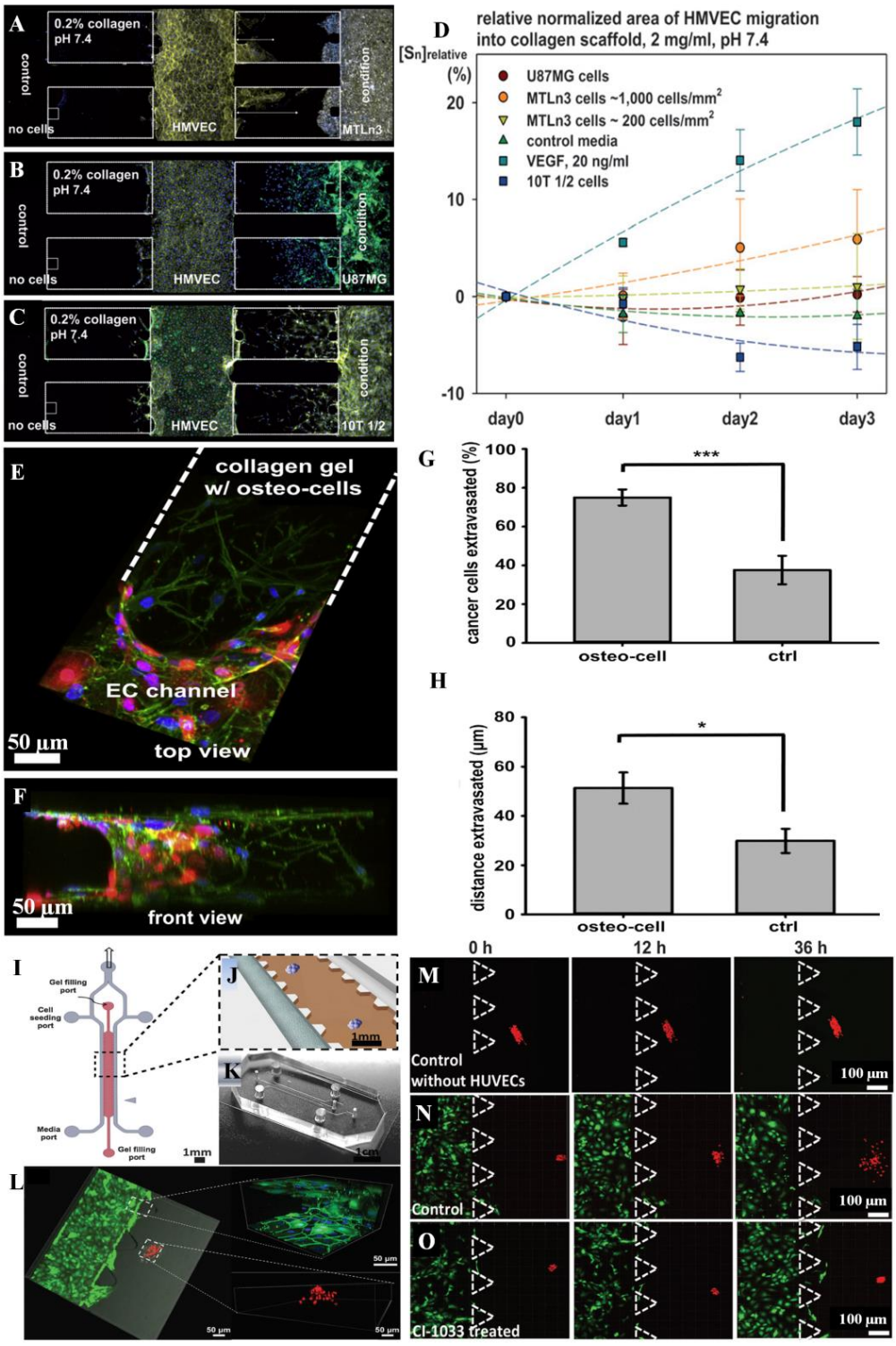

Figure 1.10: Microfluidic cancer models. Tumor angiogenesis (A) Co-culture of Human dermal microvascular endothelial cells (HMVEC) with rat mammary adenocarcinoma cells (MTLn3), (B) Co-culture of HMVEC and Human glioblastoma cell (U87MG), (c) Co-culture of HMVEC and (10T 1/2) (D) Quantification of HMVEC migration. Reprinted with permission from [55]. (E-F) Co-culture of EC and osteo cells, (G-H) Quantification of the impact of osteo environment on tumor cell extravasation. Reprinted with permission from [80] .(I-L) Microfluidic co-culture device of EC and lung adenocarcinoma (A549) cells. The chip was used to screen EMT blocking drugs. (M) Control showing dispersion of the A549 cells (red) with time in the absence of EC. (N) A549 dispersion in the presence of EC, (O) A549 dispersion in the presence of EC and endothelial growth factor receptor (EGFR) inhibitor. Reprinted with permission from [83].

h) Body-on-chip

The increasing realization of the drawbacks of using animal models for drug testing, has resulted in the development of different microfluidic models for different organs of the human body (organ-on-a-chip). But during the administration of drugs to a human body, the impact of the drug need not be specific to a particular organ. The pharmacokinetics-pharmacodynamics (PK-PD) of the drug is vital to understand its efficacy. With this in mind, researchers have created test models, by incorporating different organ-on-chip models discussed above to create a body-on-a-chip. Though not all the organs have been put together, there have been a few models incorporating breast cancer, intestine and liver, [84]with different organs in different chambers and the chambers connected by micro-channels. Another model comprising of liver, tumor and bone marrow was created to study the PK-PD profiles of anti-cancer drugs. [85] A model with different human cell types to represent lung, liver, kidney and adipose tissue were cultured on chip as a body-on-chip model for drug screening. [86] Such models can reduce the dependence on animal models. By increasing the complexity of the system, they can be used as drug screening platforms in the future. Some body-on-chip models are shown in figure 1.11.

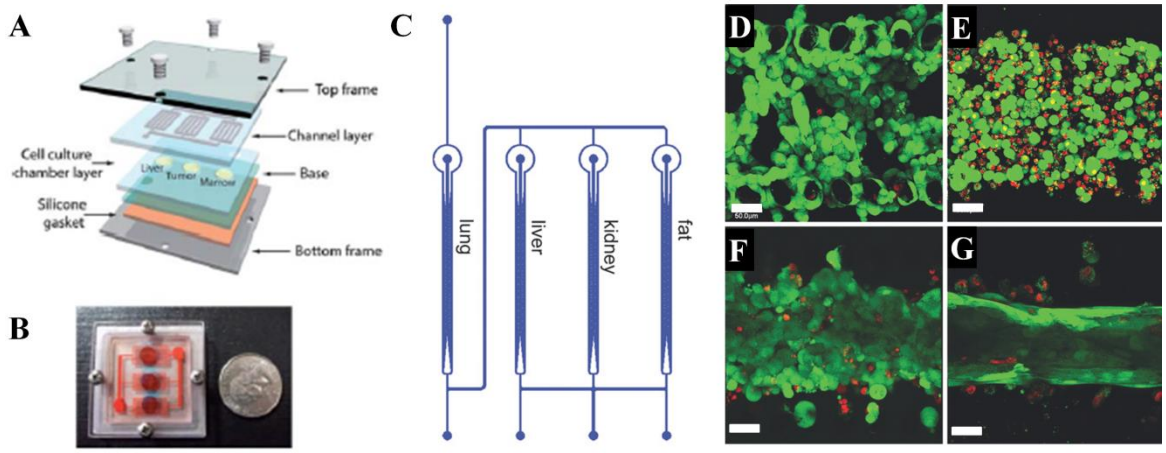

Figure 1.11: Body on a chip. (A-B) Co-culture of liver, tumor and bone marrow on chip for PK-PD analysis of a drug. Reprinted with permission from [87], (C) Culture of different organs on the same chip. Live dead staining to test the cell viability of the different cell types in the presence of TGF-β1. (D) A549 cells (Lung carcinoma),(E) C3A (Liver carcinoma) (F) HK-2 (human kidney cells) (G) Human preadipocyte cells (HPA). Scale bar: 50µm. Reprinted with permission from [86].

i) Single cell analysis

It is important to understand the interactions between different organs as well as interactions between cells especially for disease studies and drug development and

checking drug efficacy. There has also been an increasing realization of the heterogeneity between cells of the same cell type [88] because of differences in their stochastic gene expression and protein expression. Analysis of individual cells and its response to different bio-chemical conditions help in forming a better understanding of the functioning of the cells and hence help in predicting the cell behavior. Moreover, single cell analysis will also be helpful in understanding the make-up of rare cells like the cancer stem cells about which not much understanding is currently available.

Because of the ability to fabricate microfluidic channels to dimensions comparable to that of a single cell, such devices are extremely useful in performing analysis of single cells. Different microfluidic approaches have been used to achieve this task. One of the techniques of analyzing single cells is a process called chemical cytometry which involves the separation of the cells followed by performing the analysis of interest. The first step in single cell analysis is cell isolation which is normally performed using different strategies like micro valve, [89] using optical field, [90-91] electrical field [92] or magnetic field. [93] Following its isolotaion, the cells are lysed to release its components that can be further analyzed. Different analytical methods have been coupled with such isolation technique to build a lab on a chip for the analysis of gene expression, [94-95] protein detection, [96-97] as well as cell metabolites. [98] Apart from gaining a understanding about the cell, such a method helps in the screening of drugs as well as its concentration profiling. [99] Kellog et al. developed a high throughput microfluidic system with parallel channels to understand the signaling dynamics within the cell. [100] Another work by Fan et.al used a microfluidic chip for whole genome haplotyping of a single cell. [101] The cells are microscopically chosen and separated, following which they are lysed to extract the chromosomes. The chromosomes are then amplified on a chip and a 46 loci polymerase chain reaction (PCR) is used to perform the final analysis. Single cell analysis provides different advantages and microfludics is proving to be one of the best methods for studying it.

1.4 Challenges for microfluidics

Microfluidics is a fast growing area of research that has been in place for close to two decades. The breakthrough in the use of material chemistry for device fabrication has been an added advantage as these materials allow for easy fabrication of complex designs for a wide range of applications. Nevertheless there is a growing concern regarding the future of microfluidics. Though it has appeared as a promising approach especially in

biomedical engineering, the number of microfluidics products in the market is very limited. Microfluidic technology for disease studies and drug efficacy testing can save a lot of money. But the lack of experts in these markets has resulted in minimal use of microfluidics for such applications.

Sackmann et al. [102] noted that one of the reasons for failure of usage of microfluidics in biomedical engineering has been the failure of the biologists and the engineers to work together. It was noted that between 2000 and 2012, 85% of the microfluidics based studies and discoveries have been published in engineering journals. Apart from this, the biologists are comfortable and familiar with the established conventional *in vitro* models and animal models thereby and keeping microfluidic approaches as their final resort. There is a necessity to bridge the gap between the biologists and the engineers for increasing the usage of the microfluidics.

Apart from cell culture, the various assays for detection and biochemical and molecular studies for different analytes, play a vital role in the success of the method. The conventional cell culture procedures and *in vitro* models have been in use for centuries, while the different assays used for cellular analysis are matured, tried and tested over decades making them reliable in comparison to a fresher technology like microfluidics. The development of numerous on-chip analytical tools in recent times is a step in the right direction. More assays and detection tools need to be developed and incorporated with the chip so as to develop a complete lab on a chip model which is easy to use. Apart from that, educating the scientific community about the advantages of microfluidics is also an essential promoter. Hence for the future of microfluidics, it is best to forge meaningful collaborations such that specific problems faced by biologists can be targeted and engineers can work in tandem to solve the problem.

1.5 Summary

In this chapter we have discussed in brief about the current status of microfluidic *in vitro* models. With the help of microfabrication and fluid control, complex designs can be created and they can be used to replicate different organs of the human body. Though 3D culture of cells has been successfully carried out to create these organs on a chip, it may also be noticed that with efficient cell patterning techniques researchers have successfully created models that can replicate *in vivo* systems. The heart on a chip [Figure 1.5], lungs on a chip [Figure 1.6], gut on a chip [Figure 1.7] and kidney on a chip [Figure

1.8], discussed above are examples of such efficient cell patterning coupled with ability of microfabrication to enable multi-layered devices.

In this thesis, I have used cell patterning to develop a microfluidic *in vitro* model that can be used as a migration assay. I have discussed the procedure used to modify the PDMS chip to allow for efficient cell patterning inisde the chip and have also performed studies to validate the effectiveness of the chip. The model developed here also allows for the co-culture of different cell types in different channels which has been used to study tumor-stroma interactions. This co-culture model has also been used to test the selectivity and efficiency of an organic dye to bring about photodynamic therapy. The aim of the my research was to develop a microfluidic *in vitro* model, validate its effectiveness by comparing results obtained from this study to the results available from previous *in vivo* studies and apply the model to perform different studies like impact of substrate properties on cell migration and for drug testing.

Chapter 2 Objectives and methodology

2.1 Overview and objective

Cell patterning involves the organization of cells in complex formations to suit a specific study. Such patterning of cells generally involves the creation of cell adhesive areas (protein coating) on a substrate followed by culturing cells. Microfabrication and microfluidic technologies have been widely used to achieve complex cell patterns. A large number of *in vitro* models have been created by patterning cells and it has enabled the study of various cell phenomena like cell-cell interactions and cell migration. Patterning of single and multiple cell types has been reviewed previously. [15, 103-105] Patterning different cell types to create a co-culture system has been of particular interest as cells *in vivo* are present in a complex environment comprising of different cell types. Most of the cell patterned models have a two dimensional (2D) cell culture which is not the case *in vivo*. Researchers have compared the differences in cell behavior between the cells cultured in 2D to cells cultured in 3D and have observed that cells cultured in 3D show better relevance to cells *in vivo*. Nevertheless, 2D cell culture has enabled the understanding of basic cell behaviors like cell migration, cell-substrate interactions, etc, which has proved vital for the development of complex 3D cell models. Moreover culturing cells in 2D is faster with a standardized and accepted procedure and also, a large number of widely accepted assays are available to perform various biomolecular analyses in comparison to 3D cell culture. Though physiological relevance of 2D cell culture models is less, they can be used for preliminary studies before the usage of complex 3D cell culture and animal models.

Microfluidics has been widely used for the creation of co-culture models by patterning different cell types inside the microfluidic chip. The advantage of using microfluidics in biology has been already discussed in the previous chapter. The primary objective of this work is to develop a simple, easy to use microfluidic *in vitro* model that can be used to perform different cell-based studies. In alignment with this objective, in this thesis I have discussed the development of a microfluidic *in vitro* model that can be used to pattern cells (single cell type or multiple cell types) in specific compartments within the microfluidic device. Here the cells were cultured in 2D and the model was used for different studies.

1. **Cell-cell interactions**: This study was performed to validate that the *in vitro* model developed has physiological relevance. Interaction between tumor cells and stromal cells has been used to validate the model.

2. **Cell-substrate interaction**: Combinatorial impact of varying properties of the substrate on cell migration of mesenchymal stem cells.
3. **Efficacy testing**: The efficacy of an organic dye for targeted staining and targeted photodynamic therapy (PDT).

In this thesis, each of these studies has been divided into individual chapters. Since these studies are distinct from one another except for the microfluidic model, I have discussed their background individually, followed by a brief insight into the materials and methods used for the study. Following this, I have discussed the results and finally summarized each of these studies.

2.2 Basic methods

In this section, the methods and materials that have been common amongst the different studies have been discussed and summarized. PDMS is the material used for the microfluidic chip. It is commonly used in microfluidic chip fabrication because of low fabrication costs, ease of handling, good chemical and thermal stability, optical transparency, [29] permeability to gases [30] and biocompatibility [106]. Once fabricated, the chip is surface treated to control the fluid flow and facilitate cell culture. Cells are cultured on-chip and respective studies are carried out. Prior to cell culture on-chip, the compatibility of the different surface treatment procedures on cell culture was verified by cell adhesion assays and cell viability assays as well as protein retention assays. On-chip analysis, primarily involved transmitted light and fluorescent imaging of the cells on-chip to check for its viability or other cellular properties like cell spreading and migration.

2.2.1 Microfluidic chip fabrication

The microfluidic chip is fabricated using a sequence of procedures involving rapid prototyping and replica molding. [107] A brief account of the fabrication procedure is shown as a schematic in Figure 2.1. This procedure stems from the more sophisticated techniques of microfabrication, which is used widely in the silicon industry for the creation of integrated circuits (IC). Since IC fabrication is highly expensive, less expensive techniques of rapid prototyping has been widely accepted, especially in universities and other research centers for the fabrication of microfluidic chips.

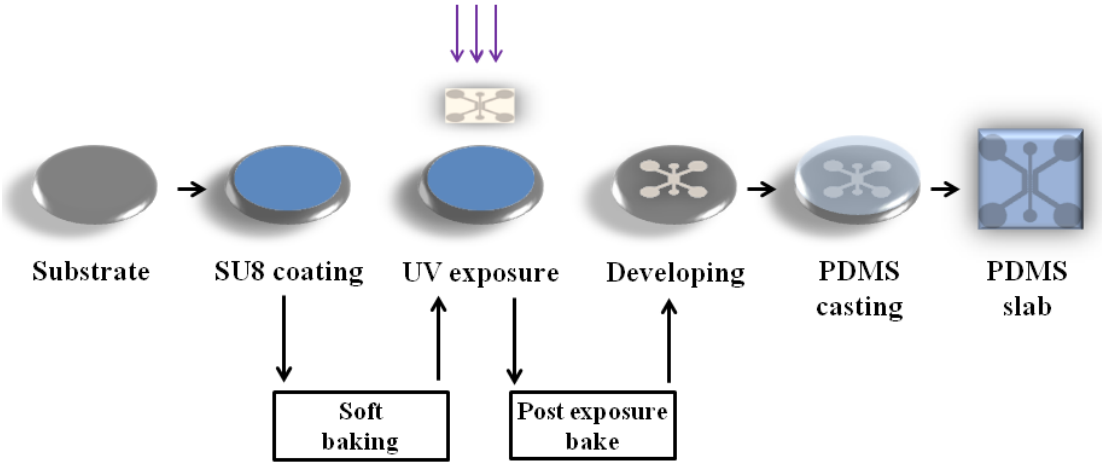

Figure 2.1: Schematic of microfluidic chip fabrication. The PDMS slab is sealed to a cover slip or another PDMS layer to obtain the microfluidic chip

In the initial step of rapid prototyping, the design of the chip is drawn using designing tools like AutoCAD (Autodesk Inc., USA) and printed onto transparent sheets. Such a printed design is called a photomask which has distinct opaque and transparent regions. The design from the photomask is transferred onto a substrate, like a silicon wafer, using photolithography. A negative photoresist SU8 2050 (Microchem, USA) is spin coated onto a 3-inch silicon wafer to get a final thickness of approximately 170 µm. The spin coated wafer is soft baked by a two step process: 5 min at 65°C and 45 min at 95°C. Following soft baking, the photomask is placed over the wafer and exposed to ultraviolet (UV) radiation (365 nm). The light passes through the transparent portions of the photomask, thus polymerizing those regions, while the region below the opaque portion of the photomask remains unpolymerized. A step of post exposure bake is performed to complete the polymerization of the SU8 by placing the sample at 65°C for 5 min and 95°C for 45 min. SU8 developer solution (Microchem, USA) is used to wash away the unpolymerized portion of the SU8 leaving behind the positive relief of the design. This wafer, with the design is called a mold. The step of replica molding follows rapid prototyping.

Replica molding is a simple step that involves casting of a prepolymer against the mold which will lead to the generation of a negative relief on the polymer. The polymer used in our study is PDMS. PDMS is a mixture of a silicone rubber base and a curing agent normally mixed in the ratio of 10: 1 by weight, respectively. Once mixed, PDMS is poured over the mold and cured at 70°C for 2 h, following which they are cut and peeled

off from the mold. Thus a replica of the mold is obtained on a PDMS slab. The mold can be reused to create another PDMS slab by following the same procedure. Holes are punched onto the PDMS slab to serve as inlets and outlets. To create a completely functional chip, the PDMS slab is sealed onto a glass cover slip (22 mm × 22 mm). This sealing is facilitated by a surface treatment procedure called plasma treatment. [108-109] In our case, the PDMS slab and the cover slip are plasma treated using an air plasma cleaner (Harrick Plasma, NY, USA) at input power of 100W and RF frequency of 8-12 MHz.

In our studies, we have used a three channel microfluidic device for compartmentalized cell culture. The three channels are separated from each other by micropillars (cross-section 200 µm × 100 µm). The maximum length of the channel is around 2 cm, while the width of the side channels are 800 µm each while that of the central channel is 500 µm. The height of the fabricated chip is approximately 170 µm.

2.2.2 Protein coating

Native PDMS does not support long term cell rowth and hence the PDMS chips were coated with fibronectin so as to enhance cell growth. 20 µg/ ml of fibronectin (Life technologies, Singapore) was introduced into the chip through the inlets and placed in a humidified incubator at 37°C and 5% CO_2. The flow of fibronectin is guided by the hydrophilicity of the surface within the chip (due to plasma treatment). The chip is washed with 1X phosphate buffer saline (PBS) and placed in an oven at 40^{o}C for 24 h to accomplish the hydrophobic recovery of PDMS. Following this, the chip is UV sterilized and a second layer of fibronectin coating was done by introducing 20 µg/ ml of fibronectin into the side channels. This is done to enhance cell attachment in these channels. To enhance the flow of liquid, the side channels were coated with gelatin using a procedure explained in chapter 3 (section 3.2.2). It could be observed that due to the hydrophilic nature of the gelatin coating in the side channels, there was no hindrance to the flow of fibronectin, while because of the lack of gelatin coating, the central channel was hydrophobic and fibronectin did not cross over to the central channel due to high surface tension (created by the combined effect of micropillars and hydrophobic central channel). The second layer of fibronectin coating was performed to enhance cell attachment in these channels. These channels are washed with 1X PBS and the chip is ready for cell seeding.

2.2.3 2D cell culture

In this thesis, different cell types have been used for different studies. But the procedure for culturing the cells is similar for these cells. The cells are cultured in Dulbecco's modified eagle medium (DMEM) supplemented with 10% fetal bovine serum (FBS) and 5% Penicillin-Streptomycin (PS). Cells were cultured in T-25 flasks till they achieve 80% confluence, following which they were resuspended using 0.25% EDTA (ethylenediaminetetraacetic acid)-trypsin to a cell density of one million cells (10^6) per ml. Approximately 50~60 µl of cell suspension (10^6 mL^{-1}) was introduced into the side channels of the microfluidic chip. The cell medium inside the microfluidic chip was changed every 24 h. The flow rate during medium change on the microfluidic chip was maintained at a very low level to prevent the cells from being damaged by the flow shear stress.

2.2.4 Cell viability/cell proliferation assay

Cell viability was quantified using the Prestoblue cell viability reagent (Life technologies, Singapore). It is a resazurin based solution which can be reduced by living cells. The degree of reduction depends on the number of cells and hence can also be used to quantify cell proliferation. In our studies we have used this as an indicator of cell viability. The advantage of using Prestoblue reagent over the widely popular MTT assay is that MTT assay is an end point assay, where the cells need to be sacrificed for measurement, while prestoblue reagent is not an endpoint assay. Hence this assay can be used to measure the viability of cells over an extended period of time. Apart from this, the incubation time is relatively short for the prestoblue assay. In brief, the working solution for the assay is prepared by diluting the prestoblue stock 10 times using FBS/PS supplemented cell culture medium. They are then incubated with the cells for approximately 1 h. Some no cell controls are also prepared simultaneously, in which the working solution is incubated in wells without any cells for 1 h. The absorbance of the reagent in each well is measured at two specific wavelengths, 570 nm and 600 nm. The absorbance values give an idea of the reduction of the prestoblue reagent due to the cell metabolism. The percentage of reduction of the reagent is a direct indicator of cell viability or proliferation.

The percentage reduction of prestoblue is calculated using the formula,

$$\frac{[O2 \times A1] - [O1 \times A2]}{[R1 \times N2] - [R2 \times N1]} \times 100$$

O1 = molar extinction coefficient of oxidized prestoblue reagent at 570 nm

O2 = molar extinction coefficient of oxidized prestoblue reagent at 600 nm

R1 = molar extinction coefficient of reduced prestoblue reagent at 570 nm

R2 = molar extinction coefficient of reduced prestoblue reagent at 600 nm

A1 = absorbance of test well at 570 nm

A2 = absorbance of test well at 600 nm

N1 = absorbance of no-cell control at 570 nm

N2 = absorbance of no-cell control at 600 nm

Wavelength	Reduced [R]	Oxidized [O]
570 nm	155677	80586
600 nm	14652	117216

Table 2-1: Molar extinction coefficients of the prestoblue reagent

2.2.5 Cell adhesion assay

Cell attachment/adhesion is one of the most vital processes that the cells need to undergo before its subsequent growth on a substrate. Hence it is one of the important parameters for substrate compatibility for cell culture. In this thesis, cell adhesion, along with cell viability has been used to show the biocompatibility of PDMS. CyQUANT® Cell Proliferation Assay Kit (Life Technologies, Singapore) was used to quantify the relative cell adhesion with respect to a control. The cells are seeded on the substrates of interest using the cell culture procedure as explained above (section 2.2.3). They are washed after 90 min using 1X PBS to remove the non-adhered cells, following which they are frozen at -80^{o}C overnight. Frozen cells are thawed and lysed with a cell lysis buffer containing 1X CyQUANT® GR Dye for 5 min. The fluorescence intensity of the dye was measured using a microplate reader (Infinite M200 series plate reader, Tecan Asia, Singapore) with excitation at 485 nm and emission at 535 nm. These readings when expressed relative to the control give an idea of cell adhesion in the different substrates with respect to the control. This method has been found to be reliable for relative quantification of cell adhesion. [110] The basic principle here is that as DNA for a cell remains constant, the quantification of DNA content (due to the fluorescence intensity) correlates to the number of cells that are adhered to the substrate.

2.2.6 Cellular imaging

The miniature size and the transparency of the microfluidic device makes the microfluidic chip compatible for microscopy. Cell staining and fluorescence imaging are reliable and widely used methods for on-chip analysis. In our studies we have used fluorescence microscope, Olympus IX71 (Olympus, Singapore) and confocal microscope laser scanning microscope (LSM 710) (Carl Zeiss, Singapore) to perform bright-field and fluorescence imaging on-chip.

2.2.7 Measurement of reactive oxygen species

Reactive oxygen species (ROS) are molecules generated within the cell as a result of mitochondrial oxidative metabolism or external factors like cytokines, bacterial invasion, etc. These are radicals that are derived from molecular oxygen and are generated by almost all the cells. Apart from playing an integral part in the human immune system, they can also be harmful to the host cells. [111] In our study, intracellular ROS was measured using 5-(and-6)-chloromethyl-2′,7′-dichlorodihydrofluorescein diacetate (CM-H2DCFDA) assay (Life Technologies, Singapore). The concentration of the final working solution is cell dependent and suitable optimization experiments were performed to identify the best concentration for individual cell types. The working solution was prepared in 1X PBS and incubated with the cells for 20 minutes prior to fluorescence imaging. The fluorescent intensity is a direct measure of the ROS generated within the cell. This was done using the ImageJ software.(National Institute of Health, USA).

2.2.8 Quantitative real time polymerase chain reaction (qRT PCR)

qRT PCR is used for the quantification of gene expression. Gene expression is a process where the information from a gene translates into a functional product, which could be a protein or functional RNA (Ribonucleic acid). Though expression of a specific gene does not necessarily mean the production of the specific protein, it still gives an idea of the proteins that might be produced. Normally gene expression quantification happens from the total RNA in the cells. The process includes the extraction of the total RNA from the cell followed by the generation of complementary DNA (cDNA) by reverse transcription. Real time PCR was performed using the cDNA, specific primer sequences to target specific genes and a fluorescent tag for detecting the the PCR product. In our studies, total cellular RNA extraction was done using the RNeasy® Mini Kit 250 (Qiagen,

Singapore), followed by which the RNA density quantification was performed using NanoDrop lite spectrophotometer (Thermo Scientific, USA). Approximately 100 ng RNA of each sample was used for reverse transcription into cDNA with iScript^{TM} Reverse Transcriptase Supermix (Biorad, Singapore). Real-time PCR was performed on 96-well optical reaction plates (Bio-Rad, USA). The solution in each well had a mixture composed of 10 µl of *Power* SYBR Green PCR Master Mix (Invitrogen, USA), 0.24 µl of forward primer, 0.24 µl of reverse primer, 10 ng of cDNA, and the remaining volume of dnase-free water. Glyceraldehyde 3-phosphate dehydrogenase (GAPDH) was used as the calibrator sample to calculate the relative linear fold change in messenger ribonucleic acid (mRNA) levels. All the primers were purchased from IDT (Singapore). Target primers are chosen according to the study performed and their details are discussed in the respective chapters. The data were analyzed with Step One software version 2.3 using the comparative cycle threshold (C_T) method $\Delta\Delta C_T$ method. [112] This is a method to normalize the C_T values obtained after real time PCR. The analysis of gene expression helps in the understanding of how an organism's genetic makeup enables it to function and respond to its environment.

2.2.9 Protein retention assay

As stated earlier, native PDMS is not a suitable substrate for cell growth and hence it is coated with a protein (fibronectin) prior to cell culture. The amount of fibronectin retained on surface was quantified using Micro BCA protein assay kit (Life Technologies, Singapore). Micro bicinchoninic acid (BCA) assay is a colorimetric assay whereby the peptide bonds in the protein react and reduce the Cu^{2+} ions to Cu^{+} ions, which is detected. The Pierce BCA protein assay kit has three reagents that need to be mixed in specific ratio by volume to obtain the working reagent; 50 parts of reagent A (alkaline tartrate-carbonate buffer) 48 parts of reagent B (bicinchonic acid solution) and 2 parts of reagent C (copper sulfate solution). The detection was performed by measuring the absorbance at 562 nm using a microplate reader (Infinite M200 Pro, Tecan Asia, Singapore). According to the absorbance measurement, the protein concentration can be determined using a standard curve. The standard curve is obtained by using different concentrations of BSA (Bovine serum albumin). Concentrations from 0 to 100 µg/ml of BSA was prepared and incubated for 1 h at 37^{o}C with the working solution of the Pierce BCA protein assay kit following which the absorbance at 562 nm is measured. The standard curve is plotted with the absorbance in the Y-axis and BSA concentration along the X-axis. A linear equation relating the protein concentration to the absorbance value is

obtained, which is used to measure the concentration of protein retained in our experiments. The standard curve is calibrated each time an unknown sample is used. To measure the concentration of fibronectin retained, PDMS samples were prepared in a 4 well plate and processed according to the procedure followed for chip preparation. Briefly, 20 µg/ ml of fibronectin was coated following plasma treatment following which the samples were placed at 40ºC for 24 h. These samples are then incubated with the working solution of the Micro BCA assay and a microplate reader is used to measure the absorbance at 562 nm. The readings obtained are substituted into the equation obtained from the standard curve to calculate the protein retained per cm^2.

2.2.10 Contact angle measurement

The wettability of the substrate is an important property in microfluidic devices. As discussed earlier, PDMS by virtue is hydrophobic. The manipulation of the PDMS wettability is important for controlling flow inside the chip. A widely used method for determining the surface wettability is using the sessile drop method where a drop (5µl) of milli-Q-water is placed on the surface and the angle that the droplet makes at the liquid-solid interface surface and liquid-air interface, can be measured as the water contact angle. If the angle is greater than 90°, it is considered hydrophobic while a value lesser than that is considered hydrophilic. In our work, an optical tensiometer (Attension Theta, Sweden) was used to measure the contact angle of water droplet on PDMS substrate, which gives a quantitative characterization of the surface wettability.

2.2.11 Atomic force microscopy

An atomic force microscope (AFM) is normally used to obtain surface profiles with high sensitivities (measurable distance of 10^{-4} Å). [113] It was built to be a combination of scanning tunneling microscope (STM) and a stylus prolifilometer (SP). It uses a cantilever connected to a spring, whose displacements help in tracing the surface profile. The displacement of the spring is measured with the help of a laser beam directed at the head of the cantilever. They are normally operated either in contact mode, tapping mode or non-contact mode. According to the measurement to be performed, the mode of operation and the cantilever are chosen. The spring constant and diameter of the cantilever and its tip, respectively, needs to be carefully selected according to the measurement to be performed. For our experiments, the surface roughness and stiffness of the PDMS were determined by atomic force microscopy (AFM, MFP-3D, Asylum Research, CA, USA). The AFM probe with a silicon tip (radius 28±10 nm and spring

constant 0.5~4.4 N/m) was used and the measurements were performed in tapping mode. 20 μm × 20 μm topographical images with resolution of 256 pixels were scanned at 0.8 Hz using a set point of 0.7 V. The probe used for stiffness measurement was a modified silicon nitride AFM cantilever (NovaScan, USA) (spring constant 0.01 N/m) with a polystyrene spherical tip (4.5 μm in diameter). For stiffness measurement, the Hertz's model was used to derive the apparent elastic modulus as given in a previous report. [114]

Chapter 3 Microfluidic chip development and cell-cell interaction study

3.1 Background

The first step in the development of any model is to check for its validity in performing the desired role. In the case of an *in vitro* model, its validity depends on how effective it is in replicating *in vivo* conditions. In this chapter I have discussed the development of the microfluidic chip following which I have tested the ability of the chip to work as an effective *in vitro* model by comparing the results obtained from a cell-cell interaction study to that obtained previously using an *in vivo* model and reported in literature.

Cell interaction is an important phenomenon, which is vital for the physiological functioning of tissues[115-116] and also for key roles in cancer biology [117-118] and wound healing.[119] For better understanding of such phenomena there is a need for *in vitro* models that can mimic such natural phenomena. To achieve such physiological relevance several innovative and effective assays, such as wound healing assays and migration assays have been developed. [120] Cell interaction may occur among cells of the same phenotype, such as between endothelial cells during wound healing.[7] It may also happen between cells of different phenotypes, such as between endothelial cells and tumor cells during tumor-induced angiogenesis.[121-122] It is therefore desirable to develop co-culture systems, where different types of cells grow on the same substrate and the cellular interactions can be induced and monitored in real time. For this purpose, cell patterning is necessary to control their spatial distribution. In many prior studies, cell patterning was achieved by active methods using forces or fields, such as standing surface acoustic waves,[123] magnetic field,[124] optical force,[125] dielectrophoresis,[126] or optoelectronic methods.[127] The other important or probably more natural strategy of cell patterning was by passive methods utilizing the biochemical or biophysical affinity between cells and functionalized microarrays or micropatterns, which were created by various microfabrication techniques, such as photolithography, soft lithography, microcontact printing,[105] inkjet printing,[128] and dip-pen lithography.[129]

In the most recent decade, microfluidics has proved to be an effective tool for many cell-based studies.[130] Among these innovative microfluidic devices, some are dedicated for co-culture system, which is a rather challenging task compared to handling a single type of cells on a chip. Previous reports have shown various designs, including valves,[131] laminar flow between immiscible liquids,[132-133] separate compartments for dynamic co-culture,[134] and detachable substrates where the cells are individually cultured

on different substrates.[135] Some researchers have also used scaffold materials such as collagen to create barriers between two cell types in a 3-dimensional co-culture system.[136] Some of the microfluidic co-culture systems created are targeted to specific applications, such as macrophage-osteoblast interaction[137] or bacterial cancer targeting.[138] It is very common that an actuating component, such as a syringe pump, is needed to control the barriers between distinct compartments for different cell types, which however makes the overall system bulky, and the operation complicated. Moreover, if two different substrates, such as polydimethylsiloxane (PDMS) and polystyrene, are used together for cell culture, the cell behaviour may vary due to different substrate properties. Therefore it is necessary to develop a model that is easy to manipulate, compact in size, and has uniform and controllable material property.

In this chapter, a simple method to create a planar co-culture system using a PDMS chip without any actuating component has been discussed. A scotch tape was used for selective surface treatment to create distinct hydrophilic and hydrophobic PDMS compartments, and hence fluid flow could be confined locally. Two types of cell models (HS5 and HuH7) were cultured in distinct hydrophilic compartments, while the hydrophobic compartment served as a barrier in between. Once both cell types reached confluence, the barrier was removed easily by introducing liquid into it thereby creating a co-culture region for cell migration and interaction. These two particular cell types were chosen for a proof-of-concept study on tumor-stromal interactions, which is of great interest and significance in cancer metastasis and subsequent survival of metastasized tumor cells. [139] The substrate hydrophobicity was characterized and various biochemical assays, such as micro BCA assay for adsorbed protein quantification, Prestoblue cell viability assay, and Cyquant cell proliferation assay for cell adhesion quantification, were carried out to evaluate the effect of this co-culture system.

3.2 Materials and methods

3.2.1 Chip fabrication

The microfluidic chip fabrication is a modified version of the process explained previously in section 2.2.1. In brief, the SU8 mold was created first using photolithography approach following which PDMS was prepared at a ratio of 10:1 (elastomer to curing agent) by weight and poured over the mold and cured at 70°C for 2 h. The PDMS slab is cut out from the mold and sealed. In this experiment, a cover slip coated with PDMS is used instead of a plain cover slip. To coat the cover slip with

PDMS, approximately 20 mg of the mixed PDMS (after mixing elastomer to curing agent) was poured on to a 22 mm×22 mm cover slip and was spin coated at 2000 rpm for 60 s following which the cover slip was heated to 70°C for 2 h for the PDMS to cure.

3.2.2 Fake channel

Apart from the many advantages of PDMS as stated above, one of the major disadvantages include poor affinity of native PDMS for living cell culture due to its strong hydrophobicity.[140] It is thus vital to modify the surface properties of PDMS so as to favor liquid perfusion and enhanced cell adhesion.[141] There are many ways of surface treatment on PDMS,[142] among which oxygen or the above mentioned air plasma is the easiest and most commonly used method.[107] On exposure to plasma, silanol bonds are formed on surface of PDMS, improving its wettability. Although plasma treatment renders the entire surface hydrophilic, it is also handy to have localized hydrophilicity of PDMS such that specific regions can be functionalized separately. In the literature, much effort has been directed towards localized plasma treatment, such as using water mask [143] or microplasma generation using high-precision electrode and AC excitation. [144] However, these methods involve nontrivial procedures and expensive materials. An economic solution was proposed [145] using a PDMS slab as a stencil to selectively pattern the protein-repelling polymeric network by plasma etching, allowing for modifying surface chemistry to enhance cell attachment. In addition, if a hydrophilic microchannel is peripherally sealed, it can be easily primed with liquid driven by capillary force. However, if the channel is not sealed peripherally, such as in an open burrow, the liquid can hardly fill the channel owing to the surface tension. This unique phenomena inspired us to form temporary or fake channels in this study to selectively change the local surface property of the PDMS channel.

We used Scotch tape (3M, MN, USA), rather than a PDMS slab, as a stencil to mask specific locations on the chip to prevent them from plasma treatment, and to create a temporary channel for biochemical functionalization through liquid perfusion. The detailed procedure is illustrated in Figure 3.1. Briefly, both side channels were coated with 0.1% gelatin (Type B from bovine skin, Sigma-Aldrich, Singapore). This enhanced the wettability of PDMS. After 24 h, it was observed that the gelatin coated PDMS regions maintained their wettability [146], while the central channel did not, owing to the ability of PDMS to undergo hydrophobic recovery with time. [147] This led to the creation of hydrophilic side channels and hydrophobic central channels.

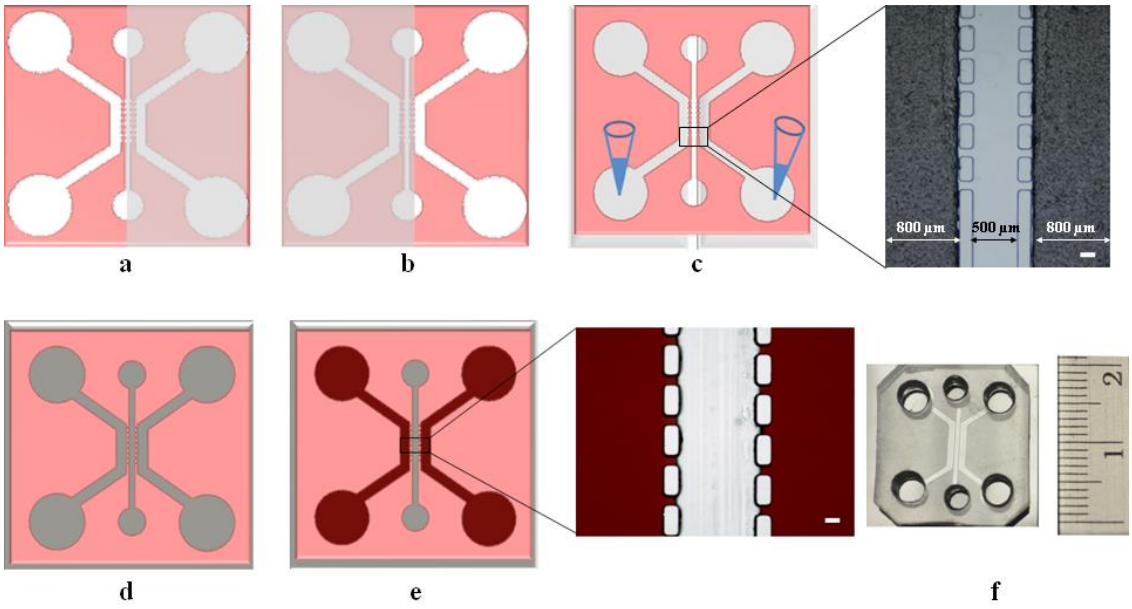

Figure 3.1: Microfluidic chip preparation. (a) Step 1: a Scotch tape is used as a stencil to cover the central channel and a side channel on the right; only the side channel on the left is plasma treated. (b) Step 2: a Scotch tape covers the central channel and the side channel on the left; only the side channel on the right is plasma treated. (c) Step 3: temporary channels are formed by covering both side channels with Scotch tapes. Inset shows a microscopic image of the tape covering the plasma treated side channels. Gelatin is introduced in both side channels and coated these channels to enhance surface wettability. Scale bar: 100 µm. (d) Step 4: a completely sealed chip is assembled by plasma treating and bonding: the surface treated (in steps 1-3) PDMS replica and a PDMS-coated glass cover slip. (e) Step 5: the entire chip is dried in the air and the central channel recovers its hydrophobicity after 24 h, while the side channels remain hydrophilic because of the gelatin coating. Inset shows the microscopic image of the side channels filled with red dye solution, while the liquid does not overflow into the central channel owing to the surface tension. Scale bar: 100 µm. (f) The final microfluidic co-culture chip ready for use.

3.2.3 Contact angle measurement

An optical tensiometer (Attension Theta, Sweden) was used to measure the contact angle of water droplet on PDMS substrate, which gives a quantitative characterization of the surface wettability under various conditions.

3.2.4 Protein coating

Fibronectin (20µg/ml) was used to coat the PDMS surface as explained in section 2.2.2 to enhance the surface biocompatibility towards cell culture.

3.2.5 Cell culture

In this study two different cell types of human bone marrow stromal cell line, HS5 (ATCC, USA) and human hepatocarcinoma cell line, HuH7, were used as the models for the co-culture system. The cells were re-suspended and introduced into the chip as explained earlier in section 2.2.2.

3.2.6 Protein retention assay

Micro BCA assay (Life Technologies, Singapore) was used to measure the concentration of fibronectin retained on the surface of PDMS. The measurement was performed as explained in section 2.2.9.

3.2.7 Cell adhesion

Cell adhesion was determined using CyQUANT® cell proliferation assay (Life Technologies, Singapore) to characterize the cell adhesion on the modified PDMS surface in a 4-well plate. The procedure is as described earlier in section 2.2.5.

3.2.8 Cell viability

Apart from cell adhesion, cell viability over extended time periods is significant as both these factors help in the understanding of compatibility of the substrate towards cell culture. The quantification was done using the Prestoblue cell viability reagent (Life technologies, Singapore) as described earlier in section 2.2.4.

3.2.9 Fluorescence imaging

The cells were fixed using formalin (Sigma-Aldrich, Singapore), stained with TRITC conjugated phalloidin (Life technologies, Singapore) for the cytoskeleton and 4',6-diamidino-2-phenylindole (DAPI) (Life technologies, Singapore) for the cell nuclei. Cell imaging was under a fluorescence microscope (IX71, Olympus, Singapore).

3.2.10 Reactive Oxygen Species

Reactive oxygen species (ROS) generated within the cells were measured using CM-H2DCFDA assay (Life Technologies, Singapore). HS5, HuH7 and a mixture of HS5 and HUH7 cells were seeded into a 96 well plate. Prior to the final batch of experiments, optimization was performed to find out the most suitable concentration of the dye as well as the incubation time. Four different concentrations (1 µM, 2 µM, 4 µM, 7.5 µM) in 1X PBS of the assay was used and three different incubation times were checked (10 min, 20 min and 30 min). It was observed that the 2 µM for 20 min was good for the two cell types used here. Hence 2µM of CM-H2DCFDA in 1X PBS was incubated with the cells after 24 hours, for 20 minutes prior to fluorescence imaging. The fluorescence intensity was calculated using the ImageJ software.(National Institute of Health, USA). The assay was performed for up to 5 days to obtain a relative increase in the ROS generation.

3.2.11 Live-Dead cell imaging

Live-dead cell staining was performed to get a qualitative estimation of the live and dead cells within the microfluidic chip. Fluorescein Diacetate (FDA) (Sigma-Aldrich, Singapore) and ethidium homodimer (EthD-1) (Life Technologies, Singapore) were used to stain the live and the dead cells respectively, prior to the fluorescence imaging.

3.3 Results and discussion

Native PDMS is hydrophobic and thus is not amicable for cell culture. Plasma treatment and protein coating can reduce the hydrophobicity and promote cell growth. In this study, development of the co-culture system primarily depends on the ability of PDMS to recover its hydrophobicity so that different cells can be confined in different compartments on the same chip. We noticed that hydrophobic recovery of PDMS depended on both temperature and time. Generally, the hydrophobic recovery becomes faster when the temperature increases. However, temperature elevation has an adverse effect on the protein retention on PDMS surface. Furthermore, over-recovered hydrophobicity would hinder the fluid flow in the microchannels to open the co-culture region. To address these issues, we applied techniques, including selective plasma treatment of gelatin coating and double coating of fibronectin, to delicately modify the wettability and enhance cell growth in the channels.

The surface wettability was measured for native and plasma-treated PDMS coated with fibronectin, gelatin, and gelatin + fibronectin combination, respectively. In Figure 3.2a, native PDMS showed very large contact angle (~ 120^o) indicating its poor wettability. For other samples, the contact angles were measured 24 h after surface treatment. The results indicated that although fibronectin reduced the contact angle, the PDMS surface was still in the hydrophobic range (>90^o); whereas for gelatin and gelatin + fibronectin coated PDMS samples, the contact angles are much smaller showing excellent wettability. In addition, the gelatin coating helped maintain the substrate wettability for at least 24 h, by when plasma-treated PDMS would have recovered its hydrophobicity. These results imply that by controlling the area of gelatin coating, distinct hydrophilic and hydrophobic regions could be created on a single substrate.

The PDMS was coated with fibronectin for 1 h and the protein retained on the surface was quantified by micro BCA assay. The absorbed fibronectin immediately after surface coating was approximately 3 μg/ cm^2 [Figure 3.2b]. As discussed earlier, in order

to create a hydrophobic barrier between different compartments for initial cell culture, the fibronectin-coated PDMS needs to be subjected to elevated temperature much higher than room temperature for rapid hydrophobic recovery. Therefore we studied the temperature effect on the protein retention. The fibronectin-coated PDMS samples were subjected to 25ºC, 37ºC and 75ºC for 24 h, respectively, followed by micro BCA assays. It was found that the protein retention decreased drastically in 24 h to almost zero when the temperature rose to 75ºC [Figure 3.2b]. The significant decay of fibronectin adsorption could be due to the protein denaturing under the high temperature in the test. To address this issue, we performed a second coating of fibronectin (20 µg/ml) after 24 h. It could be observed that double coating of fibronectin resulted in an increase of protein retention by at least 3 folds to about 10 µg / cm^2 irrespective of the temperature change [Figure 3.2b].

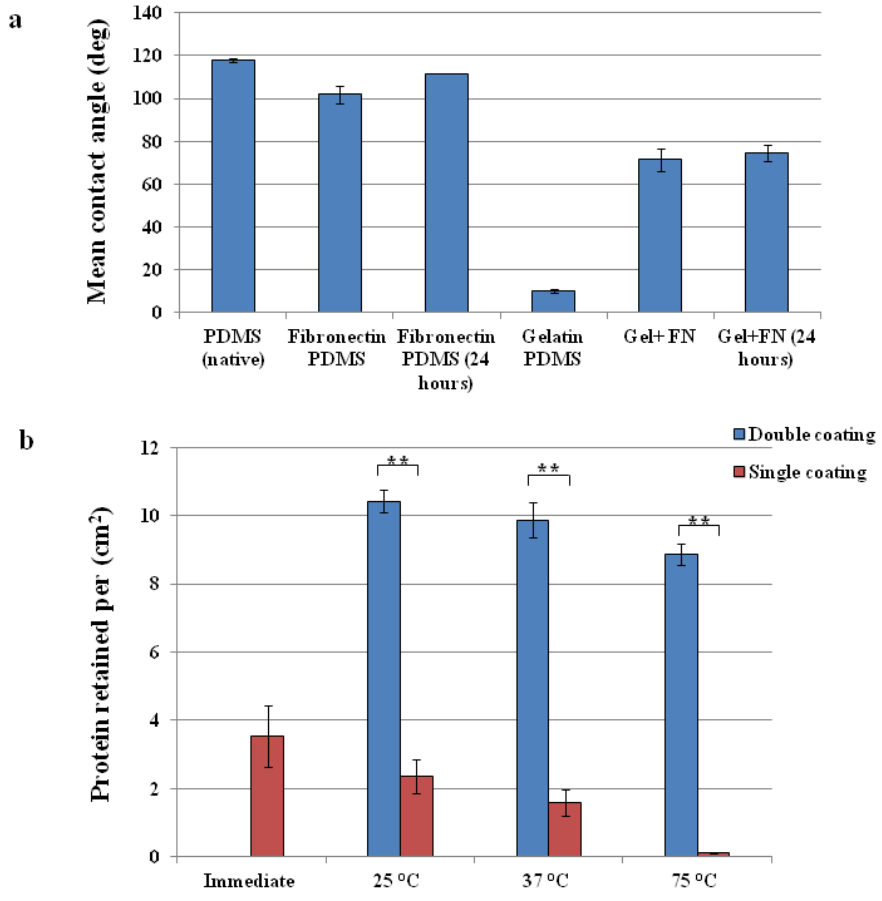

Figure 3.2: (a) Contact angle measurement of different surface-treated PDMS taken immediately and after 24 h. Statistical analysis was performed using one way ANOVA. p<0.001. (b) Micro-BCA analysis of protein retention immediately after fibronectin coating and after hydrophobic recovery (24h) under different temperatures. **p<0.005.

The impact of double coating of fibronectin on cell adhesion and viability was also studied using HS5 stromal cells. Cell adhesion on different samples was measured with respect to those on a tissue culture plate (TCP) [Figure 3.3a]. The native PDMS

without protein coating exhibited very poor biocompatibility with minimal cell adhesion. Whereas the protein-coated PDMS could support decent level of cell adhesion compared with TCP. The Prestoblue cell viability assay at day 1, day 3 and day 5 further verified the promotional effect of double protein coating on long-term cell culture. It was observed that the cell viability at day 5 was improved significantly on all PDMS surfaces with double fibronectin coating compared to those with single fibronectin coating [Figure 3.3b]. These results indicated that double coating of fibronectin on PDMS facilitated both cell adhesion and proliferation in a long term.

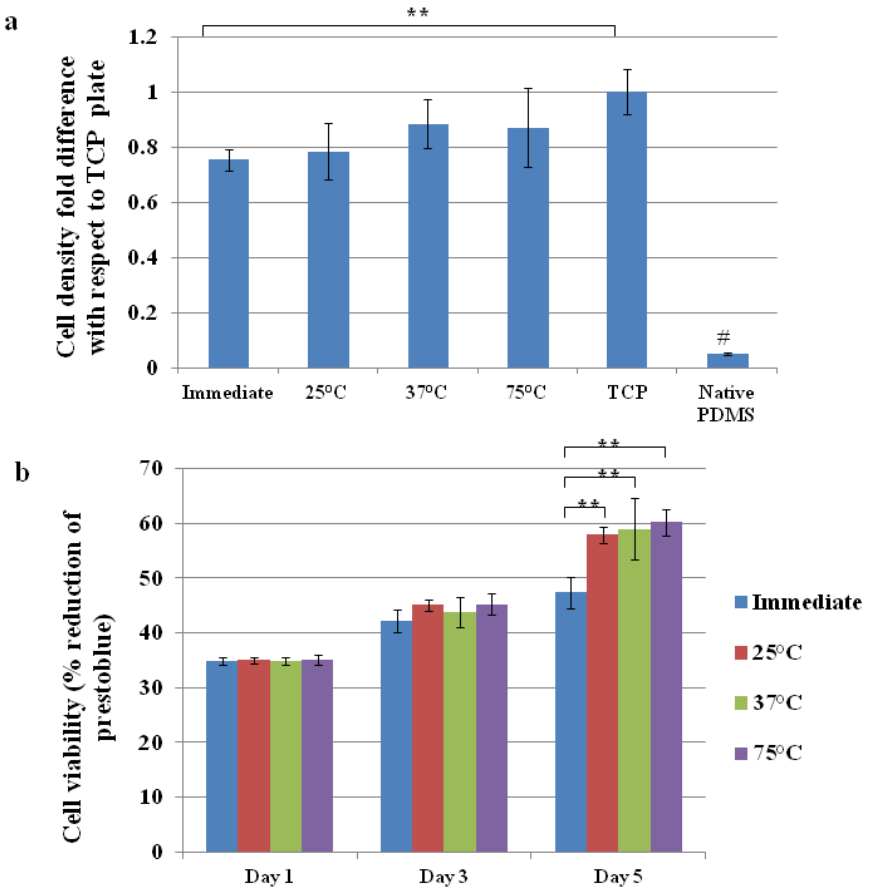

Figure 3.3: Characterization of the surface biocompatibility after fibronectin coating using HS5 stromal cells: (a) Cell adhesion. The shaded bars represent the surfaces with double fibronectin coating (b) Cell viability. Immediate refers to the samples on which cells were seeded soon after fibronectin coating. A second coating of fibronectin was performed in all other samples (before cell seeding) after incubation for 24 h under respective temperatures. (p<0.005; #p<0.001)**

As a demonstration of co-culture on this microfluidic device, HS5 and HuH7 cells were cultured respectively in distinct micro-compartments for 24 h. The cell culture medium was introduced into the central channel by applying a gentle pressure using a micropipette. This procedure removed the hydrophobic barrier and created a co-culture

region for cell interaction. The cells were cultured on the chip for up to 9 days. It was observed that highly mobile HS5 cells migrated towards HuH7 cells initially [Figure 3.4 (a-d)]. However, when the tumor cells reached confluence, they started to migrate in batches toward stromal cells [Figure 3.4 (e-f)]. After physical interaction between these two cell lines, tumor cells became more aggressive and proliferative resulting in significant death and density drop of stromal cells after day 6. A close-up view using fluorescence microscopy [Figure 3.4 (g-h)] further revealed that tumor cells generated membrane protrusions toward stromal cells during physical contact. Similar phenomenon was reported previously in a conventional co-culture system, in which the physical contact through membrane protrusion with stromal cells stimulated the papillary thyroid tumor cells and transformed moderately carcinogenic cells to highly aggressive metastatic cells.[148] These membrane protrusions are also called tunneling nanotubes (TNTs), which could serve as an intercellular channel for tumor cells to obtain the cytoplasm including mitochondria or other cellular organelles from other tissue cells and upregulate the tumor proliferation. [148-149] Moreoever in a study by Bai et al. it was observed that HS5 cells increased the proliferation, migration and invasion of Huh7 cells. [139] These results from a mice model matches with my the observation in this study.

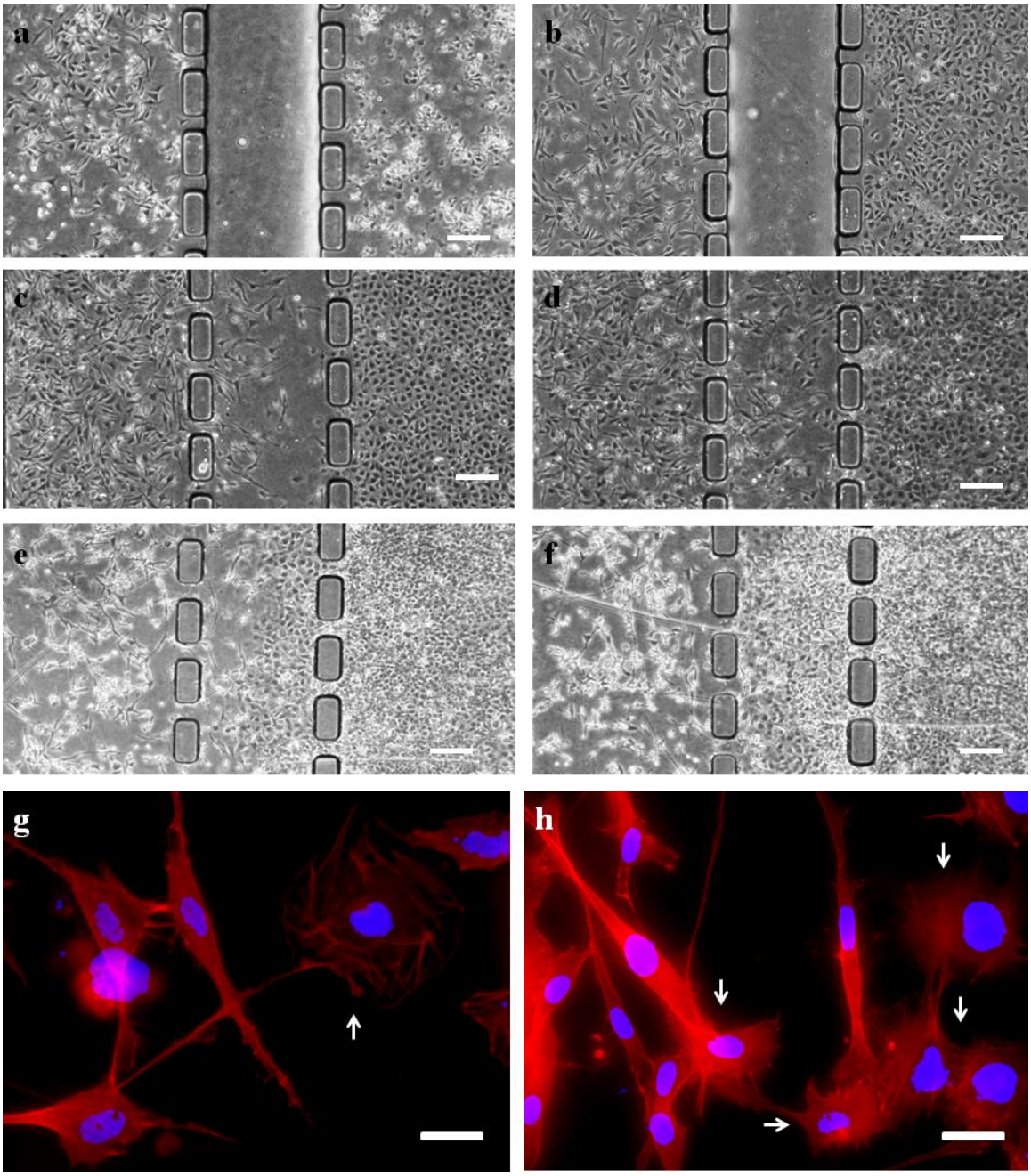

Figure 3.4: (a-f) Phase contrast images of co-culture chip taken after 2 h, and 1, 3, 5, 7 and 9 days after cell seeding. HS5 cells in the left compartment and HuH7 cells in the right. The barrier (empty channel in a and b) between the two compartments was removed after 24 h. By the 9th day, the tumor cells had occupied the central channel and the stromal cells had retreated into its own compartment and many dead stromal cells were observed. (Scale bar: 200 µm). (g-h) Fluorescence images showed the interaction between stromal cells and tumor cells. The red color is the actin filament stain and the blue color is the nucleus. The arrows indicate the tumor cells. (Scale bar: 20 µm).

It has also been reported that direct contact of tumor cells with endothelial cells results in generation of reactive oxygen species (ROS) that causes oxidation of cell membrane and DNA breakdown of the endothelial cells.[135, 150] ROS generated by the cells was quantitatively determined using the CM-H2DCFDA assay. HS5, HUH7 and a co-

culture of HS5 and HUH7 were seeded in a 96 well plate and the assay was performed on day 1, day 3 and day 5 after the initial seeding. Figure 3.5e indicates the fluorescence intensity measured in the different samples. Higher the fluorescence intensity, greater the ROS generated and it may be observed that on day 5, the ROS increase in the co-culture system seems to be approximately four times more than the mono-culture system. There are reported evidence indicating that increased ROS concentration is able to assist in tumor invasion and progression. [151-152] The area of migration of the tumor cells [figure 3.5 (a-d)] was determined by drawing contours at the leading edge and the quantification was performed using ImageJ software by calculating the area of the contours [Figure 3.5f]. It could be observed that the tumor migration increased swiftly after day 6 which is a possible consequence of an increase in ROS concentration. Live-dead cell imaging using FDA and EthD-1 [Figure 3.5 (h-j)] showed an increased cell death amongst the HS5 cells as compared to the control. This could be because of the tumor induced apoptosis as a result of paracrine signaling of ROS released by the tumor cells, normally to control the homeostasis of the local environment.[135, 150, 153] It was observed by comparing figure 3.5i and figure 3.5j that the tumor cell migration in its mono-culture is slower than in its co-culture system. This could be due to the reduced levels of ROS produced by them while in mono-culture [Figure 3.5e].

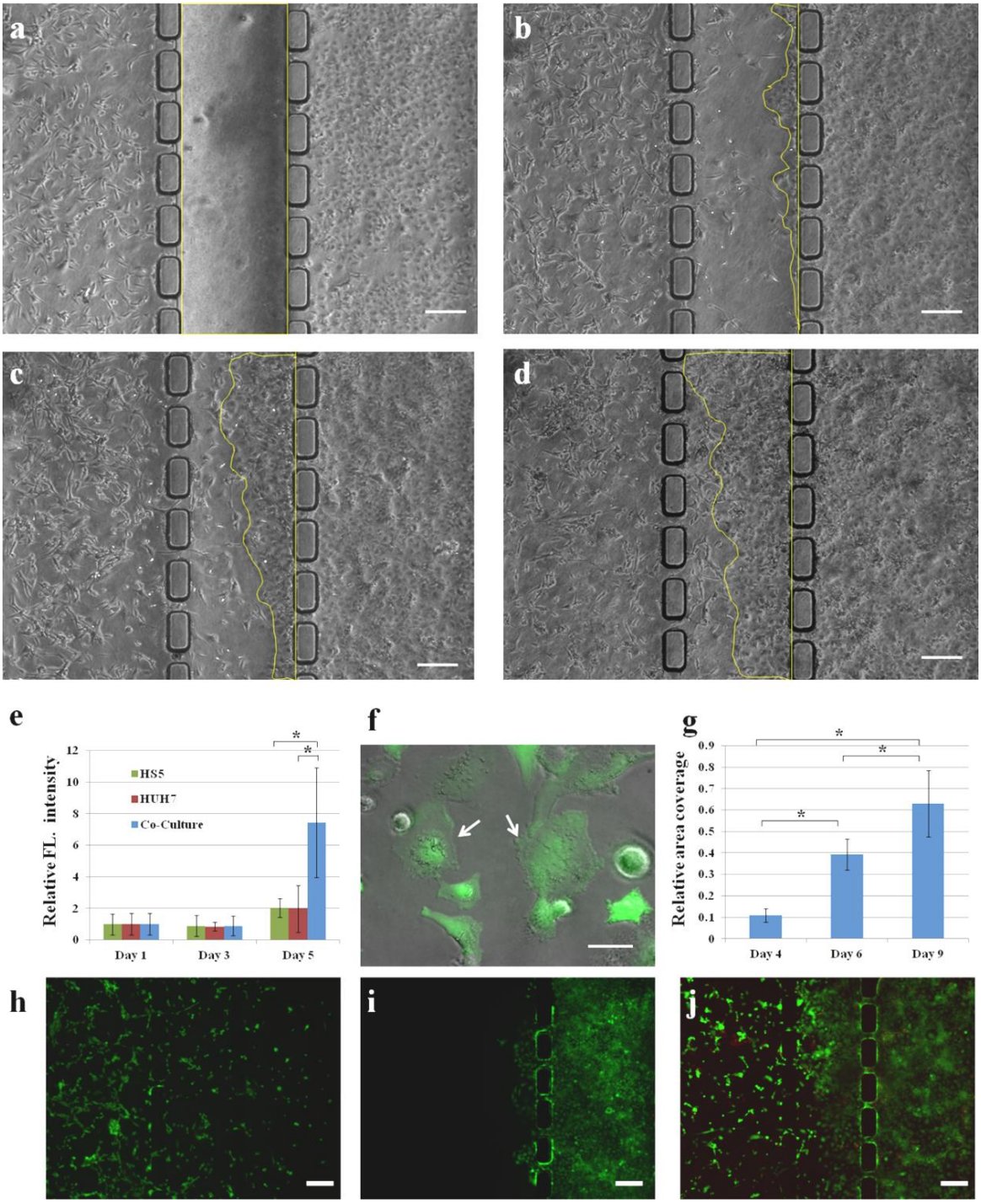

Figure 3.5: (a-d) Tumor cell migration. The change of area coverage by HuH7 cells up to day 9. (a) Day 2 after cell seeding. The yellow box indicates the total area of the central channel, which was used as gauge for normalization. (b-d) The areas covered by HuH7 cells on day 4, day 6 and day 9 respectively. e) The relative fluorescence intensity with respect to day 1 sample. The ROS generated by the cells seems to increase in day 5 with the co-culture system showing an increase of approximately four folds with respect to the cells in mono-culture. f) Fluorescence image overlaid on a phase contrast image of the co-culture of HS5 and HuH7 stained with CM-H2DCFDA for ROS determination. Arrows indicates the HuH7 cells. Scale bar: 20µm . g) Area covered by HuH7 cells with respect to the total area over a period of 6 days. h) Live-dead cell imaging of the HS5 cells mono-culture on-chip. i) Live-dead cell imaging of the HuH7 cells mono-culture on-chip. j) Live-dead cell imaging of the HS5 and HuH7 cell co-culture on-chip. Scale bar: 200 µm. *p<0.05

3.4 Summary

A very simple method was applied in this study to create a microfluidic co-culture model for *in vitro* cell-cell interaction study. A Scotch tape was utilized as a stencil for selective plasma treatment on a chip followed by surface coating with gelatin to render distinct hydrophobic and hydrophilic microchannels on the same chip. The fibronectin coating enhanced cell viability on PDMS surface. As a proof-of-concept study, stromal cells (HS5) and tumor cells (HuH7) were co-cultured on this microfluidic chip and cell migration and interaction were observed. These observations matched results reported in literature for *in vivo* models, thereby validating the functionality of the model as an effective tool for *in vitro* studies. Moreover this chip has fulfilled some key requirements as an effective co-culture system:[132] the ability to load cells into different compartments so that they can grow till they reach confluence; the ability to manipulate one cell type in the co-culture model without affecting the other cell type[58]; and also the model could allow for high-resolution imaging. Apart from these requirements, the model was highly reproducible and we have used this model to develop different *in vitro* models as discussed in the following chapters.

3.5 Declaration

A part of this chapter has already been published. Menon, N. V.; Chuah, Y. J.; Cao, B.; Lim, M.; Kang, Y. A microfluidic co-culture system to monitor tumor-stromal interactions on a chip. *Biomicrofluidics* **2014,** *8,* 064118-1-11.

Chapter 4 Cell substrate interaction

4.1 Background

The microfluidic *in* vitro model has also been applied to perform studies pertaining to the interaction between the cell and its substrate. In this chapter the influence of the physical properties of the substrate on the migration of mesenchymal stem cells (MSCs) has been observed. The purpose of such a study was because, MSC migration is significant in regenerative medicine especially ion scaffold based tissue regeneration.

Regenerative medicine involves the repair and regeneration of impaired tissues or organs due to an injury or a disease. Stem cell mediated tissue regeneration, especially for bone and cartilage repair, [154-156] has been extensively studied in the last decade due to its multi-potent therapeutic capability. The stem cells are usually introduced either as cell suspensions [157] or are homed in biodegradable scaffolds and implanted at the site of injury. [156, 158] For the latter technique, the scaffold is critical since they significantly influence the formation of extra-cellular matrix (ECM) of the regenerated tissues. The effects of ECM on cell behaviours such as viability, spreading, migration, intercellular communication and differentiation have been discussed extensively in the literature. [159-161].

Among these cell behaviours, cell migration is of particular interest and plays a vital role in many important physiological processes, such as embryogenesis, disease progression, wound healing and tissue regeneration.[162] The ECM comprises cell-secreted proteins and other biomolecules, providing physical and chemical framework and cues to the surrounding cells. The physical cues are induced by the inherent physical properties of the scaffold, including topography, stiffness, hydrophobicity, as well as other properties exhibited at the cell-scaffold interface. The chemical cues involve the biomolecular composition of the ECM, such as surface-bound ligands, adhesion proteins and chemoattractant gradient, which will activate the biochemical receptors on the cell membrane and direct their locomotion. Although these complex biophysical and biochemical cues usually work in coordination to guide the cell migration and tissue development,[162-163] recent advances in micro- and nanotechnologies have made it possible to explore the effects solely due to a single or multiple physical cues.[164-166] In scaffold-based tissue regeneration using stem cells, it is important for the cells to migrate to the site of injury, proliferate and differentiate into the desired tissues. Considering the potential toxicity of introducing artificial biochemical factors, it becomes particularly

attractive to induce and modulate cell migration by controlling the physical or mechanical properties of the biocompatible scaffold to achieve effective therapeutics. [167-168]

Conventionally, cell migration was studied using scratch assay[4] or Boyden's chamber.[169] Recently, microfluidics-based lab-on-a-chip technology has found extensive applications in many exploratory cell researches *in vitro*.[14-15] The major advantages of lab-on-a-chip devices over the conventional cell-based assays include significantly reduced sample and reagent consumption, high sensitivity, and rapid speed of assay. Some microfluidic devices are able to precisely control fluid flow and generate chemical gradient in microscale,[170-171] which is extremely difficult in the conventional migration assays such as using Boyden's chamber. A large variety of microfluidic *in vitro* models have been created and proved to be much more advantageous than conventional *in vitro* models.[55] Polydimethylsiloxane (PDMS) is a common molding material for fabricating high-resolution micro- and nano-structures in lab-on-a-chip devices owing to its chemical inertness, biocompatibility,[106] permeability to gases,[30] and optical transparency. Moreover, the surface properties of PDMS, such as stiffness, roughness and hydrophobicity, can be easily tuned by adjusting the mixing ratio of the prepolymer to the crosslinker. These features have made PDMS a capable tool to study the impact of different substrate physical properties on cell behaviours.[172-174]

Previously, the individual effects of surface property on cell migration have been studied extensively. It was shown that hydrophobic surfaces (contact angle = 98.5°±2.3°) improved endothelial cell migration as compared to hydrophilic surfaces (contact angle < 90°).[175] Moreover, the collective migration of HuH7 cancer cells was favoured on a PDMS surface with RMS roughness of 2 nm as compared to those with RMS roughness of 60 nm.[165] Additionally, the NIH 3T3 cells were observed to migrate from a softer surface towards a stiffer surface owing to the lower cell traction force required on the softer substrate, which also resulted in a faster migration rate on the softer substrates.[176] More relevant studies reported similar phenomenon that the collective migration of fibroblast and epithelial cells was promoted on substrates with lower rigidity, suggesting the weaker integrin-cytoskeleton linkages[163] and hence dynamic cell adhesion on less rigid surfaces.[177] Further studies indicated that for a specific surface ligand density, there existed an optimal substrate rigidity at which cell migration reached maximum level.[2, 178-180] As shown in these early investigations, variation of a single aspect of the surface property could affect cell migration profoundly. On the other hand, for many common

materials, the alteration of one particular substrate property may cause the change of others. For example, the stiffness of PDMS substrate can be changed by adjusting the mixing ratio of prepolymer base to the crosslinker,[181] which alters the surface roughness as well as hydrophobicity. However, these multiple aspects of substratum properties, including hydrophobicity, roughness and stiffness, and their combinatorial influence on cell migration remain to be elucidated.

In this work, we aim to understand the combinatorial impact of the PDMS substrate properties on the migration of human bone marrow stem cells (hBMSCs). hBMSC migration is a vital process during scaffold-based stem cell therapy, where the homing cells from the scaffold migrate towards the damaged tissue and eventually differentiate into specific tissues.[156] It is important to understand the optimal physical cues that would allow for improved hBMSC migration to optimize the therapeutic effect. In this proof-of-concept study, the microfluidic *in vitro* model developed earlier has been used as a migration assay using different PDMS substrates formulated with various levels of crosslinking. Cell adhesion and proliferation are firstly measured to characterize the biocompatibility of the substrate, following which the cell spreading and migration in the microfluidic chip are compared to elucidate the combinatorial impact of the substratum physical properties.

4.2 Materials and methods

4.2.1 Microfluidic chip preparation

The microfluidic chip fabrication is a modified version of process explained previously in section 2.2.1. In brief, the SU8 mold was created first using photolithography approach following which PDMS was prepared at a ratio of 10:1 (elastomer to curing agent) by weight and poured over the mold and cured at 70°C for 2 h. The PDMS slab is cut out from the mold and sealed. In this experiment, a cover slip coated with PDMS is used instead of a plain cover slip. To coat the cover slip with PDMS, approximately 20 mg of the mixed of different base to curing agent ratio (5:1, 10:1, 20:1 and 40:1) were spin-coated on glass cover slips (22 mm × 22 mm) and cured at 70°C for 3 h to create the substrates with different physical properties. The surfaces of the PDMS chips and substrates were activated using a plasma cleaner (Harrick Plasma, NY, USA) before they were bonded together. The sealed chip was further processed for cell culture following the procedures as described previously in sections 2.2.2 and 3.2.2

[Figure 3.1]. Briefly, all three compartments inside the chip were coated with 20 µg/ml fibronectin for 1 h at 37°C followed by washing with 1X PBS and drying at 40°C for 24 h. A second layer of fibronectin was coated on two side-compartments only to enhance cell attachment and proliferation.

4.2.2 Surface characterization

The surface roughness, stiffness and hydrophobicity of the PDMS substrates coated with fibronectin were characterized using the following methods. An optical tensiometer (Attension Theta, Sweden) was used to measure the surface hydrophobicity by characterizing the water contact angle. 5 µl of milli-Q water was dropped on the sample surface and the profile of the water droplet was captured using a high resolution camera. The water contact angle was calculated by the drop shape analysis software using the static sessile drop tangent method.

The surface roughness and stiffness of the PDMS substrates were determined by atomic force microscopy (AFM, MFP-3D, Asylum Research, CA, USA). The details of the probes have already been discussed in section 2.2.11. The values of roughness and stiffness were measured from 5 values taken at 5 different points of contact.

4.2.3 Mesenchymal stem cell culture and seeding

Human bone marrow mesenchymal stem cell (hBMSC) was cultured on-chip for this study. The cells were re-suspended and introduced into the chip as explained earlier in section 2.2.2.

4.2.4 Cell proliferation and cell adhesion

Equal amounts of PDMS of different crosslinking ratio are coated in different four well plates following which the cells are cultured on them. Cell proliferation and cell adhesion were quantified by the methods as stated earlier in sections 2.2.4 and 2.2.5 respectively.

4.2.5 Surface protein density

The density of fibronectin coated on the PDMS substrates was determined using micro-BCA protein assay (Thermo Scientific, Singapore) as stated in section 2.2.9. The different PDMS substrates were coated with 20 µg/ml fibronectin for 1 h at 37°C. The samples were then washed thrice with 1X PBS and placed in a drying oven at 40°C for 24

h. The substrate protein density was then measured at 562 nm using a microplate reader (Infinite M200 Pro, Tecan Asia, Singapore).

4.2.6 Cell spreading and migration

To investigate the influence of substratum property on cell spreading and migration, hBMSCs were cultured and monitored in microfluidic chips sealed onto cover slips that were pre-coated with PDMS of different crosslinking levels. The cells were initially cultured in two side-compartments in this 3-chamber microfluidic chip [Figure 4.1], while the central compartment was empty without any culture medium. After overnight culture, medium was introduced to the central compartment hence connecting both side-compartments and allowing for the cells to migrate into the centre of the chip. At the end of Day 7, the cells were stained with DAPI (for nucleus) and TRITC conjugated phalloidin (for F-actin cytoskeleton). The cytoskeleton staining allowed for measuring the spreading area of individual cells. The collective cell migration was quantified by two methods: the nucleus staining enabled cell number counting in the central channel, while the cytoskeleton staining could help measure the entire area covered by all migrating cells in the central compartment. Briefly, the cells were fixed with 10% formalin (Sigma-Aldrich, Singapore) overnight, following which they were washed with 1X PBS thrice and stained with TRITC conjugated phalloidin and DAPI as per the manufacturer's instructions. Both dyes were purchased from Life Technologies, Singapore. The cell images were taken using a fluorescence microscope (IX71, Olympus, Singapore). The areas covered by individual cells and the cell population in the central compartment were analyzed using Image-Pro Plus (Media Cybernetics, Rockville, MD, USA).

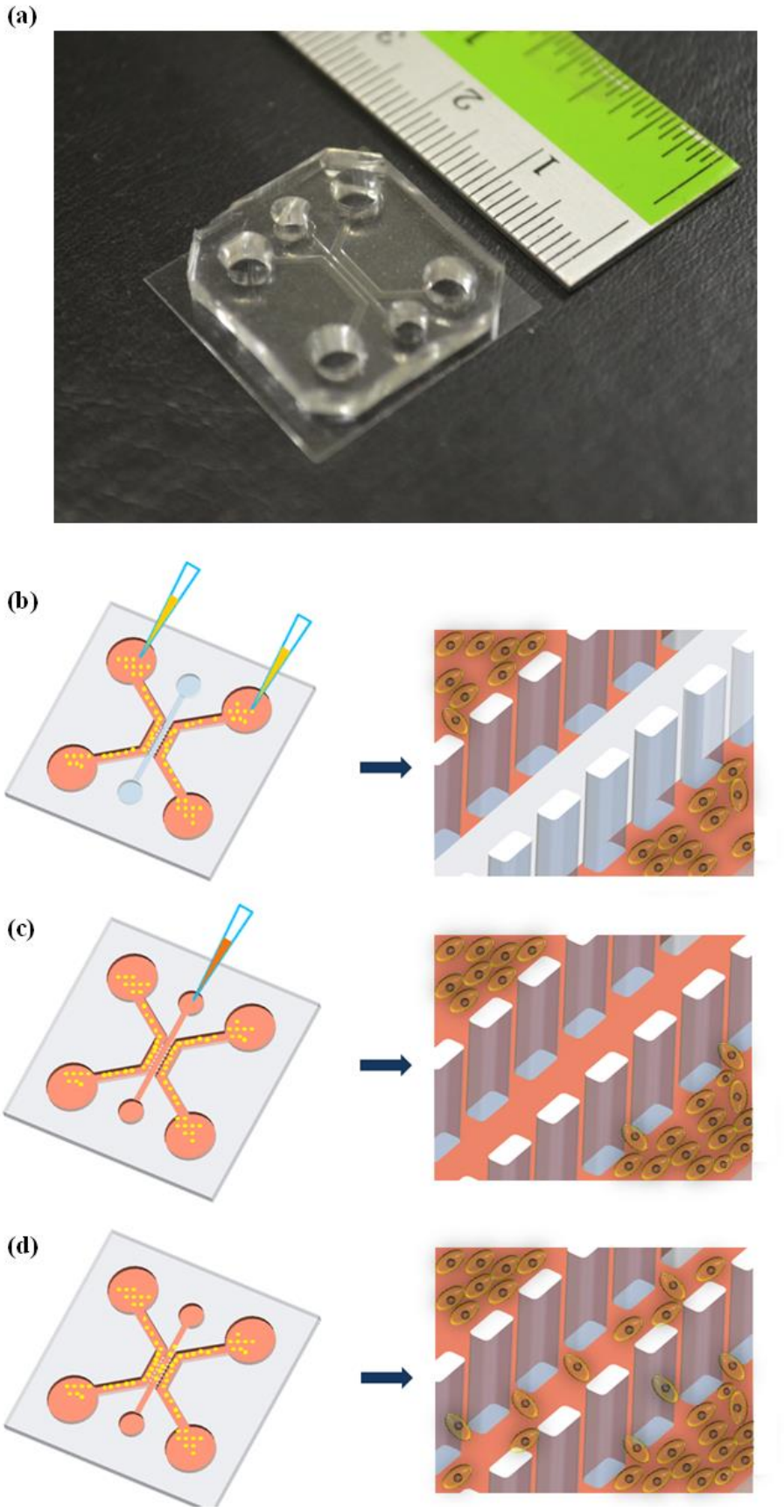

Figure 4.1: (a) The microfluidic chip design. (b) Schematic of cell seeding from the side compartments. (c) 24 h after cell seeding, cell culture medium was introduced into the central channel to allow the BMSCs to migrate into the central compartment. (d) Cell migration into the central compartment.

4.2.7 Quantitative real time polymerase chain reaction (qRT PCR)

In order to understand the effects of different PDMS substrates on the hBMSC migration, the gene expressions of cellular adhesion proteins that may influence cell migration, including, paxillin and N-cadherin,[182-183] were quantified using qRT-PCR (StepOne Plus™, Life Technologies, Singapore). Briefly, cells were seeded in 4-well plates containing different PDMS substrates pre-coated with fibronectin. After 5 days of culture, the total cellular RNA was extracted using RNeasy® Mini Kit 250 (Qiagen, Singapore). Approximately 100 ng RNA of each sample was reverse-transcribed into complementary DNA (cDNA) using iScript™ Reverse Transcriptase Supermix (Bio-Rad, Singapore). Quantitative real time PCR assays of the target genes were performed using StepOne Plus™ on a 96-well optical reaction plate (Bio-Rad, USA). Each well contained a mixture of 10 µl Power SYBR green PCR master mix (Life Technologies, Singapore), 0.24 µl forward primer and the reverse primer, and 10 µl of the reverse transcribed cDNA. The sequence of the primers is listed in Table 4.1. All primers were purchased from IDT, Singapore. The gene expression were normalized to GAPDH mRNA level in the corresponding samples and then to the expression level of the targeted gene in PDMS substrate with mixing ratio of 5:1.

Target gene	Reverse primer	Forward primer
Paxillin	5'-GGCTGCACTGCTGAAATATGAGGAAG-3';	5'-AAACCCGACTGAAACTGGAACCCT-3'
N-cadherin	5'-CAGCCTGAGCACGAAGAGTG-3'	5'-AGCTCCATTCCGACTTAGACA-3'
Ki-67	5'-TTACTACATCTGCCCATGA-3'	5'-ACTTGCCTCCTAATACGCC-3'
GAPDH	5'-TAAAAGCAGCCCTGGTGACC-3'	5'-ATGGGGAAGGTGAAGGTCG-3'

Table 4-1: Genes and the corresponding forward primer sequence used for qRT-PCR.

4.2.8 Statistical analysis

Student's t-test was used for the statistical analysis of all experimental results. A p-value of less than 0.05 ($p^*<0.05$, $n \geq 3$) was considered to be statistically significant.

4.3 Results and discussion

In this study, four different mixing ratios (5:1, 10:1, 20:1 and 40:1) of PDMS was used to change its level of cross linking and hence its surface properties. The AFM characterization illustrated the surface topography [Figure 4.2 (a-d)] of the PDMS substrates and the root-mean-square (RMS) roughness increased as the mixing ratio changed from 5:1 (0.96±0.17 nm) to 40:1 (24.83±0.76 nm) [Figure 4.2e]. The highest proportion of curing agent (5:1) rendered the smoothest PDMS surface [Figure 4.2a] due to higher level of crosslinking density. The water contact angle measurement revealed that the PDMS surface became more hydrophobic by increasing the base to crosslinker ratio [Figure 4.2f], which could be due to two important effects. Firstly, the hydrophobic methyl groups present in the prepolymer increases with the base proportion thus reducing the surface wettability.[184-185] Secondly, the increased surface nano-roughness can further reduce the wettability due to the formation of air pockets between the nano-ridges.[186-187] In addition, the surface stiffness has been suggested to be more relevant to cell-substrate interactions compared to bulk elastic modulus of the substrate material.[188] Therefore, we used AFM indentation method to measure the compressive modulus of the treated PDMS surface. It was observed that the PDMS surface stiffness decreased from 70.44±9.166 kPa to 13.8±2.315 kPa when increasing the polymer base proportion, which was corresponding to a lower level of crosslinking [Figure 4.2g].

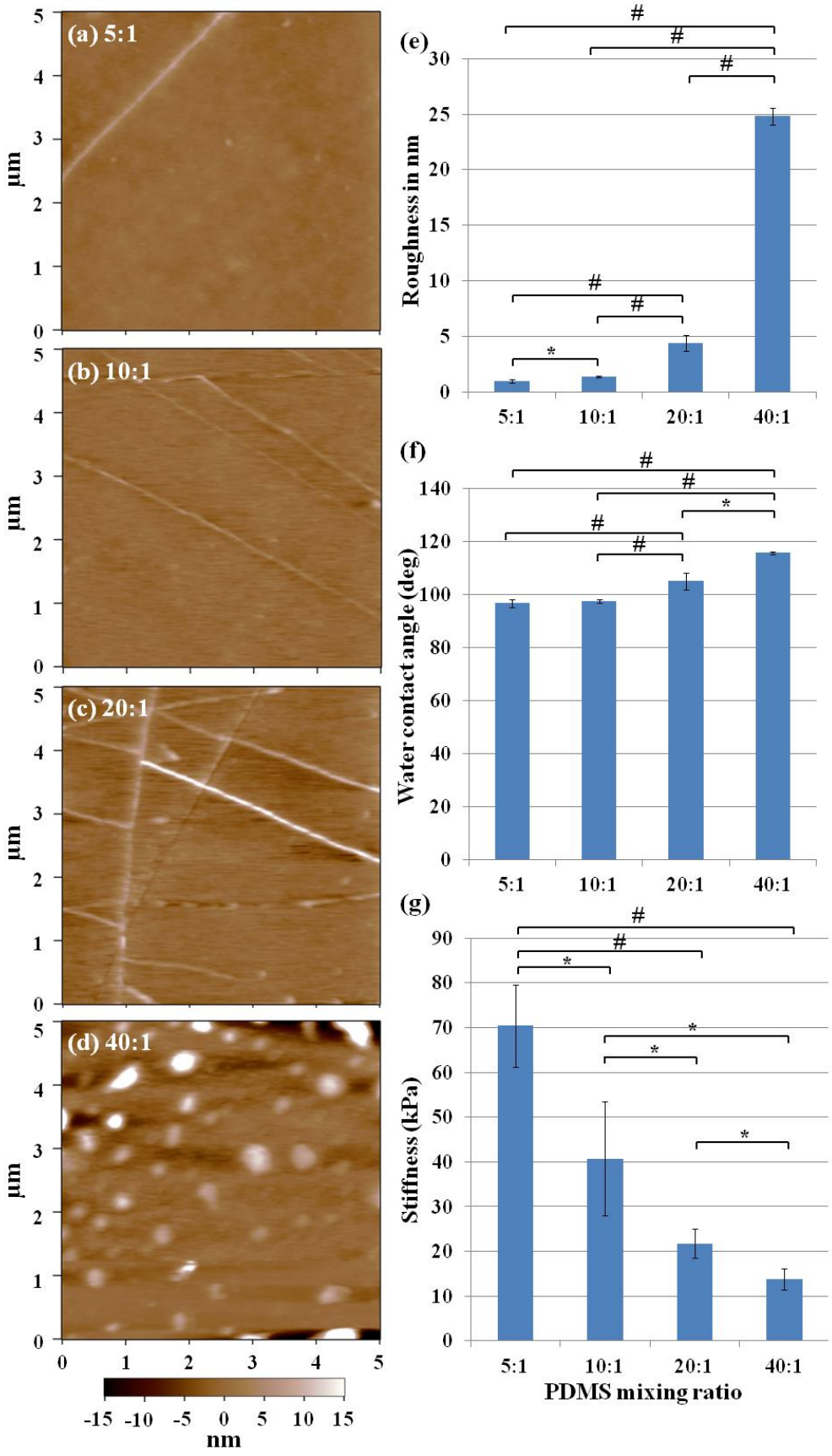

Figure 4.2: **Characterization of the surface property of the fibronectin-coated PDMS. (a-d) AFM images of the PDMS substrates made with mixing ratio of 5:1, 10:1, 20:1, and 40:1, respectively. (e) RMS roughness ($^{\#}p<0.0001$, $*p<0.05$, n = 5). (f) Water contact angle ($^{\#}p<0.0001$, $*p<0.05$, n = 4). (g) Surface stiffness ($^{\#}p<0.0001$, $*p<0.05$, n = 3).**

The initial cell adhesion and proliferation is usually an indicator of the surface biocompatibility, which depends on the chemical composition at the cell-substrate interface such as the type and density of surface ligands,[189-190] and also on the physical properties such as roughness, stiffness and hydrophobicity of the substrate.[191-193] Therefore we firstly characterized the initial cell adhesion immediately after cell seeding and also monitored the cell proliferation continuously for 7 days. Initially, variation of the combinatorial surface property of PDMS showed no significant short-term effect on the cell adhesion [Figure 4.3a] or proliferation [Figure 4.3b] at Day 1, although the coated fibronectin exhibited much higher concentration on 5:1 PDMS compared to other substrates [Figure 4.3c]. However, the long-term effect of the PDMS substrate properties on hBMSC proliferation became more obvious starting from Day 3 [Figure 4.3b], which showed that the proliferation rate was enhanced considerably on the PDMS substrates with the highest level of crosslinking (base : curing agent = 5:1). These results indicated that the PDMS formulation influenced the long-term hBMSC proliferation although it did not affect the initial cell adhesion and proliferation. It further suggested that the combinatorial effect of higher stiffness, lower hydrophobicity and lower roughness of the PDMS substrate enhanced hBMSC proliferation. These observations were consistent with prior studies on the individual effects of multiple surface properties, which reported that stiffer,[172, 194] smoother,[195] or less hydrophobic[196] surfaces could promote the proliferation of various types of stem cells.

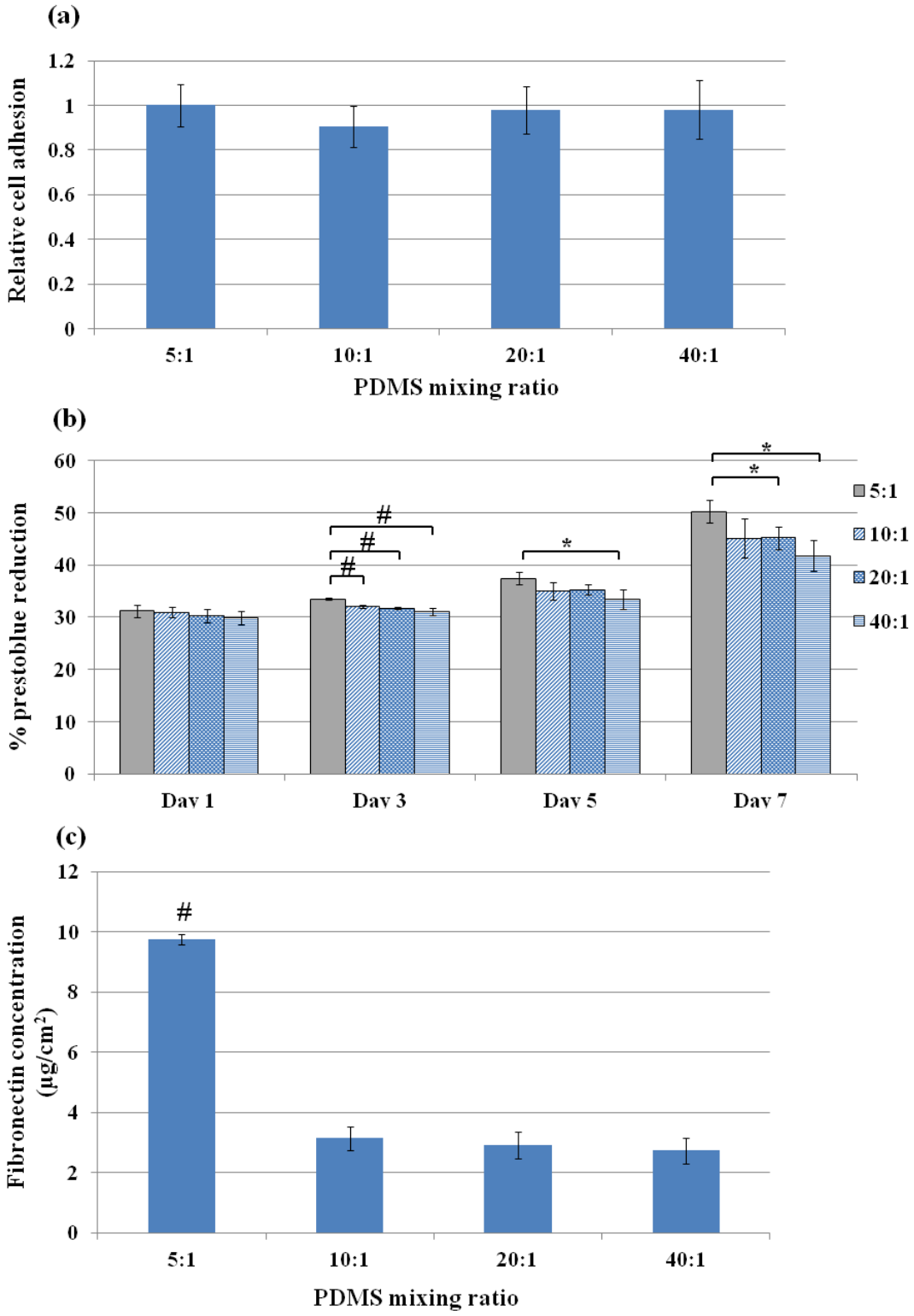

Figure 4.3: (a) Cell adhesion at 1 h after seeding normalized against the data on the 5:1 PDMS. (b) Cell viability assays over 7 days on different PDMS substrates. (c) Fibronectin concentration retained 24 h after initial fibronectin coating. $^{\#}p<0.0001$, $^{*}p<0.05$, n = 3.

The spreading and migration of hBMSCs on fibronectin-coated PDMS substrates was illustrated in figure 4.4. It was observed that most cells exhibited a typical spindle-like shape, while more cells appeared with wider spreading area and rounded shape on the PDMS substrates formulated with lower proportion of crosslinker [Figure 4.4 (a-d)]. It was previously reported that stiffer,[193, 197] roughened,[198-199] or more hydrophilic[141, 196] surfaces generally enhanced cell spreading. But in a recently published work by our group [200] we observed a higher cell spreading was observed for a PDMS sample with a roughness of 3.07±0.076 nm, stiffness of 12.1±2.71 kPa and a water contact angle of around 121.9°±0.13°. In our study we observed [Figure 4.4e] similar cell spreading for the 20:1 PDMS sample which was featured by roughness (4.37±0.72 nm) and stiffness (21.76±3.22 kPa) at intermediate level among all the samples tested while remaining slightly hydrophobic (contact angle 105.08°±3.21°). From these results we hypothesize that substrate roughness plays a prominent role for cell spreading in compared to substrate stiffness or its hydrophobicity. It was observed [Figure 4.4e] that for rougher PDMS 40:1 sample, cell spreading was smaller indicating that the substrate roughness should be at an intermediate value for optimal cell spreading.

Consistent with individual cell spreading, the total area covered by the migrating cell population also reached the maximum on the 20:1 PDMS substrate [Figure 4.4f]. In the literature, many previous studies showed that changes of a single aspect of surface property could have either promotional or inhibitory effect on cell migration. However, the variations of PDMS cross-link levels led to profound changes in many important aspects of surface property simultaneously, including stiffness, roughness and hydrophobicity [Figure 4.2], which had a combinatorial effect on cell migration [Figure 4.4] that was different from those caused by the changes of any individual aspect of surface property. As discussed above, the hBMSC spreading and migration were most favored on 20:1 PDMS substrate, which exhibited intermediate levels of roughness, stiffness and hydrophobicity.

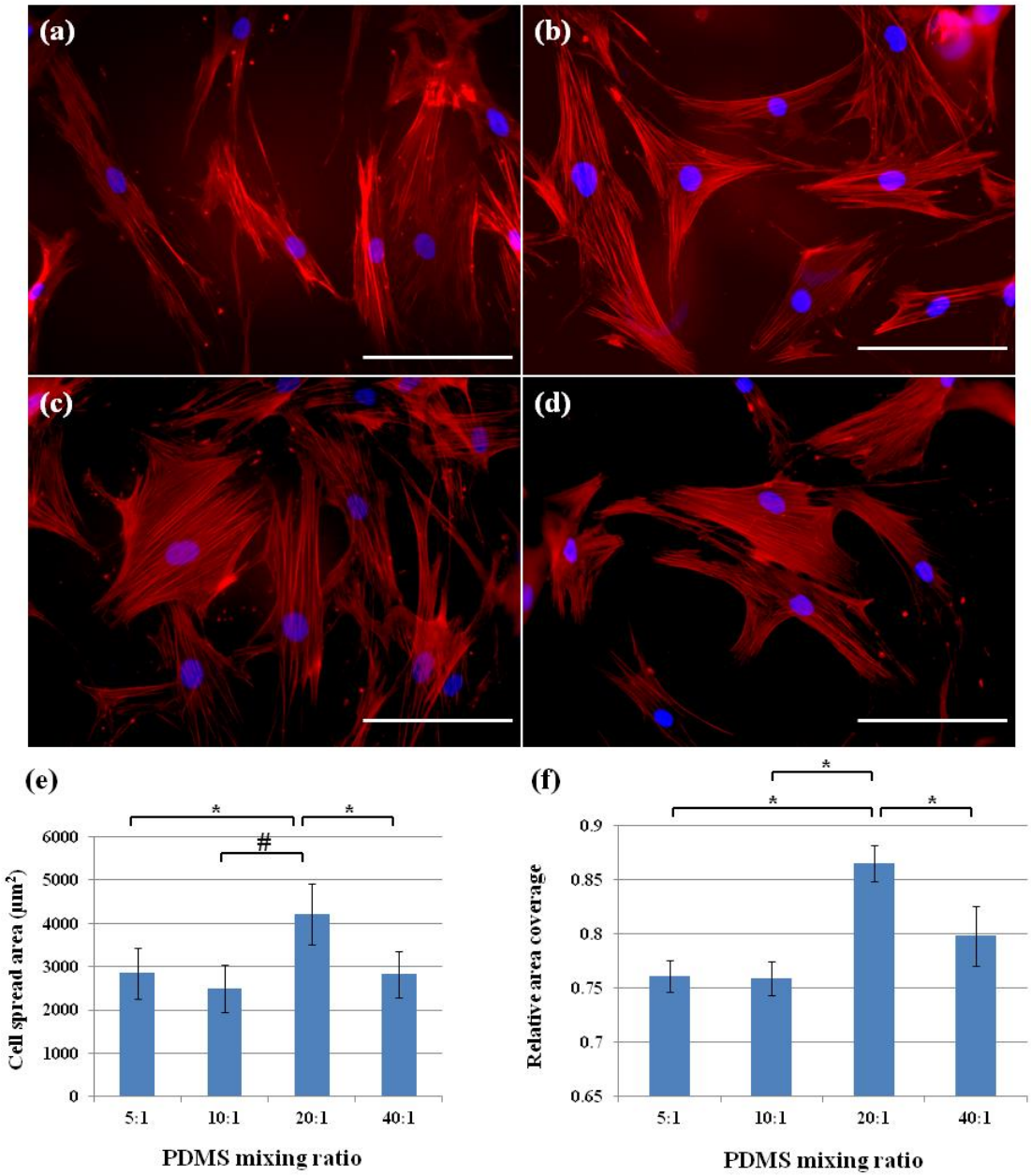

Figure 4.4: Fluorescence staining for F-actin (red) and nucleus (blue) of the cell culture on different PDMS substrates at Day 7: (a) 5:1. (b) 10:1. (c) 20:1. (d) 40:1. Scale bars: 50 μm. (e) Individual cell spreading area. (f) The total area covered by the migrating cells with respect to the total area of the central compartment. $^{\#}p<0.0001$, $^{*}p<0.05$, n = 5.

In order to understand the observed difference of cell migration on different substrates at a molecular level, quantitative real time PCR (qRT PCR) assay was performed to examine the gene expression of typical adhesion protein markers that determined the cell behavior during migration, including paxillin (cell-substrate linkage) and N-cadherin (cell-cell junction). Paxillin downregulation was shown to be associated

with decreased cell migration of hMSCs.[201] N-cadherin downregulation was shown to be associated with increased cell migration in human hematopoietic progenitor cells and smooth muscle cells,[202-203] while N-cadherin upregulation resulted in cell condensation that caused reduced migration of hMSC.[204-205] Figure 4.5 indicated that the expression of paxillin and N-cadherin in the hBMSCs on 20:1 PDMS substrates was substantially lower than those on other substrates made with different mixing ratios, while the cell spreading and migration reached optimum on 20:1 PDMS [Figure 4.4). These results were consistent with a previous report that paxillin down-regulation caused a decrease in N-cadherin expression thus resulting in enhanced migration of Hela cells.[206] Furthermore, the gene expression of proliferation marker Ki-67 (Fig. 5) showed slightly higher proliferation rate on the substrates with lower base proportions (5:1 and 10:1), which was consistent with the results by cell proliferation assay [Figure 4.3b]. The proliferation assay and gene analysis further suggested that the cell coverage in the central channel on 20:1 PDMS was mainly due to the cell migration from the side channels rather than the cell proliferation.

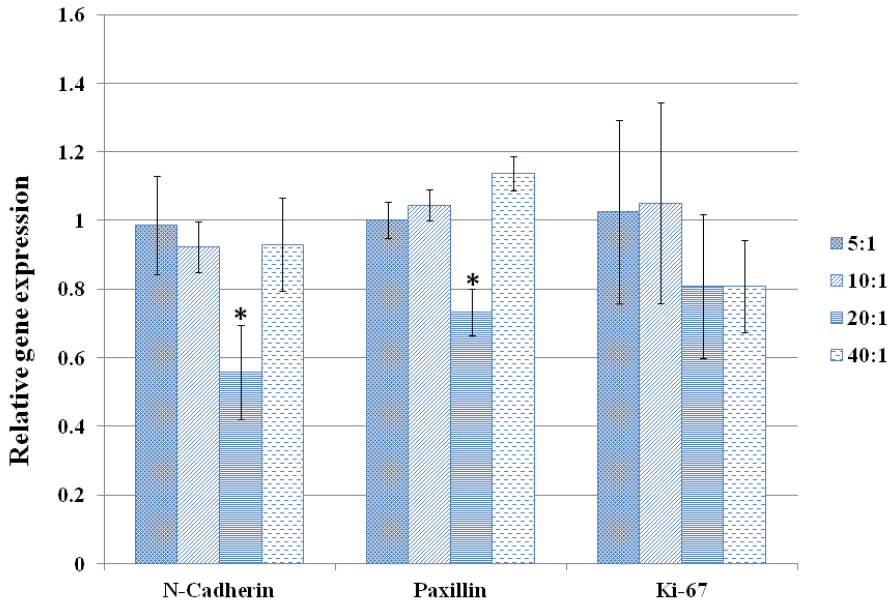

Figure 4.5: Real time PCR assays of the hBMSCs at Day 5 cultured on different PDMS substrates. All data were normalized with regard to the gene expression on 5:1 PDMS. *p<0.05, n = 3.

4.4 Summary

Hence the microfluidic *in vitro* model was modified to perform studies of cell-substrate interaction. This study has demonstrated an efficient way to study the impact of substratum properties on cell behavior using a microfluidic migration assay. The physical

properties of PDMS, including hydrophobicity, surface roughness and stiffness, can be easily tuned by varying the prepolymer to curing agent ratio. It was observed that although the initial cell adhesion and proliferation were similar on all PDMS substrates, cell spreading and migration appeared to be most favored on 20:1 PDMS that exhibited an intermediate level of roughness, stiffness and hydrophobicity. These findings indicated that multiple aspects of surface property had a combinatorial impact on cell behavior, which was different from the effects caused by the changes of any individual aspect of surface property. Since cell migration is a vital process during tissue generation, this study may elucidate the important physical cues required in the development of scaffolds with enhanced cell migration potential for stem cell-based regenerative medicine.

4.5 Declaration

12. A part of this chapter has been published. N.V. Menon, Y.J. Chuah, S. Phey, Y. Zhang, Y.N. Wu, V. Chan, Y. Kang*. "Microfluidic assay to study the combinatorial impact of substrate properties on mesenchymal stem cell migration". ***ACS Applied Materials & Interfaces***. 7 (31), 17095–17103 (2015).

Chapter 5 Efficacy testing

5.1 Background

As mentioned earlier, microfluidics *in vitro* models can play a significant role for drug efficacy testing. It was observed in a survey conducted in 2014 that the overall percentage approval of all the drugs by FDA is very poor, approximately 10% to15 %. It was also observed only 7% of the drugs for cancer are approved. [60] Such a low percentage of approval has often been blamed to be due to the use of animal models during the initial trials while the same drug's efficacy does not match with the results obtained during human trials. The high percentage of failure, results in huge financial loss to the tune of millions of dollars that goes into all the different steps preceding the human trials. Thus, there is a need to develop suitable substitutes to the animal models using cells derived from humans so that drug testing and its efficacy can be confirmed in the initial steps before proceeding towards the later phases of clinical trials. As discussed in the previous sections, microfluidic *in vitro* models can be used for filling this gap to test the efficacy of drugs as well as any targeting molecules or agents to target a specific cell type. In this chapter, the microfluidic co-culture system developed earlier has been used to check the efficacy of an organic dye to perform targeted imaging and targeted photodynamic therapy (PDT) of cancer.

Cancer is one of leading cause of death in the world and its treatment has been an area of intense research. Current state of treatment of cancer includes surgery, radiation therapy and chemotherapy. An alternative non-invasive therapeutic technique for cancer treatment is PDT. The advantages of PDT like scar-less healing, and repeatability without any genetic mutation, over the existing treatment modalities make them an extremely useful tool as a primary or an adjunctive mode of treatment for cancer. [207-208] The success of PDT for the treatment of skin cancer,[209] lung cancer, [210]. brain cancer,[211] prostrate cancer [212] has been demonstrated by the *in vitro* models as well as using clinical trials. It involves the administration of a non-toxic drug called the photosensitizer (PS) to the site of tumor growth followed by irradiation with light, preferably in the long wavelength region (600 -850 nm). This is due to the ability of the longer wavelength light to penetrate deeper through the cell layers. The primary mechanism of PDT is that upon irradiation, the PS generates singlet oxygen ($^1O_2$) by electron transfer (type I) or energy transfer (type II) mechanisms, in the presence of oxygen which leads to an increase in the intracellular reactive oxygen species (ROS). This increase in ROS within the cell causes cell death. An efficient production of singlet oxygen is possible only if the PS has a sharp absorption

coefficient, high quantum yield of the triplet state and low cytotoxicity in the absence of light irradiation. A number of photosensitizers have been developed for PDT and have been used for the treatment of different types of cancer. [208] Squaraine is one such PS exhibiting excellent photo-physical properties in the red to near infra red (NIR) region. [213-214] It has been used for a large number of biological applications including metal ion sensing, [215] NIR fluorescent labeling, [216] protein sensing,[217] detection and estimation of thiol containing amino acids [218] as well in PDT. [219-222]

In our present study, an unsymmetric squaraine dye has been used as the PS for PDT. The hydrophobic nature of the squaraine dye results in its aggregation in aqueous solution. Hence carriers, like nanoparticles. nanoliposomes, polymeric micelles [223-228] need to be used for effective delivery of the PS to the target cells. Pluronic F127 is a type of polymeric micelle that has been widely used as a carrier for hydrophobic drugs. [229] Such a micelle has been shown to improve the bioavailability of the drug and protection against the harsh environment of the gastro-intestinal tract *in vivo*. Tumor targeting by these micelles can be by passive targeting due to the enhanced permeability and retention (EPR) generally observed in tumor sites or by active targeting with the help of targeting moieties specific to the tumor. There has been an increasing interest in drug delivery by active targeting of cancer cells [230-234] specially to improve drug specificity and to reduce the adverse effects of the drug on non-cancerous cells. Targeting cancer cell surface receptors is one of the methods for active targeting and folate receptor (FR) [233, 235] is one such cancer surface receptor that is highly expressed in some cancer cells of the kidney, ovary, brain, lung, breasts, cervix and endometrium. A very commonly used targeting ligand for FR is folic acid. In this work, folic acid coupled pluronic F-127 micelle has been used to encapsulate the squaraine dye.

FR positive cancer cell lines	FR negative cancer cell lines
1. Breast cancer cell lines	**1. Lung carcinoma**
MDA-MB-231	A549
MCF-7	**2. Liver cancer**
2. Ovarian cancer	HepG2
SKOV3	Huh7
IGROV1	**3. Osteosarcoma**
OV-90	MG-63
	143B

3. Lung cancer	**4. Kidney cancer**
H460	CAKI-1
4. Cervical cancer	**5. Leukemia**
Hela	KG-1
5. Colorectal cancer	Kcl-22
Caco-2	K-562
HT29	NB-4
6. Placenta cancer/choriocarcinoma	
JAR	
7. Endometrial cancer	
Ishikawa	

Table 5-1: Folate receptor expression in cancer cells

Microfluidics has been used as an effective tool for the generation of smart *in vitro* models because of its ability to mimic physiological conditions to a great extent. Microfluidic *in vitro* models have been used as preclinical trial models for studying various physiological phenomena such as disease progression and also to perform drug studies as well as to develop organs on chip. [80, 236-237] In this work, squaraine dye (SQ) was encapsulated within a micellar system, modified with folic acid (FA). The potential of the modified micelle system as an agent for targeted imaging and targeted PDT has been verified using a microfluidic co-culture model. The schematic of the workflow is as shown in Figure 5.1. Four types of cells have been used: Cervical cancer cell (Hela) , hepatocarcinoma (HuH7), human mesenchymal stem cell (hMSC) and human bone marrow stroma (HS5). Hela (FR positive) was co-cultured with FR negative cells HuH7, hMSC and HS5 in individual microfluidic chips. A single color light emitting diode (LED) with a wavelength of 655 nm was used as the light source. Confocal imaging and flow cytometry were used to check the targeting potential of the folic acid conjugated micelle. The cytotoxicity of the micelle-dye system in the dark was checked using prestoblue cell viability assay while live -dead staining was performed to determine the cell viability of the different cells in the co-culture microfluidic chip thereby showing the efficiency of targeted PDT.

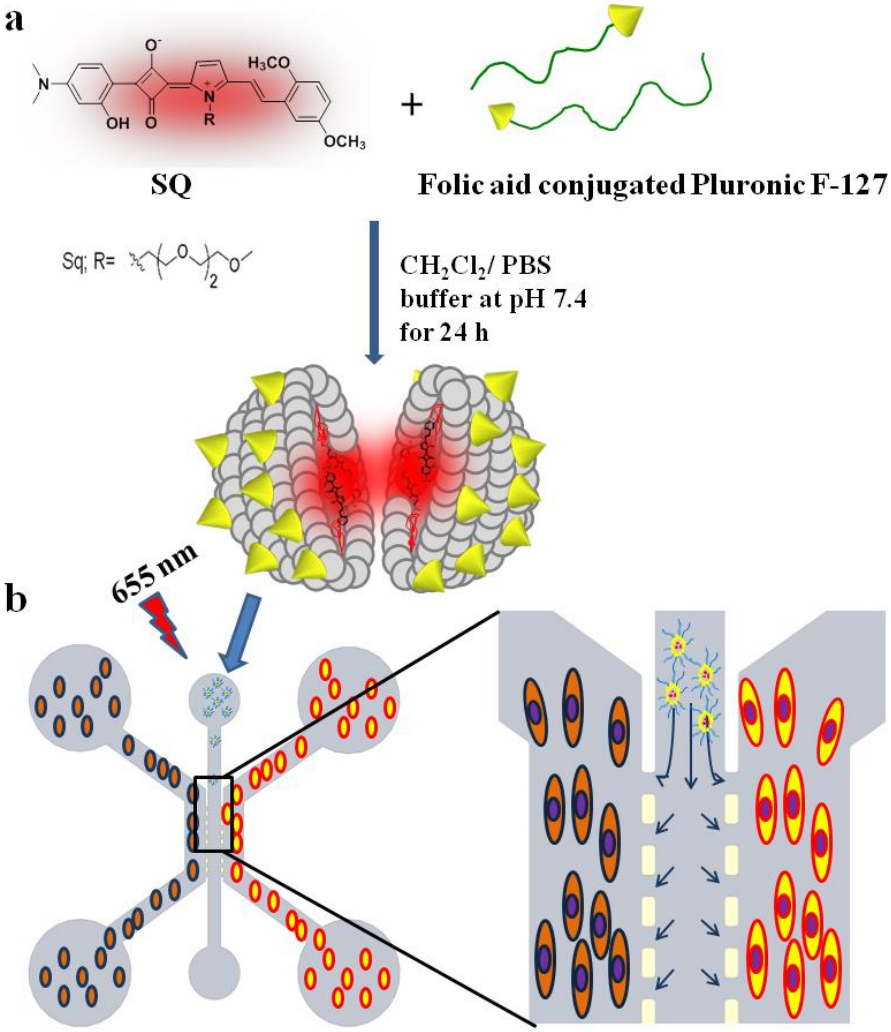

Figure 5.1: (a) Schematic of the squaraine dye SQ encapsulation within a modified micellar system. (b) Schematic of the microfluidic co-culture chip for testing efficacy.

5.2 Materials and methods

The chemicals required for chemical synthesis were purchased from Sigma-Aldrich, Singapore. The solvents were of reagent grade and all the solvents were dried and distilled prior to use.

5.2.1 Synthesis of squaraine dye (SQ)

The unsymmetric squaraine dye was synthesized by the condensation of half-squaraine derivative (**5**) (218 mg, 1.0 mmol) with styrylpyrrolechromophore (**6**) (375 mg, 1.0 mmol) in 1:1 butanol/benzene mixture (80 mL) under azeotropic conditions [Figure 5.2]. The reaction mixture was refluxed for 12 h following which they were cooled to room temperature and the solvent was removed. The product was precipitated from

petroleum ether, filtered and re-dissolved in chloroform ($CHCl_3$). The crude product obtained was later purified using column chromatography over silica gel using 3% methanol/dichloromethane.

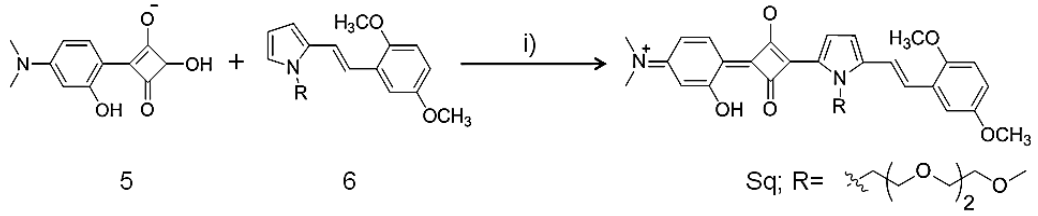

Figure 5.2: Synthesis of squaraine dye (SQ)

5.2.2 Synthesis of FA conjugated micelle

The synthesis of FA conjugated pluronic F127 (PF127) was synthesized using a modified procedure described earlier by Zhang et.al. [238] In brief, purification of PF127 was performed by dissolving it in acetone followed by precipitating in a excess cooled hexane and drying in vacuum. Once purified, PF127 (1 mM) was dissolved in dry acetonitrile and added to an excess amount of N,N′- Carbonyldiimidazole (CDI) (10 mM in dry acetonitrile) at room temperature in a nitrogen environment for 2 h. The mixture was stirred for an additional 4 h. The solution was concentrated using a rotary evaporator and poured into excess ethyl ether. This purification was repeated multiple times to remove any untreated CDI. The PF127-CDI was dried under vacuum and collected. Following the addition of imidazole groups onto the PF127, the product was reacted with a compound like 1,2-ethylenediamine to create amino terminated PF127. The product ($PF127\text{-}NH_2$) was purified and dehydrated in vacuum. FA conjugated PF127 is produced from the synthesized $PF127\text{-}NH_2$. $PF127\text{-}NH_2$, folic acid, HATU (1-[Bis(dimethylamino)methylene]-1H-1,2,3-triazolo[4,5-b]pyridinium 3-oxid hexafluorophosphate) are dissolved in DMF (dimethylformamide) in the presence of DIPEA (N, N-Diisopropylethylamine). The supernatant is dialyzed against deionized water for 24 h to remove impurities and unwanted products. The mixture was stirred in the dark for 18 h in a nitrogen atmosphere followed by lyophilization. The schematic of the procedure is illustrated in figure 5.3.

5.2.3 Preparation of SQ loaded micelle

To load the dye into the micelles, the squaraine dye (SQ) (1 mg mL^{-1}) and the modified micelles, PF127-FA (1.5×10^{-4} M) was dissolved in 10 ml of dichloromethane. An equal volume of PBS buffer (pH 7.4) was added and the mixture was stirred at room

temperature for 24 h. This led to the complete evaporation of dichloromethane leaving behind the dye encapsulated within the PF127-FA micelle. The solution is filtered and dialyzed in deionized water for 24 h to remove any impurities or any big particles.

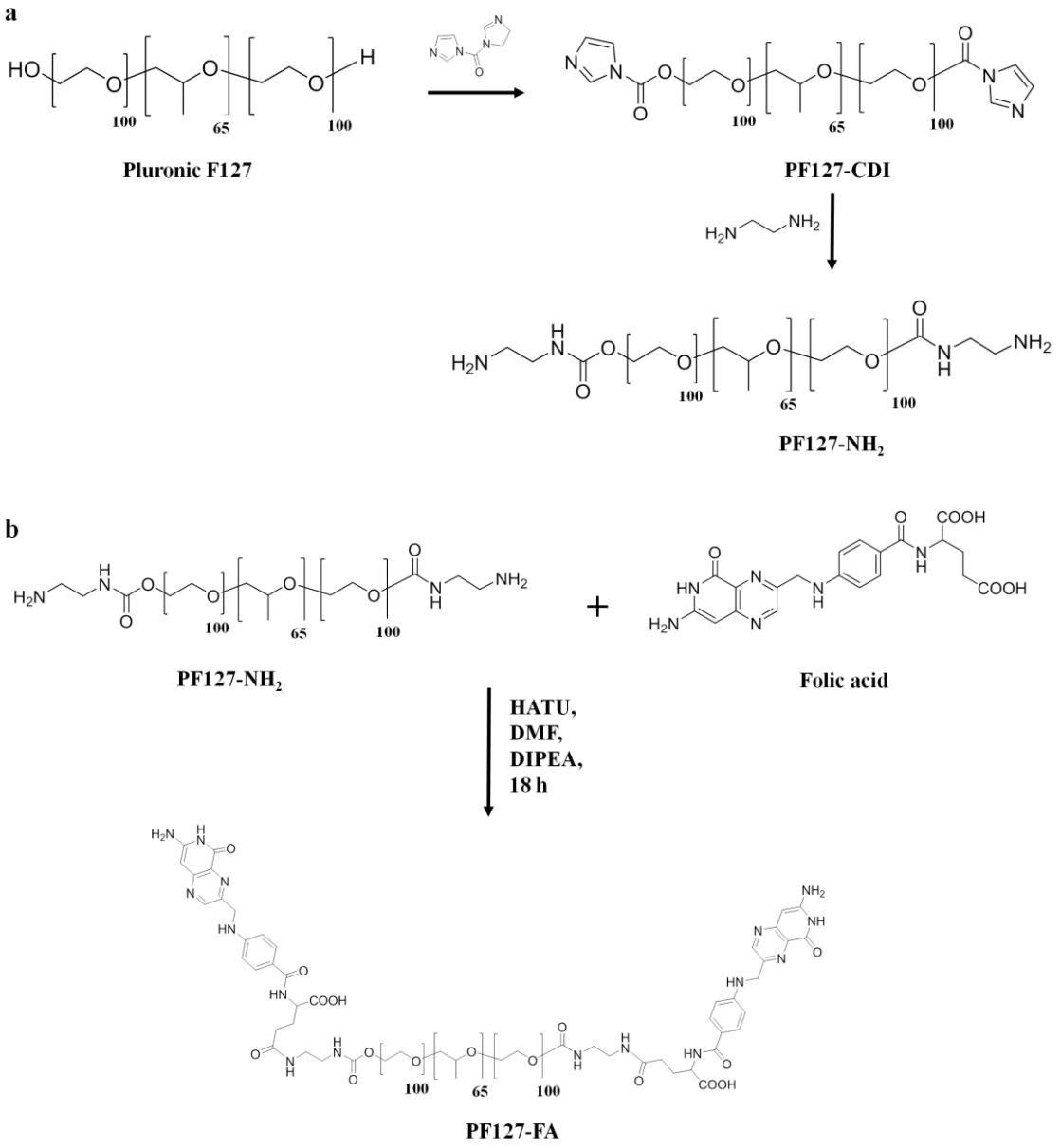

Figure 5.3: Schematic of synthesis of the modified micelle system.

5.2.4 Micelle characterisation

The size of the dye loaded micelle was measured using a transmission electron micrscope (TEM) and its hydrodynamic radius in aqueous solution was measured using dynamic light scattering (DLS) techniques using Malvern Zetasizer Naso ZS (Malvern, UK). For TEM, a JEM 1400 electron microscope (JEOL, Japan) (120 kV) equiped with slow scan CCD using cold cathode field emission as the gun was used. For sample preparation, a drop of the sample solution is placed on a TEM grid (copper grid, 300

meshes, coated with carbon film). The sample is then allowed to air-dry. The absorption spectra was measured using a UV-3600 spectrophotometer (Shimadzu, Singapore), while the emission spectra was measured using a RF-5301 PC spectrofluorophotometer (Shimadzu .Singapore)

5.2.5 Microfluidic chip fabrication

The chip preparation was carried out following the same procedure as discussed earlier in section 2.2.1. The silicon mold was fabricated and the PDMS device was obtained. The PDMS slab was plasma treated and sealed onto a glass slide. Fibronectin coating was performed in the channels within the microfluidic device followed by cell seeding.

5.2.6 Cell culture

Cervical cancer cells (Hela), hepatocarcinoma (HuH7), human bone marrow stroma(HS5) and human mesenchymal stem cells (hMSCs) were used in our study. All the cells were cultured as explained earlier 2.2.3. Three co-culture systems, Hela and HS5, Hela and HuH7 and Hela and hMSCs, were prepared using three microfluidic chips.

5.2.7 Photodynamic therapy on chip

After overnight cell culture on chip, 0.5μM of the SQ-FA micelle was introduced into the central channel, allowing the micelle to flow into the side channels with the cells. After a 15 minute incubation, the cells are washed with 1X PBS and DMEM supplemented with FBS/PS is introduced into the chips following which the cells are incubated for 2 h at 37°C in an incubator with humidified atmosphere and 5% CO_2, before its exposure to light radiation. An LED (Luxeon Star LEDs, USA) with a wavelength range of 655 nm and a fluence rate of 300 mW/cm^2, was used to irradiate the co-culture chips for 20 minutes, following which the chips are incubated in a humidified incubator at 37°C and 5% CO_2.

5.2.8 Dark Cytotoxicity

The dark cytotoxicity of the PDT agent was performed using prestoblue cell viability reagent (Life technologies, Singapore) as discussed in section 2.2.4. For this study, aproximately 5×10^3 Hela cells were cultured in a 96 well plate overnight. Different concentrations of the micelle was incubated with the cells for 15 minutes following which 1X PBS was used to wash the cells and the cells were incubated in the cell culture

medium at 37°C in a humidified environment with 5% CO2. After 2 hr., the cells were washed and incubated with 10% prestoblue reagent for 1 h following which its absorbance was measured at 570 nm and 600 nm using a microplate reader (Infinite M200 Pro, Tecan Asia, Singapore) from which the cell viability was calculated.

5.2.9 Detection of ROS inside the cancer cells *in vitro*

The ability of the PS to produce intracellular ROS generated within the cells was measured using CM-H2DCFDA assay (Life Technologies, Singapore). Approximately 1×10^4 Hela cells were seeded into each well of two 4 well plates. The cells are incubated with the 0.5µM of the PS in DMEM for 15 mins, washed thrice with 1X PBS and then incubated for 2 hours in DMEM at 37°C in an incubator with humidified atmosphere and 5% CO_2. The concentration of the dye was optimized for the Hela cells. We used 4 different concentrations (2 µM, 3 µM, 4.5 µM , 5 µM) in 1X PBS and incubated the dye for 20 min (as explained before in section 3.2.10) 4.5 µM of CM-H2DCFDA in 1X PBS was determined to be good and 4.5 µM of the dye was incubated with the cells for 20 min prior to fluorescence imaging. One of the 4-well plates was exposed to the LED with a wavelength range of 650 nm to 670 nm for 5 minutes. The fluorescence intensity of the cells in the well plate with and without irradiation was calculated using the ImageJ software (National Institute of Health, USA).

5.2.10 Flow cytometry

Approximately 1×10^5 cells of each cell type were seeded separately in 6 well plates overnight and were then incubated with SQ-FA-micelle and SQ-micelle (without folic acid) for 15 minutes. The cells were washed thrice with 1X PBS and eventually suspended in 1X PBS solution. A flow cytometer (LSR II, BD Biosciences, Singapore) was used to quantify the number of cells that have uptaken the SQ-FA-micelle. The sample fluorescence was measured for 10,000 cycles using the Allophycocyanin (APC) filter (Ex- 633 nm/ Em 640nm -680 nm). Flowjo data analysis software (FlowJo, LLC, USA) was used to quantify the cells that had up-taken the SQ-FA-micelle. This was done by setting a threshold value. The maximum value of APC for the SQ-micelle (without FA) was set as the threshold value. Cells with APC values lesser than the threshold are given a negative value while cells with APC values more than the threshold value are given positive values. The data analysis software allows for cell counting for cells with positive values and ones with negative values. From the cell count it will be easy to calculate the fold increase in the number of cells stained by the micelle. The principle of

this calculation is that the SQ-FA micelle will target only the FR positive cells. The presence of FA allows for faster uptake of the micelle by the FR positive cells. Hence for the same time frame, FR positive cells will uptake more SQ-FA-micelle in comparison to SQ-micelle. The FR negative cells will be stained almost equally by SQ-FA micelle or by SQ-micelle.

5.2.11 Live-dead cell imaging

The ability of the SQ-FA micelle for effective killing of FR positive cancer cells was determined using the microfluidic co-culture chip. Two sets of co-culture chips were created, one for assessing the targeted PDT of Hela cells and the other to act as control to compare the selectivity of the PDT. SQ-FA micelle was introduced into both the sets of co-culture chips, while the control set was maintained in the dark, while the other set was irradiated with light of wavelength in the range of 650 nm to 670 nm. . The live-dead cell count in the co-culture chips were done using FDA (Sigma-Aldrich, Singapore) for live cells and EthD-1 (Life technologies, Singapore) for the dead cells. A fluorescence microscope (Olympus IX71, Singapore) was used to capture the fluorescent images and the live-dead cell count was performed using the ImageJ software (National Institute of Health, USA).

5.2.12 Confocal imaging

A confocal microscope (Carl Zeiss LSM 710 meta, Singapore) was used to image the cells stained by the SQ-FA-micelle and DAPI (nucleus stain). The cells inside the co-culture chip were incubated with SQ-FA-micelle for 15 minutes following which the cells were washed with 1X PBS and incubated at 37°C in a humidified incubator with 5% CO2. The cells are then fixed with 10% formalin for 15 minutes, following which they are stained for their nucleus using DAPI stain (Life technologies, Singapore). The chips were then imaged using the confocal microscope and the intensity profile of the cells was measured using the ImageJ software (National Institute of Health, USA).

5.3 Results and discussion

The squaraine dye synthesized and used here has been used before and its characterization has been done elsewhere. [239] In this work, Parijat et.al used the same dye, SQ, for photooxidation of phenol using the singlet oxygen generation potential of the dye and a significant generation of singlet oxygen was observed having a singlet oxygen quantum yield of approximately 10%.

The SQ-FA-micelle was characterized to understand its various properties like absorption and emission, cytotoxicity as well as its size. The absorption and emission results are as shown in figure 5.4. The absorption and emission were measured for three samples: the dye, dye within a micelle (without FA) and dye within a FA-modified micelle. It was observed that the absorption maximum of SQ in all the three samples were almost the same (672 nm). It may also be observed that there is a peak in the region <400 nm in the SQ-FA sample which corresponds to the absorption of folic acid. A small hump was observed for the measurement of SQ micelle without folic acid. This is a consequence of aggregation of the hydrophobic SQ in aqueous environment. The maxima for the emission spectrum was observed at around 685 nm, while a very small blue shift was observed amongst the different samples. This was due to the encapsulation of the dye within a hydrophobic environment.

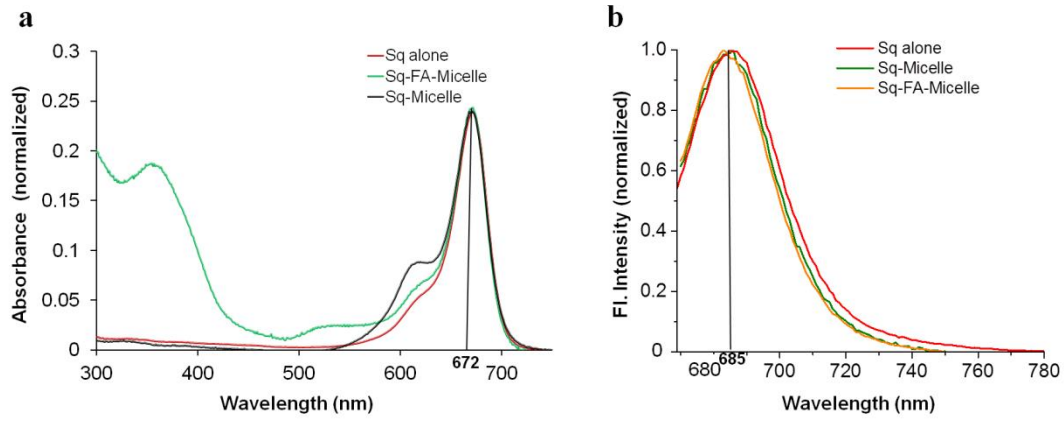

Figure 5.4: Photophysical properties of the micelle system. (a) Absorption spectrum, (b) Emission spectrum

The size of the SQ-FA-micelle was measured using TEM and its hydrodynamic radius was measured using the DLS technique. From the TEM images, the diameter of the micelle was measured to be approximately 75 nm [Figure 5.5a]. The hydrodynamic radius of the same micelle was slightly greater than the one observed by TEM and the measured particle size is 78 nm [Figure 5.5b].

Apart from the physical characterization of the micelle, it is extremely important to understand its dark cytotoxicity of the PS. Different concentrations of the solution with SQ-FA micelle, was incubated with the Hela cells for 15 minutes with a maximum concentration of 1 µM. The dilutions for these different concentrations were achieved

using the cell culture medium. The cytotoxicity measured due to the different concentrations was comparable to that of the control [Figure 5.5c], indicating the limited dark cytotoxicity of the SQ-FA micelle on the cells.

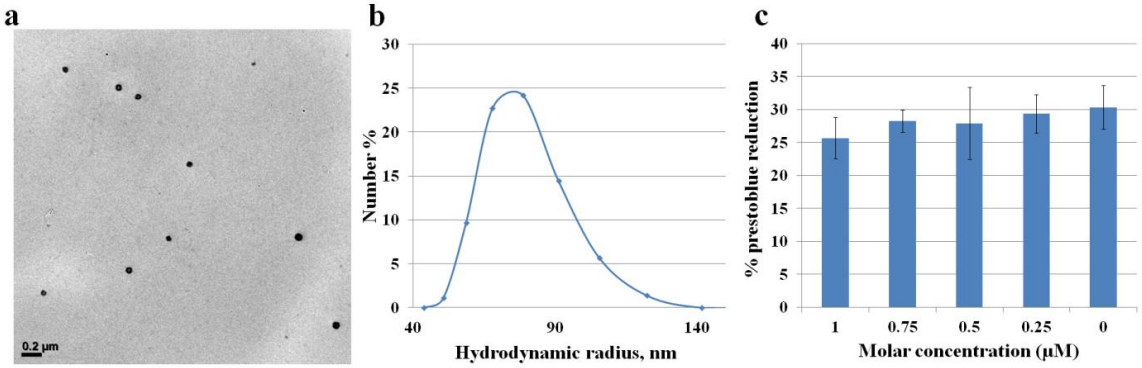

Figure 5.5: (a) TEM image of the SQ-FA micelle, (b) Hydrodynamic radius of SQ-FA micelle, (c) dark cytotoxicity.

Moreover, the absorption/emission spectrum of the dye suggests that they can be used as fluorescing agents with excitation/emission wavelengths in the red region. Due to the broad excitation of the SQ dye, in our experiments we have used an excitation wavelength of 633 nm and an emission wavelength between 650 nm to 700 nm. By functionalizing the micelle encapsulating the SQ dye using folic acid, we can target FR positive cells. This strategy allows for targeted imaging as well as its singlet oxygen yield will allow for targeted therapy. Flow cytometry and confocal imaging were used to observe targeted imaging due to Sq-FA-micelle. For flow cytometry the threshold was set and cell count with positive and negative threshold values were determined. It was observed that, while HS5, hMSC and HuH7 cells had very little staining due to SQ-FA micelle, the Hela cells had a significant increase in staining due to the micelle with FA. On calculating the fold increase of cells fluorescing due to SQ-FA-micelle with respect to SQ-micelle, for Hela cells, there was almost a 120 times increase while for the other cell types, the fold increase was less than 2 times [Figure 5.6].

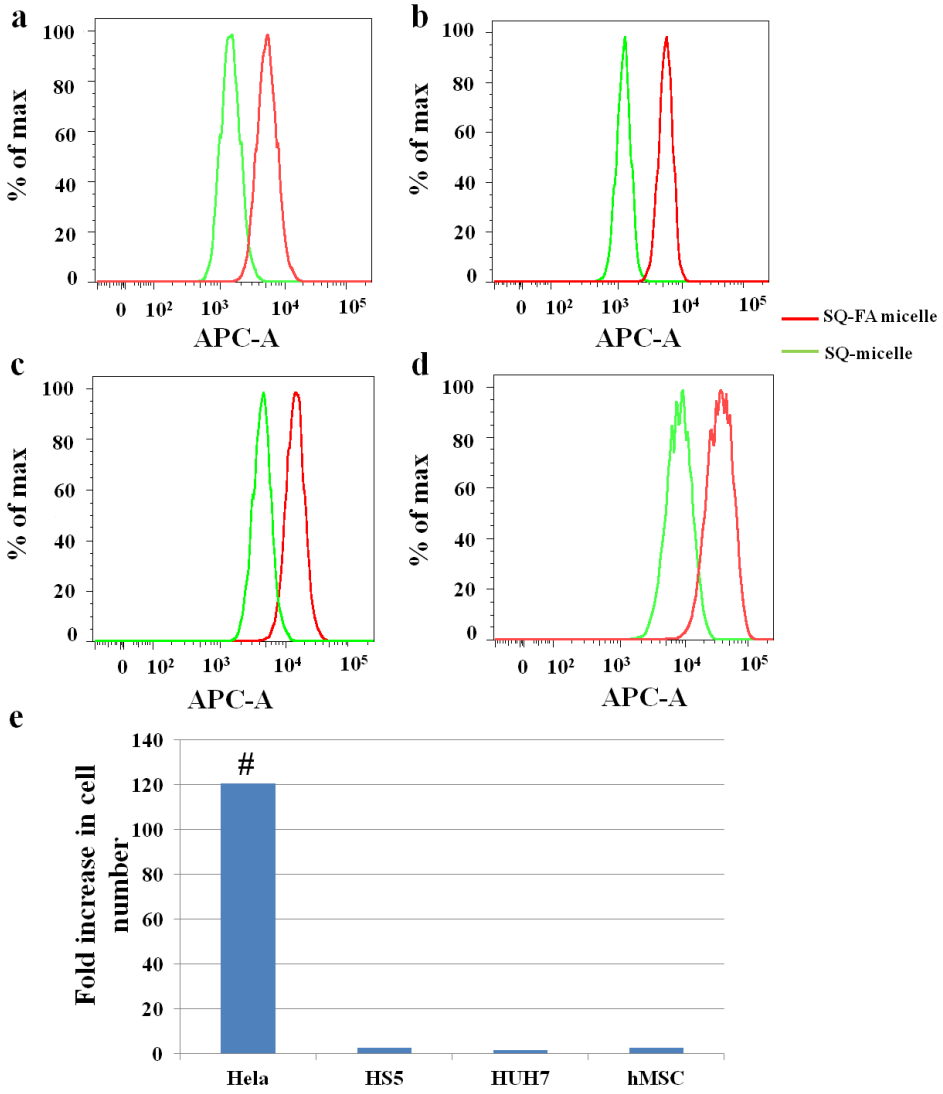

Figure 5.6: Flow cytometry. Fluorescence intensity profiles of cells due to SQ-FA micelle and SQ-micelle. (a) HS5, (b) Hela, (c) HuH7, (d) hMSC. (e) Fold increase in number of cells tagged by SQ-FA micelle relative to SQ micelle. #p<0.0001

The microfluidic co-culture chip was used to test the efficacy of the micelle system to perform targeted staining as well as targeted PDT. The scheme of cell seeding is exactly similar to the method used previously in chapter 2. Three different co-culture systems were used: HS5-Hela, HuH7-Hela and hMSC-Hela. The SQ-FA-micelle in cell culture medium (0.5 µM) was introduced through the central channel so that solution can spread to the side channels at the same instant as well as at a uniform concentration [Figure 5.1b]. To visualize the SQ localization in the cell, confocal microscopy was used. The cells were fixed and stained with DAPI prior to confocal imaging. From the images obtained, it could be observed that SQ dye does not enter the nucleus and localizes largely in the peri-nuclear region. This is of good significance in PDT applications as the probability of the dyes causing any damage to the DNA (resulting in genetic disorders or

mutations) is reduced [Figure 5.7a,c and e]. ImageJ software was used to process the images to obain the intensity profiles of the SQ fluorescence from the confocal images. These results seemed to be in agreement with the results obtained from the flow cytometer. The SQ-FA-micelle uptake by the Hela cells was much more compared to the other cell types used. This reiterates the ability of such a micellar conjugation to enhance targeted imaging of cancer.

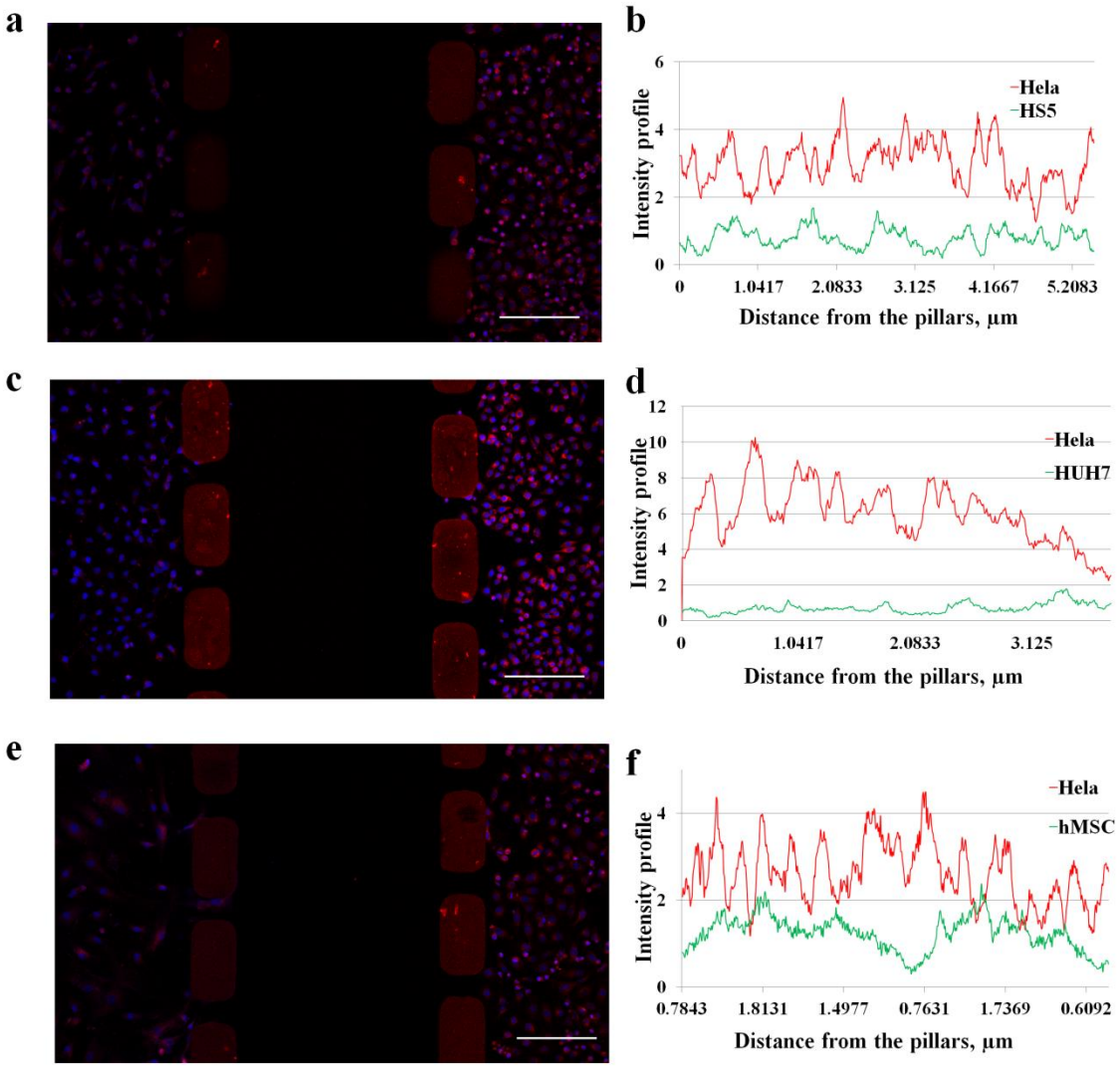

Figure 5.7: Confocal imaging of the chip with Hela cells on the right side channel and the other co-cultured cells on the left side channel. The cells were also stained for DAPI to see SQ localization in the nucleus. (a) HS5-Hela co-culture and (b) the intensity profile of the SQ dye. (c) and (d) HuH7 and Hela co-culture and intensity profile, respectively. (e) and (f) hMSC and Hela co-culture with their intensity profiles. Scale bar: 200 µm.

PDT can be performed on chip because of the ability to build co-culture models as well as due to the transparency of PDMS. Ideally, a laser source of 672 nm should be used to obtain the maximum singlet oxygen generation from the SQ dye. In this work we have capitalized on the broad absorption spectrum of SQ dye and we have used a low cost

single wavelength LED (655 nm) as the light source. When the sample is exposed to light irradiation, singlet oxygen is generated that leads to an increase in the intracellular ROS which in turn leads to cell death. The ROS quantification was done using the CM-H2DCFDA probe (Life Technologies, Singapore). Some challenges that occurred during the measurement of ROS involve the procedure followed during light irradiation. Light irradiation using the 655 nm LED normally is done outside the incubator inside the bio-safety cabinet (BSC). In such a case there tends to be a small increase in oxidative stress as the medium used DMEM normally requires 5% CO_2 to maintain its pH. And moreover, during PDT analysis, the cells are incubated for 2 h after light irradiation. But during control studies it was observed that the CM-H2DCFDA stain photobleaches extremely fast and a time point of more than 30 min leads to increased noise in the images. In order to overcome this issue of oxidative stress, we used a CO_2 independent medium (Life Technologies, Singapore) that can maintain its pH in the absence of CO_2 and also can facilitate cell growth over long periods of time outside an incubator. Also, to maintain better correlation of the ROS observed in the irradiated sample and the non-irradiated sample, both the samples were maintained in the CO_2 independent medium during the course of the experiment and imaging was performed with minimal time delay between the samples. From the fluorescence intensity measurement using ImageJ a significant difference in the ROS values was observed between the two samples [Figure 5.8h].

Live and dead staining was performed to understand the PDT efficacy of the SQ-FA micelle. Briefly, the cells were incubated with the micelle system followed by light irradiation for 20 min. The cells were stained for live and dead cells after 48 hours after the irradiation. Figure 5.8(a-f) shows the different chips with live-dead staining. The first column indicates control samples (without irradiation) and the second column indicates samples that have been irradiated while each row signifies a specific co-culture model. Cell counting was performed using ImageJ software and the results were quantified. The percentage of dead cells was calculated by from the total number of cells (number of dead cells + number of live cells). Approximately 60-70% cell death of Hela cells was observed; while the cell death in the other cells was significantly lower [Figure 5.8g] re-affirming the success of the strategy employed in this work.

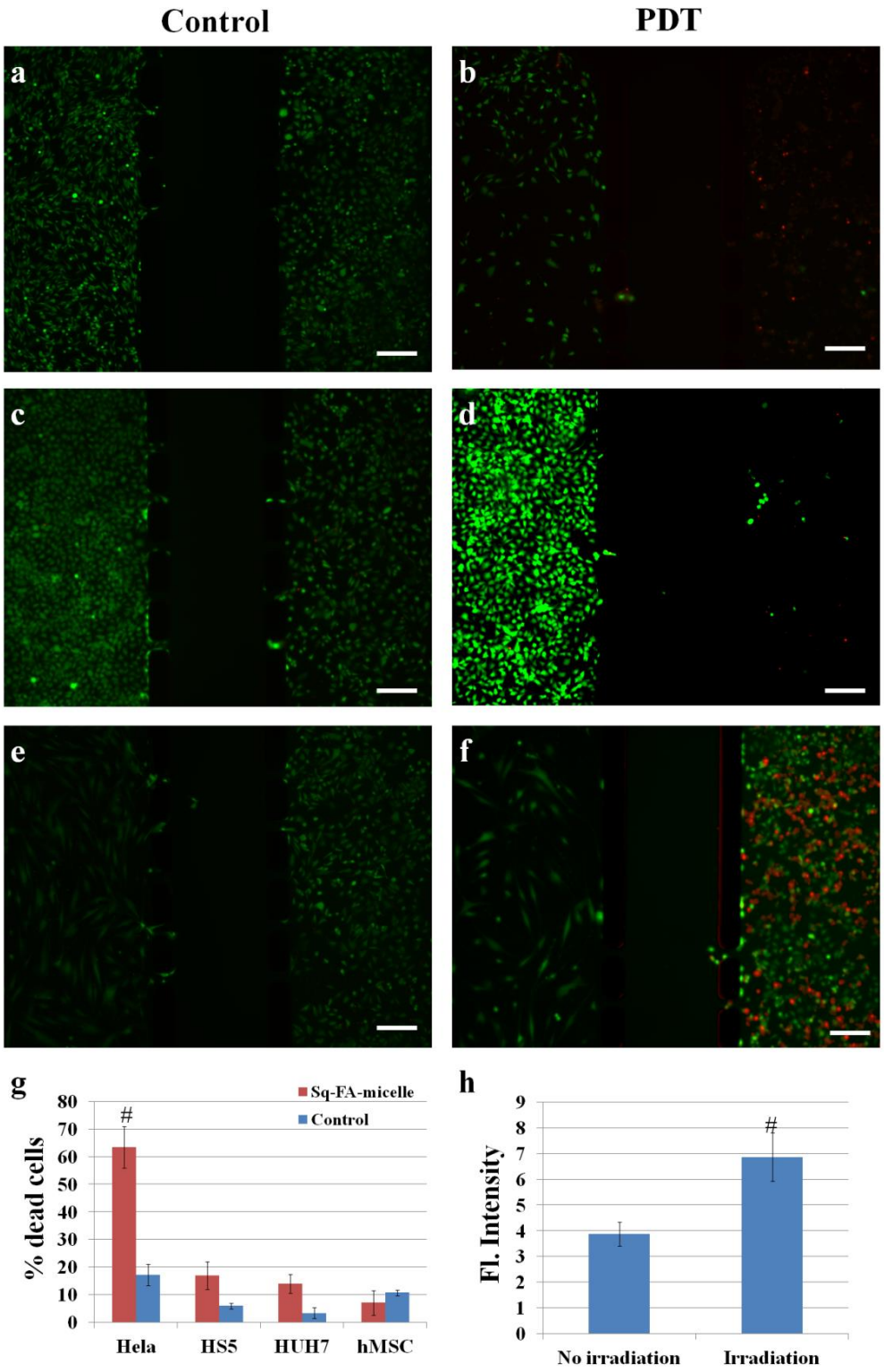

Figure 5.8:Live dead staining. (a) and (b) Live dead staining of control and PDT chip for HS5-Hela system. (c) and (d) Live dead staining of control and PDT chip for HuH7-Hela system.(e) and (f) Live dead staining of control and PDT chip for hMSC-Hela system. Scale bar: 200 µm. (g) Percentage of dead cells. (h) ROS determination from the fluorescence intensity of the cells after CMH2DCFDA staining. #p<0.0001.

5.4 Summary

In this chapter we have studied the use of a squaraine dye as potential PS for PDT. We have successfully encapsulated the dye within folic acid conjugated pluronic F127 micelle and have observed the selectivity of this dye-micelle system for targeting the folate receptor of the cancer cells using flow cytometry as well as using microscopy. Its potential as a PS for targeted PDT was confirmed by observing its ability to increase intracellular ROS within a FR positive cell type (Hela cells). With this study we have shown the ability to use the microfluidic chip for testing the efficacy of drugs. Such a model can act as the first phase during drug testing to see the impact of the drugs on human cells before proceeding for more complex organ on chip models as well as animal models.

Chapter 6 Conclusion and future work

Microfluidics has been proved to be an effective tool for many cell-based studies. Compared to conventional methods, the miniature size of microfluidic devices helps create a microenvironment that better mimics the natural cellular environment. In addition, the ability to precisely control flows and generation of biochemical gradient also helps adjust and maintain particular conditions favourable to cell growth and introduce biochemical cues to influence the cell fate. Researchers have taken advantage of these microfluidic platforms and successfully developed *in vitro* models for studying various important physiological phenomena, such as wound healing, cancer metastasis, and vascular angiogenesis.

In this research I have developed a simple and easy to use microfluidic *in vitro* model. The model was developed by a series of steps that involved selective plasma treatment, gelatin coating (to improve surface hydrophilicity), fibronectin coating followed by hydrophobic recovery at 40°C. Usage of 40°C ensured that there is better protein retention on the substrate. A second layer of protein coating was also performed so as to improve the cell adhesion and viability. The advantage of using such a protocol is that it allows for the culture of cells in separate compartments. To validate the functionality of the chip as an *in vitro* model we observed the interaction between hepatocarcinoma (Huh7) and bone marrow stroma (HS5). The observations from this study matched with those in literature from *in vivo* models thereby proving that such a model can be used as an *in vitro* model with good physiological relevance.

Once the validation was complete, the chip was used to understand the influence of substrate physical properties on hBMSC migration. In this study hBMSC migration on PDMS was observed. This was because the substrate properties (roughness, stiffness and hydrophobicity) of PDMS can be easily altered by changing its formulation (prepolymer to curing agent ratio). Cover slips spin coated with different PDMS formulations was used to seal the PDMS chips. The chip was modified using the protocol as discussed earlier and instead of co-culture, hBMSCs were cultured inside the chip. The cells were allowed to migrate for a week and its area of migration was calculated using image processing softwares (ImageJ). The molecular basis of the cell migration was also determined by quantifying the gene expression of cell adhesion proteins of N-cadherin and paxillin. From these results it was evident that cell migration was the maximum in a substrate having an intermediate level of roughness, stiffness and hydrophobicity unlike the studies in literature which indicate a direct or inverse relationship between physical properties and cell migration. The uniqueness of this study is that most studies that have

been conducted thus far have studied the impact of single properties (roughness or stiffness or hydrophobicity) on cell migration unlike in this study where the combinatorial impact of different substrate properties on hBMSC migration was studied.

Another application that I have focussed using the *in vitro* model is to test the efficacy of drugs. In this study, I have used the microfluidic co-culture model in order test the efficiency and selectivity of SQ encapsulated within a FA conjugated micelle to perform targeted imaging and PDT of cancer. The co-culture model developed involved a FR positive cell type and a FR negative cell type. Confocal microscopy and flow cytometry was performed to understand the selectivity of the PS. PDT was performed on chip by using a LED of 655 nm wavelength. From the results it was clear that the PS was highly selective to the FR positive cells and also SQ is efficient in bringing about photodynamic ttreatment of cancer. Hence such a microfluidic model will be of great use for performing preliminary studies for hypothesis testing.

In future we will add different parameters to the chip so as to increase its complexity. We intend to divulge from the current static systems to perfusion systems with the help of peristaltic or syringe pumps. Moreover studies have shown role of hypoxia in tumor development. *In-vivo,* solid tumors are less oxygenated with respect to the other cell types and studies have shown the impact of tumor hypoxia towards drug resistance. Hence it is important to develop suitable models that can replicate such conditions to form a better understanding of tumor progression. For chip development to mimic hypoxia, some easy methods are available in literature, like coating the chip with parylene or also by using an oxygen deficient incubator for performing cell culture.

Squaraine dye used in the study shows good photodynamic potential. Though only a 65% efficiency was achieved, the dye can be easily modified and with the use of a better light source (a laser source with 670 nm wavelength), the photodynamic efficiency can be increased further. The PS can be tested on 3D tissue culture models to optimize the dosage required for effective treatment following which the PS can be tested in an *in vivo* model.

I am also interested in extending the cell-substrate interaction work by using the model to test hBMSC migration on more physiologically relevant scaffolds like collagen, collagen-hydroxyapatite scaffolds, poly-L-lactic acid, etc which are scaffolds which have been used in regenerative tissue engineering. Once the relationship between these scaffold properties and hBMSC migration has been determined, it would be interesting to develop

a common mathematical model relating hBMSC migration to scaffold physical properties. Such a model can be extremely useful in regenerative tissue engineering as it may assist clinicians in deciding on ideal scaffold based on the injury.

Another future direction that we are currently working on is extending the results from these works from a 2D cell environment to a 3D cell environment. As stated earlier, such 3D models have been found to have better physiological relevance to the *in-vivo* environment as the cells in a 2D space and a 3D space behave differently. A similar 3-channel model can be used to develop such models by filing the central channel with a suitable scaffold like collagen, hydrogel or matrigel. The scaffold will act as a matrix supporting 3D migration or 3D interaction by the cells [240]. Apart from the creation of 3D migration models, as discussed in chapter 1 [Figure 1.4 (c-d)], cells can be cultured within inside a matrix like collagen or fibrin gel which is similar to a tissue culture procedure. In the example shown in Figure 1.4, Kim et al., [57] successfully created a 3D perfusable microvascular network which allowed for flow of microbeads through them. Similar techniques can be used for the creation of more complex tissue structures on chip. Apart from the use of scaffolds I would like to explore more avenues of microfluidic research, such as the usage of 3D microfluidics. 3D microfluidic system is one which involves multiple chips cascaded on top of each other and interconnected with each other. Such chips allow for efficient fluid control which can be used to design complex *in vitro* models.

With the involvement of clinicians into the developments of such models, microfluidics can indeed be used as an alternative to *in vivo* models and may serve as efficient tool in gaining a better understanding of the human physiology.

References

1. MacGowan, A.; Rogers, C.; Bowker, K. In Vitro Models, in Vivo Models, and Pharmacokinetics: What Can We Learn from in Vitro Models? *Clinical Infectious Diseases* **2001,** *33*, S214-S220.

2. DiMilla, P. A.; Stone, J. A.; Quinn, J. A.; Albelda, S. M.; Lauffenburger, D. A. Maximal Migration of Human Smooth Muscle Cells on Fibronectin and Type Iv Collagen Occurs at an Intermediate Attachment Strength. *Journal of Cell Biology* **1993,** *122*, 729-737.

3. Hendrix, M. J. C.; Seftor, E. A.; Seftor, R. E. B.; Fidler, I. J. A Simple Quantitative Assay for Studying the Invasive Potential of High and Low Human Metastatic Variants. *Cancer Letters* **1987,** *38*, 137-147.

4. Mace, K. A.; Hansen, S. L.; Myers, C.; Young, D. M.; Boudreau, N. Hoxa3 Induces Cell Migration in Endothelial and Epithelial Cells Promoting Angiogenesis and Wound Repair. *Journal of Cell Science* **2005,** *118*, 2567-2577.

5. Rojas, J. D.; Sennoune, S. R.; Maiti, D.; Bakunts, K.; Reuveni, M.; Sanka, S. C.; Martinez, G. M.; Seftor, E. A.; Meininger, C. J.; Wu, G.; Wesson, D. E.; Hendrix, M. J. C.; Martínez-Zaguilán, R. Vacuolar-Type H+-Atpases at the Plasma Membrane Regulate Ph and Cell Migration in Microvascular Endothelial Cells. *American Journal of Physiology - Heart and Circulatory Physiology* **2006,** *291*, H1147-H1157.

6. Sagnella, S. M.; Kligman, F.; Anderson, E. H.; King, J. E.; Murugesan, G.; Marchant, R. E.; Kottke-Marchant, K. Human Microvascular Endothelial Cell Growth and Migration on Biomimetic Surfactant Polymers. *Biomaterials* **2004,** *25*, 1249-1259.

7. Shizukuda, Y.; Tang, S.; Yokota, R.; Ware, J. A. Vascular Endothelial Growth Factor-Induced Endothelial Cell Migration and Proliferation Depend on a Nitric Oxide-Mediated Decrease in Protein Kinase Cδ Activity. *Circulation Research* **1999,** *85*, 247-256.

8. I., K. A. 2d- and 3d-Cell Culture. *Biopolymers and Cell* **2011,** *27*, 17-24.

9. Baker, B. M.; Chen, C. S. Deconstructing the Third Dimension – How 3d Culture Microenvironments Alter Cellular Cues. *Journal of Cell Science* **2012,** *125*, 3015-3024.

10. Rangarajan, A.; Weinberg, R. A. Comparative Biology of Mouse Versus Human Cells: Modelling Human Cancer in Mice. *Nature Reviews Cancer* **2003,** *3*, 952-959.

11. Seok, J.; Warren, H. S.; Cuenca, A. G.; Mindrinos, M. N.; Baker, H. V.; Xu, W.; Richards, D. R.; McDonald-Smith, G. P.; Gao, H.; Hennessy, L.; Finnerty, C. C.; López, C. M.; Honari, S.; Moore, E. E.; Minei, J. P.; Cuschieri, J.; Bankey, P. E.; Johnson, J. L.; Sperry, J.; Nathens, A. B.; Billiar, T. R.; West, M. A.; Jeschke, M. G.; Klein, M. B.; Gamelli, R. L.; Gibran, N. S.; Brownstein, B. H.; Miller-Graziano, C.; Calvano, S. E.; Mason, P. H.; Cobb, J. P.; Rahme, L. G.; Lowry, S. F.; Maier, R. V.; Moldawer, L. L.; Herndon, D. N.; Davis, R. W.; Xiao, W.; Tompkins, R. G.; Inflammation, t.; Host Response to Injury, L. S. C. R. P. Genomic Responses in Mouse Models Poorly Mimic Human Inflammatory Diseases. *Proceedings of the National Academy of Sciences of the United States of America* **2013,** *110*, 3507-3512.

12. May, J. E.; Morse, H. R.; Xu, J.; Donaldson, C. Development of a Novel, Physiologically Relevant Cytotoxicity Model: Application to the Study of Chemotherapeutic Damage to Mesenchymal Stromal Cells. *Toxicology and Applied Pharmacology* **2012,** *263*, 374-389.

13. Lo, K. A.; Labadorf, A.; Kennedy, N. J.; Han, M. S.; Yap, Y. S.; Matthews, B.; Xin, X.; Sun, L.; Davis, R. J.; Lodish, H. F.; Fraenkel, E. Analysis of in Vitro Insulin-Resistance Models and Their Physiological Relevance to in Vivo Diet-Induced Adipose Insulin Resistance. *Cell reports* **2013,** *5*, 259-270.

14. Meyvantsson, I.; Beebe, D. J. Cell Culture Models in Microfluidic Systems. *Annual Review of Analytical Chemistry* **2008,** *1*, 423-449.

15. Voldman, J.; Gray, M. L.; Schmidt, M. A. Microfabrication in Biology and Medicine. *Annual Review of Biomedical Engineering* **1999,** *1*, 401-425.

16. Inamdar, N. K.; Borenstein, J. T. Microfluidic Cell Culture Models for Tissue Engineering. *Current Opinion in Biotechnology* **2011,** *22*, 681-689.

17. Xue, P.; Wu, Y.; Menon, N.; Kang, Y. Microfluidic Synthesis of Monodisperse Pegda Microbeads for Sustained Release of 5-Fluorouracil. *Microfluidics and Nanofluidics* **2015,** *18*, 333-342.

18. Anna, S. L.; Bontoux, N.; Stone, H. A. Formation of Dispersions Using "Flow Focusing" in Microchannels. *Applied Physics Letters* **2003,** *82*, 364-366.

19. Davies, R. T.; Kim, J.; Jang, S. C.; Choi, E.-J.; Gho, Y. S.; Park, J. Microfluidic Filtration System to Isolate Extracellular Vesicles from Blood. *Lab on a Chip* **2012,** *12*, 5202-5210.

20. Berry, S. M.; Maccoux, L. J.; Beebe, D. J. Streamlining Immunoassays with Immiscible Filtrations Assisted by Surface Tension. *Analytical Chemistry* **2012,** *84*, 5518-5523.

21. Lee, S. H.; Heinz, A. J.; Shin, S.; Jung, Y.-G.; Choi, S.-E.; Park, W.; Roe, J.-H.; Kwon, S. Capillary Based Patterning of Cellular Communities in Laterally Open Channels. *Analytical Chemistry* **2010,** *82*, 2900-2906.

22. Phillips, T. W.; Lignos, I. G.; Maceiczyk, R. M.; deMello, A. J.; deMello, J. C. Nanocrystal Synthesis in Microfluidic Reactors: Where Next? *Lab on a Chip* **2014,** *14*, 3172-3180.

23. Dexter, J. P.; Parker, W. Parallel Combinatorial Chemical Synthesis Using Single-Layer Poly(Dimethylsiloxane) Microfluidic Devices. *Biomicrofluidics* **2009,** *3*, 034106-1-9.

24. Culbertson, C. T.; Mickleburgh, T. G.; Stewart-James, S. A.; Sellens, K. A.; Pressnall, M. Micro Total Analysis Systems: Fundamental Advances and Biological Applications. *Analytical Chemistry* **2014,** *86*, 95-118.

25. Kovarik, M. L.; Gach, P. C.; Ornoff, D. M.; Wang, Y.; Balowski, J.; Farrag, L.; Allbritton, N. L. Micro Total Analysis Systems for Cell Biology and Biochemical Assays. *Analytical Chemistry* **2012,** *84*, 516-540.

26. Cosson, S.; Lutolf, M. P. Hydrogel Microfluidics for the Patterning of Pluripotent Stem Cells. *Scientific Reports* **2014,** *4*, 1-6.

27. Cheng, S.-Y.; Heilman, S.; Wasserman, M.; Archer, S.; Shuler, M. L.; Wu, M. A Hydrogel-Based Microfluidic Device for the Studies of Directed Cell Migration. *Lab on a Chip* **2007,** *7*, 763-769.

28. Friend, J.; Yeo, L. Fabrication of Microfluidic Devices Using Polydimethylsiloxane. *Biomicrofluidics* **2010,** *4*, 026502-1-5.

29. Xia, Y.; Whitesides, G. M. Soft Lithography. *Annual Review of Materials Science* **1998,** *28*, 153-184.

30. Leclerc, E.; Sakai, Y.; Fujii, T. Cell Culture in 3-Dimensional Microfluidic Structure of Pdms (Polydimethylsiloxane). *Biomedical Microdevices* **2003,** *5*, 109-114.

31. Shevkoplyas, S. S.; Gifford, S. C.; Yoshida, T.; Bitensky, M. W. Prototype of an in Vitro Model of the Microcirculation. *Microvascular Research* **2003,** *65*, 132-136.

32. Yap, B.; Kamm, R. D. Mechanical Deformation of Neutrophils into Narrow Channels Induces Pseudopod Projection and Changes in Biomechanical Properties. *Journal of Applied Physiology* **2005,** *98*, 1930-1939.

33. Higgins, J. M.; Eddington, D. T.; Bhatia, S. N.; Mahadevan, L. Sickle Cell Vasoocclusion and Rescue in a Microfluidic Device. *Proceedings of the National Academy of Sciences of the United States of America* **2007,** *104*, 20496-20500.

34. Quinto-Su, P. A.; Kuss, C.; Preiser, P. R.; Ohl, C.-D. Red Blood Cell Rheology Using Single Controlled Laser-Induced Cavitation Bubbles. *Lab on a Chip* **2011,** *11*, 672-678.

35. Ye, T.; Li, H.; Lam, K. Y. Motion, Deformation and Aggregation of Two Cells in a Microchannel by Dielectrophoresis. *Electrophoresis* **2011,** *32*, 3147-3156.

36. Shao, J.; Wu, L.; Wu, J.; Zheng, Y.; Zhao, H.; Jin, Q.; Zhao, J. Integrated Microfluidic Chip for Endothelial Cells Culture and Analysis Exposed to a Pulsatile and Oscillatory Shear Stress. *Lab on a Chip* **2009,** *9*, 3118-3125.

37. Khan, O. F.; Sefton, M. V. Endothelial Cell Behaviour within a Microfluidic Mimic of the Flow Channels of a Modular Tissue Engineered Construct. *Biomedical Microdevices* **2011,** *13*, 69-87.

38. Chau, L.; Doran, M.; Cooper-White, J. A Novel Multishear Microdevice for Studying Cell Mechanics. *Lab on a Chip* **2009,** *9*, 1897-1902.

39. Gordon, J. L. Extracellular Atp: Effects, Sources and Fate. *Biochemical Journal* **1986,** *233*, 309-319.

40. Zhu, H.; Zennadi, R.; Xu, B. X.; Eu, J. P.; Torok, J. A.; Telen, M. J.; McMahon, T. J. Impaired Atp Release from Red Blood Cells Promotes Their Adhesion to Endothelial Cells: A Mechanism of Hypoxemia after Transfusion. *Critical care medicine* **2011,** *39*, 2478-2486.

41. Subasinghe, W.; Spence, D. M. Simultaneous Determination of Cell Aging and Atp Release from Erythrocytes and Its Implications in Type 2 Diabetes. *Analytica Chimica Acta* **2008,** *618*, 227-233.

42. Moehlenbrock, M. J.; Price, A. K.; Martin, R. S. Use of Microchip-Based Hydrodynamic Focusing to Measure the Deformation-Induced Release of Atp from Erythrocytes. *Analyst* **2006,** *131*, 930-937.

43. Price, A. K.; Martin, R. S.; Spence, D. M. Monitoring Erythrocytes in a Microchip Channel That Narrows Uniformly: Towards an Improved Microfluidic-Based Mimic of the Microcirculation. *Journal of Chromatography A* **2006,** *1111*, 220-227.

44. Wan, J.; Ristenpart, W. D.; Stone, H. A. Dynamics of Shear-Induced Atp Release from Red Blood Cells. *Proceedings of the National Academy of Sciences of the United States of America* **2008,** *105*, 16432-16437.

45. Liang, C.-C.; Park, A. Y.; Guan, J.-L. In Vitro Scratch Assay: A Convenient and Inexpensive Method for Analysis of Cell Migration in Vitro. *Nature Protocols* **2007,** *2*, 329-333.

46. Van Horssen, R.; ten Hagen, T. L. Crossing Barriers: The New Dimension of 2d Cell Migration Assays. *Journal of Cellular Physiology* **2011,** *226*, 288-290.

47. Felder, M.; Sallin, P.; Barbe, L.; Haenni, B.; Gazdhar, A.; Geiser, T.; Guenat, O. Microfluidic Wound-Healing Assay to Assess the Regenerative Effect of Hgf on Wounded Alveolar Epithelium. *Lab on a Chip* **2012,** *12*, 640-646.

48. Van der Meer, A. D.; Vermeul, K.; Poot, A. A.; Feijen, J.; Vermes, I. A Microfluidic Wound-Healing Assay for Quantifying Endothelial Cell Migration. *American Journal of Physiology - Heart and Circulatory Physiology* **2010,** *298*, H719-H725.

49. Punde, T. H.; Wen-Hao, W.; Po-Chen, S.; Chien-Yu, F.; Tsung-Pao, W.; Long, H.; Hawn-You, C.; Cheng-Hsien, L., A 3-D Capillary-Endothelium-Mimetic Microfluidic Chip for Studying the Extravasation Behaviour of Neutrophils. In *Solid-State Sensors, Actuators and Microsystems Conference (Transducers), 2011 16th International*, Beijing, **2011**; pp 2251-2254.

50. Han, S.; Yan, J.-J.; Shin, Y.; Jeon, J. J.; Won, J.; Eun Jeong, H.; Kamm, R. D.; Kim, Y.-J.; Chung, S. A Versatile Assay for Monitoring in Vivo-Like Transendothelial Migration of Neutrophils. *Lab on a Chip* **2012,** *12*, 3861-3865.

51. Li, Y.-H.; Zhu, C. A Modified Boyden Chamber Assay for Tumor Cell Transendothelial Migration In vitro. *Clin Exp Metastasis* **1999,** *17*, 423-429.

52. Jeong, G. S.; Han, S.; Shin, Y.; Kwon, G. H.; Kamm, R. D.; Lee, S. H.; Chung, S. Sprouting Angiogenesis under a Chemical Gradient Regulated by Interactions with an Endothelial Monolayer in a Microfluidic Platform. *Analytical Chemistry* **2011,** *83*, 8454-8459.

53. Chung, S.; Sudo, R.; Zervantonakis, I. K.; Rimchala, T.; Kamm, R. D. Surface-Treatment-Induced Three-Dimensional Capillary Morphogenesis in a Microfluidic Platform. *Advanced Materials* **2009,** *21*, 4863-4867.

54. Shin, Y.; Jeon, J. S.; Han, S.; Jung, G.-S.; Shin, S.; Lee, S.-H.; Sudo, R.; Kamm, R. D.; Chung, S. In Vitro 3d Collective Sprouting Angiogenesis under Orchestrated Ang-1 and Vegf Gradients. *Lab on a Chip* **2011,** *11*, 2175-2181.

55. Chung, S.; Sudo, R.; Mack, P. J.; Wan, C.-R.; Vickerman, V.; Kamm, R. D. Cell Migration into Scaffolds under Co-Culture Conditions in a Microfluidic Platform. *Lab on a Chip* **2009,** *9*, 269-275.

56. Sudo, R.; Chung, S.; Zervantonakis, I. K.; Vickerman, V.; Toshimitsu, Y.; Griffith, L. G.; Kamm, R. D. Transport-Mediated Angiogenesis in 3d Epithelial Coculture. *The FASEB journal* **2009,** *23*, 2155-2164.

57. Kim, S.; Lee, H.; Chung, M.; Jeon, N. L. Engineering of Functional, Perfusable 3d Microvascular Networks on a Chip. *Lab on a Chip* **2013,** *13*, 1489-1500.

58. Golden, A. P.; Tien, J. Fabrication of Microfluidic Hydrogels Using Molded Gelatin as a Sacrificial Element. *Lab on a Chip* **2007,** *7*, 720-725.

59. Chrobak, K. M.; Potter, D. R.; Tien, J. Formation of Perfused, Functional Microvascular Tubes in Vitro. *Microvascular Research* **2006,** *71*, 185-196.

60. Hay, M.; Thomas, D. W.; Craighead, J. L.; Economides, C.; Rosenthal, J. Clinical Development Success Rates for Investigational Drugs. *Nature Biotechnology* **2014,** *32*, 40-51.

61. McCain, M. L.; Sheehy, S. P.; Grosberg, A.; Goss, J. A.; Parker, K. K. Recapitulating Maladaptive, Multiscale Remodeling of Failing Myocardium on a Chip. *Proceedings of the National Academy of Sciences of the United States of America* **2013,** *110*, 9770-9775.

62. Mathur, A.; Loskill, P.; Shao, K.; Huebsch, N.; Hong, S.; Marcus, S. G.; Marks, N.; Mandegar, M.; Conklin, B. R.; Lee, L. P.; Healy, K. E. Human Ipsc-Based Cardiac Microphysiological System for Drug Screening Applications. *Scientific Reports* **2015,** *5*, 1-7.

63. Huh, D.; Leslie, D. C.; Matthews, B. D.; Fraser, J. P.; Jurek, S.; Hamilton, G. A.; Thorneloe, K. S.; McAlexander, M. A.; Ingber, D. E. A Human Disease Model of Drug

Toxicity-Induced Pulmonary Edema in a Lung-on-a-Chip Microdevice. *Science Translational Medicine* **2012,** *4*, 159ra147-1-8.

64. Huh, D.; Matthews, B. D.; Mammoto, A.; Montoya-Zavala, M.; Hsin, H. Y.; Ingber, D. E. Reconstituting Organ-Level Lung Functions on a Chip. *Science* **2010,** *328*, 1662-1668.

65. Tavana, H.; Zamankhan, P.; Christensen, P. J.; Grotberg, J. B.; Takayama, S. Epithelium Damage and Protection During Reopening of Occluded Airways in a Physiologic Microfluidic Pulmonary Airway Model. *Biomedical Microdevices* **2011,** *13*, 731-742.

66. Esch, E. W.; Bahinski, A.; Huh, D. Organs-on-Chips at the Frontiers of Drug Discovery. *Nature Reviews Drug Discovery* **2015,** *14*, 248-260.

67. Ho, C.-T.; Lin, R.-Z.; Chang, W.-Y.; Chang, H.-Y.; Liu, C.-H. Rapid Heterogeneous Liver-Cell on-Chip Patterning Via the Enhanced Field-Induced Dielectrophoresis Trap. *Lab on a Chip* **2006,** *6*, 724-734.

68. Lee, J.; Kim, S. H.; Kim, Y.-C.; Choi, I.; Sung, J. H. Fabrication and Characterization of Microfluidic Liver-on-a-Chip Using Microsomal Enzymes. *Enzyme and Microbial Technology* **2013,** *53*, 159-164.

69. Lee, S.-A.; No, D. Y.; Kang, E.; Ju, J.; Kim, D.-S.; Lee, S.-H. Spheroid-Based Three-Dimensional Liver-on-a-Chip to Investigate Hepatocyte-Hepatic Stellate Cell Interactions and Flow Effects. *Lab on a Chip* **2013,** *13*, 3529-3537.

70. Kim, H. J.; Huh, D.; Hamilton, G.; Ingber, D. E. Human Gut-on-a-Chip Inhabited by Microbial Flora That Experiences Intestinal Peristalsis-Like Motions and Flow. *Lab on a Chip* **2012,** *12*, 2165-2174.

71. Kim, H. J.; Ingber, D. E. Gut-on-a-Chip Microenvironment Induces Human Intestinal Cells to Undergo Villus Differentiation. *Integrative Biology* **2013,** *5*, 1130-1140.

72. Snouber, L. C.; Letourneur, F.; Chafey, P.; Broussard, C.; Monge, M.; Legallais, C.; Leclerc, E. Analysis of Transcriptomic and Proteomic Profiles Demonstrates Improved Madin–Darby Canine Kidney Cell Function in a Renal Microfluidic Biochip. *Biotechnology Progress* **2012,** *28*, 474-484.

73. Huang, H.-C.; Chang, Y.-J.; Chen, W.-C.; Harn, H. I. C.; Tang, M.-J.; Wu, C.-C. Enhancement of Renal Epithelial Cell Functions through Microfluidic-Based Coculture with Adipose-Derived Stem Cells. *Tissue Engineering Part A* **2013,** *19*, 2024-2034.

74. Jang, K.-J.; Suh, K.-Y. A Multi-Layer Microfluidic Device for Efficient Culture and Analysis of Renal Tubular Cells. *Lab on a Chip* **2010,** *10*, 36-42.

75. Jang, K.-J.; Mehr, A. P.; Hamilton, G. A.; McPartlin, L. A.; Chung, S.; Suh, K.-Y.; Ingber, D. E. Human Kidney Proximal Tubule-on-a-Chip for Drug Transport and Nephrotoxicity Assessment. *Integrative Biology* **2013,** *5*, 1119-1129.

76. Torisawa, Y.-s.; Spina, C. S.; Mammoto, T.; Mammoto, A.; Weaver, J. C.; Tat, T.; Collins, J. J.; Ingber, D. E. Bone Marrow–on–a–Chip Replicates Hematopoietic Niche Physiology in Vitro. *Nature Methods* **2014,** *11*, 663-669.

77. Chung, S.; Sudo, R.; Vickerman, V.; Zervantonakis, I. K.; Kamm, R. D. Microfluidic Platforms for Studies of Angiogenesis, Cell Migration, and Cell-Cell Interactions: Sixth International Bio-Fluid Mechanics Symposium and Workshop March 28-30, 2008 Pasadena, California. *Annals of Biomedical Engineering* **2010,** *38*, 1164-1177.

78. Zervantonakis, I. K.; Hughes-Alford, S. K.; Charest, J. L.; Condeelis, J. S.; Gertler, F. B.; Kamm, R. D. Three-Dimensional Microfluidic Model for Tumor Cell Intravasation and Endothelial Barrier Function. *Proceedings of the National Academy of Sciences of the United States of America* **2012,** *109*, 13515-13520.

79. Sung, K. E.; Yang, N.; Pehlke, C.; Keely, P. J.; Eliceiri, K. W.; Friedl, A.; Beebe, D. J. Transition to Invasion in Breast Cancer: A Microfluidic in Vitro Model Enables Examination of Spatial and Temporal Effects. *Integrative Biology* **2011,** *3*, 439-450.

80. Bersini, S.; Jeon, J. S.; Dubini, G.; Arrigoni, C.; Chung, S.; Charest, J. L.; Moretti, M.; Kamm, R. D. A Microfluidic 3d In vitro Model for Specificity of Breast Cancer Metastasis to Bone. *Biomaterials* **2014,** *35*, 2454-2461.

81. Walsh, C. L.; Babin, B. M.; Kasinskas, R. W.; Foster, J. A.; McGarry, M. J.; Forbes, N. S. A Multipurpose Microfluidic Device Designed to Mimic Microenvironment Gradients and Develop Targeted Cancer Therapeutics. *Lab on a Chip* **2009,** *9*, 545-554.

82. Vidi, P.-A.; Maleki, T.; Ochoa, M.; Wang, L.; Clark, S. M.; Leary, J. F.; Lelievre, S. A. Disease-on-a-Chip: Mimicry of Tumor Growth in Mammary Ducts. *Lab on a Chip* **2014,** *14*, 172-177.

83. Aref, A. R.; Huang, R. Y.-J.; Yu, W.; Chua, K.-N.; Sun, W.; Tu, T.-Y.; Bai, J.; Sim, W.-J.; Zervantonakis, I. K.; Thiery, J. P.; Kamm, R. D. Screening Therapeutic Emt Blocking Agents in a Three-Dimensional Microenvironment. *Integrative Biology* **2013,** *5*, 381-389.

84. Imura, Y.; Sato, K.; Yoshimura, E. Micro Total Bioassay System for Ingested Substances: Assessment of Intestinal Absorption, Hepatic Metabolism, and Bioactivity. *Analytical Chemistry* **2010,** *82*, 9983-9988.

85. Sung, J. H.; Shuler, M. L. A Micro Cell Culture Analog ([Small Micro]Cca) with 3-D Hydrogel Culture of Multiple Cell Lines to Assess Metabolism-Dependent Cytotoxicity of Anti-Cancer Drugs. *Lab on a Chip* **2009,** *9*, 1385-1394.

86. Zhang, C.; Zhao, Z.; Abdul Rahim, N. A.; van Noort, D.; Yu, H. Towards a Human-on-Chip: Culturing Multiple Cell Types on a Chip with Compartmentalized Microenvironments. *Lab on a Chip* **2009,** *9*, 3185-3192.

87. Sung, J. H.; Kam, C.; Shuler, M. L. A Microfluidic Device for a Pharmacokinetic-Pharmacodynamic (Pk-Pd) Model on a Chip. *Lab on a Chip* **2010,** *10*, 446-455.

88. Phelps, M. S.; Verbeck, G. F. A Lipidomics Demonstration of the Importance of Single Cell Analysis. *Analytical Methods* **2015,** *7*, 3668-3670.

89. Wu, H.; Wheeler, A.; Zare, R. N. Chemical Cytometry on a Picoliter-Scale Integrated Microfluidic Chip. *Proceedings of the National Academy of Sciences of the United States of America* **2004,** *101*, 12809-12813.

90. Hellmich, W.; Pelargus, C.; Leffhalm, K.; Ros, A.; Anselmetti, D. Single Cell Manipulation, Analytics, and Label-Free Protein Detection in Microfluidic Devices for Systems Nanobiology. *Electrophoresis* **2005,** *26*, 3689-3696.

91. Huang, N.-T.; Zhang, H.-l.; Chung, M.-T.; Seo, J. H.; Kurabayashi, K. Recent Advancements in Optofluidics-Based Single-Cell Analysis: Optical on-Chip Cellular Manipulation, Treatment, and Property Detection. *Lab on a Chip* **2014,** *14*, 1230-1245.

92. Hunt, T. P.; Westervelt, R. M. Dielectrophoresis Tweezers for Single Cell Manipulation. *Biomedical Microdevices* **2006,** *8*, 227-230.

93. Lim, B.; Reddy, V.; Hu, X.; Kim, K.; Jadhav, M.; Abedini-Nassab, R.; Noh, Y.-W.; Lim, Y. T.; Yellen, B. B.; Kim, C. Magnetophoretic Circuits for Digital Control of Single Particles and Cells. *Nature Communication* **2014,** *5*, 1-10.

94. Marcy, Y.; Ouverney, C.; Bik, E. M.; Lösekann, T.; Ivanova, N.; Martin, H. G.; Szeto, E.; Platt, D.; Hugenholtz, P.; Relman, D. A.; Quake, S. R. Dissecting Biological "Dark Matter" with Single-Cell Genetic Analysis of Rare and Uncultivated Tm7 Microbes from the Human Mouth. *Proceedings of the National Academy of Sciences of the United States of America* **2007,** *104*, 11889-11894.

95. Toriello, N. M.; Douglas, E. S.; Thaitrong, N.; Hsiao, S. C.; Francis, M. B.; Bertozzi, C. R.; Mathies, R. A. Integrated Microfluidic Bioprocessor for Single-Cell Gene Expression Analysis. *Proceedings of the National Academy of Sciences of the United States of America* **2008,** *105*, 20173-20178.

96. Huang, B.; Wu, H.; Bhaya, D.; Grossman, A.; Granier, S.; Kobilka, B. K.; Zare, R. N. Counting Low-Copy Number Proteins in a Single Cell. *Science* **2007,** *315*, 81-84.

97. Salehi-Reyhani, A.; Kaplinsky, J.; Burgin, E.; Novakova, M.; Demello, A. J.; Templer, R. H.; Parker, P.; Neil, M. A. A.; Ces, O.; French, P.; Willison, K. R.; Klug, D. A First Step Towards Practical Single Cell Proteomics: A Microfluidic Antibody Capture Chip with Tirf Detection. *Lab on a Chip* **2011,** *11*, 1256-1261.

98. Amantonico, A.; Urban, P. L.; Oh, J. Y.; Zenobi, R. Interfacing Microfluidics and Laser Desorption/Ionization Mass Spectrometry by Continuous Deposition for Application in Single Cell Analysis. *Chimia* **2009,** *63*, 185-188.

99. Brouzes, E.; Medkova, M.; Savenelli, N.; Marran, D.; Twardowski, M.; Hutchison, J. B.; Rothberg, J. M.; Link, D. R.; Perrimon, N.; Samuels, M. L. Droplet Microfluidic Technology for Single-Cell High-Throughput Screening. *Proceedings of the National Academy of Sciences of the United States of America* **2009,** *106*, 14195-14200.

100. Kellogg, R. A.; Gómez-Sjöberg, R.; Leyrat, A. A.; Tay, S. High-Throughput Microfluidic Single-Cell Analysis Pipeline for Studies of Signaling Dynamics. *Nature Protocols* **2014,** *9*, 1713-1726.

101. Fan, H. C.; Wang, J.; Potanina, A.; Quake, S. R. Whole-Genome Molecular Haplotyping of Single Cells. *Nature Biotechnology* **2011,** *29*, 51-57.

102. Sackmann, E. K.; Fulton, A. L.; Beebe, D. J. The Present and Future Role of Microfluidics in Biomedical Research. *Nature* **2014,** *507*, 181-189.

103. Folch, A.; Toner, M. Microengineering of Cellular Interactions. *Annual Review of Biomedical Engineering* **2000,** *2*, 227-256.

104. Rhee, S. W.; Taylor, A. M.; Tu, C. H.; Cribbs, D. H.; Cotman, C. W.; Jeon, N. L. Patterned Cell Culture inside Microfluidic Devices. *Lab on a Chip* **2005,** *5*, 102-107.

105. Goubko, C. A.; Cao, X. Patterning Multiple Cell Types in Co-Cultures: A Review. *Materials Science and Engineering: C* **2009,** *29*, 1855-1868.

106. Sia, S. K.; Whitesides, G. M. Microfluidic Devices Fabricated in Poly(Dimethylsiloxane) for Biological Studies. *Electrophoresis* **2003,** *24*, 3563-3576.

107. McDonald, J. C.; Duffy, D. C.; Anderson, J. R.; Chiu, D. T.; Wu, H.; Schueller, O. J.; Whitesides, G. M. Fabrication of Microfluidic Systems in Poly(Dimethylsiloxane). *Electrophoresis* **2000,** *21*, 27-40.

108. Owen, M. J.; Smith, P. J. Plasma Treatment of Polydimethylsiloxane. *Journal of Adhesion Science and Technology* **1994,** *8*, 1063-1075.

109. Bhattacharya, S.; Datta, A.; Berg, J. M.; Gangopadhyay, S. Studies on Surface Wettability of Poly(Dimethyl) Siloxane (Pdms) and Glass under Oxygen-Plasma Treatment and Correlation with Bond Strength. *Journal of Microelectromechanical Systems* **2005,** *14*, 590-597.

110. Crouzier, T.; Jang, H.; Ahn, J.; Stocker, R.; Ribbeck, K. Cell Patterning with Mucin Biopolymers. *Biomacromolecules* **2013,** *14*, 3010-3016.

111. Kohchi, C.; Inagawa, H.; Nishizawa, T.; Soma, G. Ros and Innate Immunity. *Anticancer Research* **2009,** *29*, 817-21.

112. Livak, K. J.; Schmittgen, T. D. Analysis of Relative Gene Expression Data Using Real-Time Quantitative Pcr and the 2−Δδct Method. *Methods* **2001,** *25*, 402-408.

113. Binnig, G.; Quate, C. F.; Gerber, C. Atomic Force Microscope. *Physical Review Letters* **1986,** *56*, 930-933.

114. Wu, Y.-N.; Law, J. B. K.; He, A. Y.; Low, H. Y.; Hui, J. H. P.; Lim, C. T.; Yang, Z.; Lee, E. H. Substrate Topography Determines the Fate of Chondrogenesis from Human Mesenchymal Stem Cells Resulting in Specific Cartilage Phenotype Formation. *Nanomedicine: Nanotechnology, Biology and Medicine* **2014,** *10*, 1507-1516.

115. Clark, B. R.; Keating, A. Biology of Bone Marrow Stroma. *Annals of the New York Academy of Sciences* **1995,** *770*, 70-78.

116. Bhatia, S. N.; Balis, U. J.; Yarmush, M. L.; Toner, M. Effect of Cell–Cell Interactions in Preservation of Cellular Phenotype: Cocultivation of Hepatocytes and Nonparenchymal Cells. *The FASEB Journal* **1999,** *13*, 1883-1900.

117. Chaffer, C. L.; Weinberg, R. A. A Perspective on Cancer Cell Metastasis. *Science* **2011,** *331*, 1559-1564.

118. Ingber, D. E. Cancer as a Disease of Epithelial–Mesenchymal Interactions and Extracellular Matrix Regulation. *Differentiation* **2002,** *70*, 547-560.

119. Grinnell, F. Wound Repair, Keratinocyte Activation and Integrin Modulation. *Journal of Cell Science* **1992,** *101*, 1-5.

120. Kramer, N.; Walzl, A.; Unger, C.; Rosner, M.; Krupitza, G.; Hengstschläger, M.; Dolznig, H. In Vitro Cell Migration and Invasion Assays. *Reviews in Mutation Research* **2013,** *752*, 10-24.

121. Brown, N.; Bicknell, R., Cell Migration and the Boyden Chamber. In *Metastasis Research Protocols*, Brooks, S.; Schumacher, U., Eds. Humana Press: **2001**; Chapter 5, pp 47-54.

122. Kozien, D.; Gerol, M.; Hendey, B.; RayChaudhury, A. A Novel in Vitro Model of Tumor Angiogenesis. *In Vitro Cell.Dev.Biol.-Animal* **2000,** *36*, 555-558.

123. Shi, J.; Ahmed, D.; Mao, X.; Lin, S.-C. S.; Lawit, A.; Huang, T. J. Acoustic Tweezers: Patterning Cells and Microparticles Using Standing Surface Acoustic Waves (Ssaw). *Lab on a Chip* **2009,** *9*, 2890-2895.

124. Ino, K.; Ito, A.; Honda, H. Cell Patterning Using Magnetite Nanoparticles and Magnetic Force. *Biotechnology and Bioengineering* **2007,** *97*, 1309-1317.

125. Odde, D. J.; Renn, M. J. Laser-Guided Direct Writing of Living Cells. *Biotechnology and Bioengineering* **2000,** *67*, 312-318.

126. Lin, R.-Z.; Ho, C.-T.; Liu, C.-H.; Chang, H.-Y. Dielectrophoresis Based-Cell Patterning for Tissue Engineering. *Biotechnology Journal* **2006,** *1*, 949-957.

127. Yang, S.-M.; Yu, T.-M.; Huang, H.-P.; Ku, M.-Y.; Hsu, L.; Liu, C.-H. Dynamic Manipulation and Patterning of Microparticles and Cells by Using Tiopc-Based Optoelectronic Dielectrophoresis. *Optics Letters* **2010,** *35*, 1959-1961.

128. Roth, E. A.; Xu, T.; Das, M.; Gregory, C.; Hickman, J. J.; Boland, T. Inkjet Printing for High-Throughput Cell Patterning. *Biomaterials* **2004,** *25*, 3707-3715.

129. Lee, K. B.; Park, S. J.; Mirkin, C. A.; Smith, J. C.; Mrksich, M. Protein Nanoarrays Generated by Dip-Pen Nanotithography. *Science* **2002,** *295*, 1702-1705.

130. Tehranirokh, M.; Kouzani, A. Z.; Francis, P. S.; Kanwar, J. R. Microfluidic Devices for Cell Cultivation and Proliferation. *Biomicrofluidics* **2013,** *7*, 051502-1-32.

131. Gao, Y.; Majumdar, D.; Jovanovic, B.; Shaifer, C.; Lin, P. C.; Zijlstra, A.; Webb, D.; Li, D. A Versatile Valve-Enabled Microfluidic Cell Co-Culture Platform and Demonstration of Its Applications to Neurobiology and Cancer Biology. *Biomedical Microdevices* **2011,** *13*, 539-548.

132. Brewer, B.; Shi, M.; Edd, J.; Webb, D.; Li, D. A Microfluidic Cell Co-Culture Platform with a Liquid Fluorocarbon Separator. *Biomedical Microdevices* **2014,** *16*, 311-323.

133. Zhao, B.; Moore, J. S.; Beebe, D. J. Surface-Directed Liquid Flow inside Microchannels. *Science* **2001,** *291*, 1023-1026.

134. Ciofani, G.; Migliore, A.; Raffa, V.; Menciassi, A.; Dario, P. Bicompartmental Device for Dynamic Cell Coculture: Design, Realisation and Preliminary Results. *Journal of Bioscience and Bioengineering* **2008,** *105*, 536-544.

135. Kaji, H.; Yokoi, T.; Kawashima, T.; Nishizawa, M. Controlled Cocultures of Hela Cells and Human Umbilical Vein Endothelial Cells on Detachable Substrates. *Lab on a Chip* **2009,** *9*, 427-432.

136. Zervantonakis, I. K.; Kothapalli, C. R.; Chung, S.; Sudo, R.; Kamm, R. D. Microfluidic Devices for Studying Heterotypic Cell-Cell Interactions and Tissue Specimen Cultures under Controlled Microenvironments. *Biomicrofluidics* **2011,** *5*, 013406-1-14.

137. Wei, C.-W.; Cheng, J.-Y.; Young, T.-H. Elucidating in Vitro Cell-Cell Interaction Using a Microfluidic Coculture System. *Biomedical Microdevices* **2006,** *8*, 65-71.

138. Hong, J. W.; Song, S.; Shin, J. H. A Novel Microfluidic Co-Culture System for Investigation of Bacterial Cancer Targeting. *Lab on a Chip* **2013,** *13*, 3033-3040.

139. Bai, H.; Weng, Y.; Bai, S.; Jiang, Y.; Li, B.; He, F.; Zhang, R.; Yan, S.; Deng, F.; Wang, J.; Shi, Q. Ccl5 Secreted from Bone Marrow Stromal Cells Stimulates the Migration and Invasion of Huh7 Hepatocellular Carcinoma Cells Via the Pi3k-Akt Pathway. *International journal of oncology* **2014,** *45*, 333-43.

140. Lee, J. N.; Jiang, X.; Ryan, D.; Whitesides, G. M. Compatibility of Mammalian Cells on Surfaces of Poly(Dimethylsiloxane). *Langmuir* **2004,** *20*, 11684-11691.

141. Kuddannaya, S.; Chuah, Y. J.; Lee, M. H. A.; Menon, N. V.; Kang, Y.; Zhang, Y. Surface Chemical Modification of Poly(Dimethylsiloxane) for the Enhanced Adhesion and Proliferation of Mesenchymal Stem Cells. *ACS Applied Materials & Interfaces* **2013,** *5*, 9777-9784.

142. Makamba, H.; Kim, J. H.; Lim, K.; Park, N.; Hahn, J. H. Surface Modification of Poly(Dimethylsiloxane) Microchannels. *Electrophoresis* **2003,** *24*, 3607-3619.

143. Dinh, N.-D.; Chiang, Y.-Y.; Hardelauf, H.; Baumann, J.; Jackson, E.; Waide, S.; Sisnaiske, J.; Frimat, J.-P.; Thriel, C. v.; Janasek, D.; Peyrin, J.-M.; West, J. Microfluidic Construction of Minimalistic Neuronal Co-Cultures. *Lab on a Chip* **2013,** *13*, 1402-1412.

144. Priest, C.; Gruner, P. J.; Szili, E. J.; Al-Bataineh, S. A.; Bradley, J. W.; Ralston, J.; Steele, D. A.; Short, R. D. Microplasma Patterning of Bonded Microchannels Using High-Precision "Injected" Electrodes. *Lab on a Chip* **2011,** *11*, 541-544.

145. Tourovskaia, A.; Barber, T.; Wickes, B. T.; Hirdes, D.; Grin, B.; Castner, D. G.; Healy, K. E.; Folch, A. Micropatterns of Chemisorbed Cell Adhesion-Repellent Films Using Oxygen Plasma Etching and Elastomeric Masks. *Langmuir* **2003,** *19*, 4754-4764.

146. Białopiotrowicz, T.; Jańczuk, B. Changes of the Surface Free Energy of the Adsorptive Gelatin Films. *European Polymer Journal* **2001,** *37*, 1047-1051.

147. Fritz, J. L.; Owen, M. J. Hydrophobic Recovery of Plasma-Treated Polydimethylsiloxane. *The Journal of Adhesion* **1995,** *54*, 33-45.

148. Castellone, M. D.; Laatikainen, L. E.; Laurila, J. P.; Langella, A.; Hematti, P.; Soricelli, A.; Salvatore, M.; Laukkanen, M. O. Brief Report: Mesenchymal Stromal Cell Atrophy in Coculture Increases Aggressiveness of Transformed Cells. *STEM CELLS* **2013,** *31*, 1218-1223.

149. Vallabhaneni, K. C.; Haller, H.; Dumler, I. Vascular Smooth Muscle Cells Initiate Proliferation of Mesenchymal Stem Cells by Mitochondrial Transfer Via Tunneling Nanotubes. *Stem cells and development* **2012,** *21*, 3104-3113.

150. Paduch, R.; Walter-Croneck, A.; Zdzisińska, B.; Szuster-Ciesielska, A.; Kandefer-Szerszeń, M. Role of Reactive Oxygen Species (Ros), Metalloproteinase-2 (Mmp-2) and

Interleukin-6 (Il-6) in Direct Interactions between Tumour Cell Spheroids and Endothelial Cell Monolayer. *Cell Biology International* **2005,** *29*, 497-505.

151. Fiaschi, T.; Chiarugi, P. Oxidative Stress, Tumor Microenvironment, and Metabolic Reprogramming: A Diabolic Liaison. *International Journal of Cell Biology* **2012,** *2012*, 1-8.

152. Ubaldo E. Martinez-Outschoorn, R. M. B., Dayana Rivadeneira, Barbara Chiavarina, Stephanos Pavlides, Chenguang Wang, Diana Whitaker-Menezes, Kristin Daumer, Zhao Lin, Agnieszka Witkiewicz, Neal Flomenberg, Anthony Howell, Richard Pestell, Erik Knudsen, Federica Sotgia & Michael P. Lisanti Oxidative Stress in Cancer Associated Fibroblasts Drives Tumor-Stroma Co-Evolution. *Cell Cycle* **2010,** *9*, 3256-3276.

153. Lin, R. Z.; Wang, T. P.; Hung, R. J.; Chuang, Y. J.; Chien, C. C.; Chang, H. Y. Tumor-Induced Endothelial Cell Apoptosis: Roles of Nad(P)H Oxidase-Derived Reactive Oxygen Species. *Journal of Cellular Physiolology* **2011,** *226*, 1750-1762.

154. Arthur, A.; Zannettino, A.; Gronthos, S. The Therapeutic Applications of Multipotential Mesenchymal/Stromal Stem Cells in Skeletal Tissue Repair. *Journal of Cellular Physiology* **2009,** *218*, 237-245.

155. Barry, F. P.; Murphy, J. M. Mesenchymal Stem Cells: Clinical Applications and Biological Characterization. *The International Journal of Biochemistry & Cell Biology* **2004,** *36*, 568-584.

156. Sundelacruz, S.; Kaplan, D. L. Stem Cell- and Scaffold-Based Tissue Engineering Approaches to Osteochondral Regenerative Medicine. *Seminars in Cell & Developmental Biology* **2009,** *20*, 646-655.

157. Barbash, I. M.; Chouraqui, P.; Baron, J.; Feinberg, M. S.; Etzion, S.; Tessone, A.; Miller, L.; Guetta, E.; Zipori, D.; Kedes, L. H.; Kloner, R. A.; Leor, J. Systemic Delivery of Bone Marrow–Derived Mesenchymal Stem Cells to the Infarcted Myocardium: Feasibility, Cell Migration, and Body Distribution. *Circulation* **2003,** *108*, 863-868.

158. Drury, J. L.; Mooney, D. J. Hydrogels for Tissue Engineering: Scaffold Design Variables and Applications. *Biomaterials* **2003,** *24*, 4337-4351.

159. Kim, D.-H.; Provenzano, P. P.; Smith, C. L.; Levchenko, A. Matrix Nanotopography as a Regulator of Cell Function. *The Journal of Cell Biology* **2012,** *197*, 351-360.

160. Kleinman, H. K.; Philp, D.; Hoffman, M. P. Role of the Extracellular Matrix in Morphogenesis. *Current Opinion in Biotechnology* **2003,** *14*, 526-532.

161. Watt, F. M. The Extracellular Matrix and Cell Shape. *Trends in Biochemical Sciences* **1986,** *11*, 482-485.

162. Reig, G.; Pulgar, E.; Concha, M. L. Cell Migration: From Tissue Culture to Embryos. *Development* **2014,** *141*, 1999-2013.

163. Li, S.; Guan, J.-L.; Chien, S. Biochemstry and Biomechanics of Cell Motility. *Annual Review of Biomedical Engineering* **2005,** *7*, 105-150.

164. Brandl, F.; Sommer, F.; Goepferich, A. Rational Design of Hydrogels for Tissue Engineering: Impact of Physical Factors on Cell Behavior. *Biomaterials* **2007,** *28*, 134-146.

165. Han, J.; Menon, N. V.; Kang, Y.; Tee, S.-Y. An in Vitro Study on the Collective Tumor Cell Migration on Nanoroughened Poly(Dimethylsiloxane) Surfaces. *Journal of Materials Chemistry B* **2015,** *3*, 1565-1572.

166. Shin, H. Fabrication Methods of an Engineered Microenvironment for Analysis of Cell–Biomaterial Interactions. *Biomaterials* **2007,** *28*, 126-133.

167. Zhu, J.; Marchant, R. E. Design Properties of Hydrogel Tissue-Engineering Scaffolds. *Expert Review of Medical Devices* **2011,** *8*, 607-626.

168. Bose, S.; Roy, M.; Bandyopadhyay, A. Recent Advances in Bone Tissue Engineering Scaffolds. *Trends in Biotechnology* **2012,** *30*, 546-554.

169. Chen, H. C. Boyden Chamber Assay. *Methods in molecular biology (Clifton, N.J.)* **2005,** *294*, 15-22.

170. Beebe, D. J.; Mensing, G. A.; Walker, G. M. Physics and Applications of Microfluidics in Biology. *Annual Review of Biomedical Engineering* **2002,** *4*, 261-286.

171. Cimetta, E.; Cannizzaro, C.; James, R.; Biechele, T.; Moon, R. T.; Elvassore, N.; Vunjak-Novakovic, G. Microfluidic Device Generating Stable Concentration Gradients for Long Term Cell Culture: Application to Wnt3a Regulation of [Small Beta]-Catenin Signaling. *Lab on a Chip* **2010,** *10*, 3277-3283.

172. Eroshenko, N.; Ramachandran, R.; Yadavalli, V. K.; Rao, R. R. Effect of Substrate Stiffness on Early Human Embryonic Stem Cell Differentiation. *Journal of biological engineering* **2013,** *7*, 1-8.

173. Palchesko, R. N.; Zhang, L.; Sun, Y.; Feinberg, A. W. Development of Polydimethylsiloxane Substrates with Tunable Elastic Modulus to Study Cell Mechanobiology in Muscle and Nerve. *PLoS ONE* **2012,** *7*, e51499-1-13.

174. Park, J.; Yoo, S.; Lee, E.-J.; Lee, D.; Kim, J.; Lee, S.-H. Increased Poly(Dimethylsiloxane) Stiffness Improves Viability and Morphology of Mouse Fibroblast Cells. *BioChip J* **2010,** *4*, 230-236.

175. Shen, Y.; Wang, G.; Huang, X.; Zhang, Q.; Wu, J.; Tang, C.; Yu, Q.; Liu, X. Surface Wettability of Plasma Sio(X):H Nanocoating-Induced Endothelial Cells' Migration and the Associated Fak-Rho Gtpases Signalling Pathways. *Journal of the Royal Society Interface* **2012,** *9*, 313-327.

176. Lo, C. M.; Wang, H. B.; Dembo, M.; Wang, Y. L. Cell Movement Is Guided by the Rigidity of the Substrate. *Biophysical Journal* **2000,** *79*, 144-152.

177. Pelham, R. J.; Wang, Y.-l. Cell Locomotion and Focal Adhesions Are Regulated by Substrate Flexibility. *Proceedings of the National Academy of Sciences of the United States of America* **1997,** *94*, 13661-13665.

178. Hansen, T. D.; Koepsel, J. T.; Le, N. N.; Nguyen, E. H.; Zorn, S.; Parlato, M.; Loveland, S. G.; Schwartz, M. P.; Murphy, W. L. Biomaterial Arrays with Defined Adhesion Ligand Densities and Matrix Stiffness Identify Distinct Phenotypes for Tumorigenic and Non-Tumorigenic Human Mesenchymal Cell Types. *Biomaterials Science* **2014,** *2*, 745-756.

179. Peyton, S. R.; Putnam, A. J. Extracellular Matrix Rigidity Governs Smooth Muscle Cell Motility in a Biphasic Fashion. *Journal of Cellular Physiology* **2005,** *204*, 198-209.

180. Stroka, K. M.; Aranda-Espinoza, H. Neutrophils Display Biphasic Relationship between Migration and Substrate Stiffness. *Cell Motility and the Cytoskeleton* **2009,** *66*, 328-341.

181. Mih, J. D.; Marinkovic, A.; Liu, F.; Sharif, A. S.; Tschumperlin, D. J. Matrix Stiffness Reverses the Effect of Actomyosin Tension on Cell Proliferation. *Journal of Cell Science* **2012,** *125*, 5974-5983.

182. Li, D.; Ding, J.; Wang, X.; Wang, C.; Wu, T. Fibronectin Promotes Tyrosine Phosphorylation of Paxillin and Cell Invasiveness in the Gastric Cancer Cell Line Ags. *Tumori journal* **2009,** *95*, 769-779.

183. Rago, L.; Beattie, R.; Taylor, V.; Winter, J. Mir379-410 Cluster Mirnas Regulate Neurogenesis and Neuronal Migration by Fine-Tuning N-Cadherin. *The EMBO journal* **2014,** *33*, 906-920.

184. Fuard, D.; Tzvetkova-Chevolleau, T.; Decossas, S.; Tracqui, P.; Schiavone, P. Optimization of Poly-Di-Methyl-Siloxane (Pdms) Substrates for Studying Cellular Adhesion and Motility. *Microelectronic Engineering* **2008,** *85*, 1289-1293.

185. Michael, J. O., Siloxane Surface Activity. In *Silicon-Based Polymer Science*, American Chemical Society: **1989**; Chapter 40, pp 705-739.

186. Borgioli, F.; Galvanetto, E.; Bacci, T. Influence of Surface Morphology and Roughness on Water Wetting Properties of Low Temperature Nitrided Austenitic Stainless Steels. *Materials Characterization* **2014,** *95*, 278-284.

187. Yoshimitsu, Z.; Nakajima, A.; Watanabe, T.; Hashimoto, K. Effects of Surface Structure on the Hydrophobicity and Sliding Behavior of Water Droplets. *Langmuir* **2002,** *18*, 5818-5822.

188. Seo, J.-H.; Sakai, K.; Yui, N. Adsorption State of Fibronectin on Poly(Dimethylsiloxane) Surfaces with Varied Stiffness Can Dominate Adhesion Density of Fibroblasts. *Acta biomaterialia* **2013,** *9*, 5493-5501.

189. Chastain, S. R.; Kundu, A. K.; Dhar, S.; Calvert, J. W.; Putnam, A. J. Adhesion of Mesenchymal Stem Cells to Polymer Scaffolds Occurs Via Distinct Ecm Ligands and Controls Their Osteogenic Differentiation. *Journal of Biomedical Materials Research Part A* **2006,** *78A*, 73-85.

190. Lee, J. W.; Kim, Y. H.; Park, K. D.; Jee, K. S.; Shin, J. W.; Hahn, S. B. Importance of Integrin B1-Mediated Cell Adhesion on Biodegradable Polymers under Serum Depletion in Mesenchymal Stem Cells and Chondrocytes. *Biomaterials* **2004,** *25*, 1901-1909.

191. Ayala, R.; Zhang, C.; Yang, D.; Hwang, Y.; Aung, A.; Shroff, S. S.; Arce, F. T.; Lal, R.; Arya, G.; Varghese, S. Engineering the Cell–Material Interface for Controlling Stem Cell Adhesion, Migration, and Differentiation. *Biomaterials* **2011,** *32*, 3700-3711.

192. Gail, M. H.; Boone, C. W. Cell-Substrate Adhesivity: A Determinant of Cell Motility. *Experimental Cell Research* **1972,** *70*, 33-40.

193. Li, J.; Han, D.; Zhao, Y.-P. Kinetic Behaviour of the Cells Touching Substrate: The Interfacial Stiffness Guides Cell Spreading. *Scientific Reports* **2014,** *4*, 1-10.

194. Rowlands, A. S.; George, P. A.; Cooper-White, J. J. Directing Osteogenic and Myogenic Differentiation of Mscs: Interplay of Stiffness and Adhesive Ligand Presentation. *Cell Physiology* **2008,** *295*, C1037-C1044.

195. Kawahara, H.; Soeda, Y.; Niwa, K.; Takahashi, M.; Kawahara, D.; Araki, N. In Vitro Study on Bone Formation and Surface Topography from the Standpoint of Biomechanics. *J Mater Sci: Mater Med* **2004,** *15*, 1297-1307.

196. Hao, L.; Yang, H.; Du, C.; Fu, X.; Zhao, N.; Xu, S.; Cui, F.; Mao, C.; Wang, Y. Directing the Fate of Human and Mouse Mesenchymal Stem Cells by Hydroxyl-Methyl Mixed Self-Assembled Monolayers with Varying Wettability. *Journal of Materials Chemistry B* **2014,** *2*, 4794-4801.

197. Yeung, T.; Georges, P. C.; Flanagan, L. A.; Marg, B.; Ortiz, M.; Funaki, M.; Zahir, N.; Ming, W.; Weaver, V.; Janmey, P. A. Effects of Substrate Stiffness on Cell Morphology, Cytoskeletal Structure, and Adhesion. *Cell Motility and the Cytoskeleton* **2005,** *60*, 24-34.

198. Lampin, M.; Warocquier-Clérout, R.; Legris, C.; Degrange, M.; Sigot-Luizard, M. F. Correlation between Substratum Roughness and Wettability, Cell Adhesion, and Cell Migration. *Journal of Biomedical Materials Research* **1997,** *36*, 99-108.

199. Lipski, A. M.; Pino, C. J.; Haselton, F. R.; Chen, I. W.; Shastri, V. P. The Effect of Silica Nanoparticle-Modified Surfaces on Cell Morphology, Cytoskeletal Organization and Function. *Biomaterials* **2008,** *29*, 3836-3846.

200. Chuah, Y. J.; Zhang, Y.; Wu, Y.; Menon, N. V.; Goh, G. H.; Lee, A. C.; Chan, V.; Zhang, Y.; Kang, Y. Combinatorial Effect of Substratum Properties on Mesenchymal Stem Cell Sheet Engineering and Subsequent Multi-Lineage Differentiation. *Acta biomaterialia* **2015**.

201. Yun, S. P.; Ryu, J. M.; Han, H. J. Involvement of Beta1-Integrin Via Pip Complex and Fak/Paxillin in Dexamethasone-Induced Human Mesenchymal Stem Cells Migration. *Journal of Cellular Physiology* **2011,** *226*, 683-692.

202. Wein, F.; Pietsch, L.; Saffrich, R.; Wuchter, P.; Walenda, T.; Bork, S.; Horn, P.; Diehlmann, A.; Eckstein, V.; Ho, A. D.; Wagner, W. N-Cadherin Is Expressed on Human

Hematopoietic Progenitor Cells and Mediates Interaction with Human Mesenchymal Stromal Cells. *Stem Cell Research* **2010,** *4*, 129-139.

203. Blindt, R.; Bosserhoff, A.-K.; Dammers, J.; Krott, N.; Demircan, L.; Hoffmann, R.; Hanrath, P.; Weber, C.; Vogt, F., *Downregulation of N-Cadherin in the Neointima Stimulates Migration of Smooth Muscle Cells by Rhoa Deactivation*. **2004**; Vol. 62, p 212-222.

204. DeLise, A. M.; Tuan, R. S. Alterations in the Spatiotemporal Expression Pattern and Function of N-Cadherin Inhibit Cellular Condensation and Chondrogenesis of Limb Mesenchymal Cells in Vitro. *Journal of Cellular Biochemistry* **2002,** *87*, 342-359.

205. Gao, L.; McBeath, R.; Chen, C. S. Stem Cell Shape Regulates a Chondrogenic Versus Myogenic Fate through Rac1 and N-Cadherin. *Stem cells* **2010,** *28*, 564-572.

206. Yano, H.; Mazaki, Y.; Kurokawa, K.; Hanks, S. K.; Matsuda, M.; Sabe, H. Roles Played by a Subset of Integrin Signaling Molecules in Cadherin-Based Cell–Cell Adhesion. *The Journal of Cell Biology* **2004,** *166*, 283-295.

207. Ethirajan, M.; Chen, Y.; Joshi, P.; Pandey, R. K. The Role of Porphyrin Chemistry in Tumor Imaging and Photodynamic Therapy. *Chemical Society reviews* **2011,** *40*, 340-362.

208. Anand, S.; Ortel, B. J.; Pereira, S. P.; Hasan, T.; Maytin, E. V. Biomodulatory Approaches to Photodynamic Therapy for Solid Tumors. *Cancer Letters* **2012,** *326*, 8-16.

209. Blume, J. E.; Oseroff, A. R. Aminolevulinic Acid Photodynamic Therapy for Skin Cancers. *Dermatologic Clinics* **2007,** *25*, 5-14.

210. Moghissi, K. Photodynamic Therapy for Lung Cancer 30 Years On. *Photodiagnosis and Photodynamic Therapy* **2013,** *10*.

211. Quirk, B. J.; Brandal, G.; Donlon, S.; Vera, J. C.; Mang, T. S.; Foy, A. B.; Lew, S. M.; Girotti, A. W.; Jogal, S.; LaViolette, P. S.; Connelly, J. M.; Whelan, H. T. Photodynamic Therapy (Pdt) for Malignant Brain Tumors – Where Do We Stand? *Photodiagnosis and Photodynamic Therapy* **2015**.

212. Moore, C. M.; Pendse, D.; Emberton, M. Photodynamic Therapy for Prostate Cancer--a Review of Current Status and Future Promise. *Nature Clinical Practice Urology* **2009,** *6*, 18-30.

213. Ajayaghosh, A. Chemistry of Squaraine-Derived Materials: Near-Ir Dyes, Low Band Gap Systems, and Cation Sensors. *Accounts of Chemical Research* **2005,** *38*, 449-459.

214. Ajayaghosh, A. Donor-Acceptor Type Low Band Gap Polymers: Polysquaraines and Related Systems. *Chemical Society Reviews* **2003,** *32*, 181-191.

215. Ajayaghosh, A.; Carol, P.; Sreejith, S. A Ratiometric Fluorescence Probe for Selective Visual Sensing of Zn2+. *Journal of the American Chemical Society* **2005,** *127*, 14962-14963.

216. Renard, B.-L.; Aubert, Y.; Asseline, U. Fluorinated Squaraine as near-Ir Label with Improved Properties for the Labeling of Oligonucleotides. *Tetrahedron Letters* **2009,** *50*, 1897-1901.

217. Anees, P.; Sreejith, S.; Ajayaghosh, A. Self-Assembled near-Infrared Dye Nanoparticles as a Selective Protein Sensor by Activation of a Dormant Fluorophore. *Journal of the American Chemical Society* **2014,** *136*, 13233-13239.

218. Sreejith, S.; Divya, K. P.; Ajayaghosh, A. A near-Infrared Squaraine Dye as a Latent Ratiometric Fluorophore for the Detection of Aminothiol Content in Blood Plasma. *Angewandte Chemie International Edition* **2008,** *47*, 7883-7887.

219. Arunkumar, E.; Sudeep, P. K.; Kamat, P. V.; Noll, B. C.; Smith, B. D. Singlet Oxygen Generation Using Iodinated Squaraine and Squaraine-Rotaxane Dyes. *New Journal of Chemistry* **2007,** *31*, 677-683.

220. Prostota, Y.; Kachkovsky, O. D.; Reis, L. V.; Santos, P. F. New Unsymmetrical Squaraine Dyes Derived from Imidazo[1,5-a]Pyridine. *Dyes and Pigments* **2013,** *96*, 554-562.

221. Ramaiah, D.; Eckert, I.; Arun, K. T.; Weidenfeller, L.; Epe, B. Squaraine Dyes for Photodynamic Therapy: Study of Their Cytotoxicity and Genotoxicity in Bacteria and Mammalian Cells¶‡. *Photochemistry and Photobiology* **2002,** *76*, 672-677.

222. Avirah, R. R.; Jayaram, D. T.; Adarsh, N.; Ramaiah, D. Squaraine Dyes in Pdt: From Basic Design to in Vivo Demonstration. *Organic & Biomolecular Chemistry* **2012,** *10*, 911-920.

223. Biswas, S.; Torchilin, V. P. Nanopreparations for Organelle-Specific Delivery in Cancer. *Advanced Drug Delivery Reviews* **2014,** *66*, 26-41.

224. Kim, C. K.; Ghosh, P.; Pagliuca, C.; Zhu, Z.-J.; Menichetti, S.; Rotello, V. M. Entrapment of Hydrophobic Drugs in Nanoparticle Monolayers with Efficient Release into Cancer Cells. *Journal of the American Chemical Society* **2009,** *131*, 1360-1361.

225. Derycke, A. S. L.; de Witte, P. A. M. Liposomes for Photodynamic Therapy. *Advanced Drug Delivery Reviews* **2004,** *56*, 17-30.

226. Tang, W.; Xu, H.; Park, E. J.; Philbert, M. A.; Kopelman, R. Encapsulation of Methylene Blue in Polyacrylamide Nanoparticle Platforms Protects Its Photodynamic Effectiveness. *Biochemical and Biophysical Research Communications* **2008,** *369*, 579-583.

227. van Nostrum, C. F. Polymeric Micelles to Deliver Photosensitizers for Photodynamic Therapy. *Advanced Drug Delivery Reviews* **2004,** *56*, 9-16.

228. Ding, H.; Yu, H.; Dong, Y.; Tian, R.; Huang, G.; Boothman, D. A.; Sumer, B. D.; Gao, J. Photoactivation Switch from Type Ii to Type I Reactions by Electron-Rich Micelles for Improved Photodynamic Therapy of Cancer Cells under Hypoxia. *Journal of Controlled Release* **2011,** *156*, 276-280.

229. Basak, R.; Bandyopadhyay, R. Encapsulation of Hydrophobic Drugs in Pluronic F127 Micelles: Effects of Drug Hydrophobicity, Solution Temperature, and Ph. *Langmuir* **2013,** *29*, 4350-4356.

230. Beduneau, A.; Saulnier, P.; Hindre, F.; Clavreul, A.; Leroux, J. C.; Benoit, J. P. Design of Targeted Lipid Nanocapsules by Conjugation of Whole Antibodies and Antibody Fab' Fragments. *Biomaterials* **2007,** *28*, 4978-90.

231. Hong, M.; Zhu, S.; Jiang, Y.; Tang, G.; Pei, Y. Efficient Tumor Targeting of Hydroxycamptothecin Loaded Pegylated Niosomes Modified with Transferrin. *Journal of Controlled Release* **2009,** *133*, 96-102.

232. Zensi, A.; Begley, D.; Pontikis, C.; Legros, C.; Mihoreanu, L.; Wagner, S.; Buchel, C.; von Briesen, H.; Kreuter, J. Albumin Nanoparticles Targeted with Apo E Enter the Cns by Transcytosis and Are Delivered to Neurones. *Journal of Controlled Release* **2009,** *137*, 78-86.

233. Huang, P.; Xu, C.; Lin, J.; Wang, C.; Wang, X.; Zhang, C.; Zhou, X.; Guo, S.; Cui, D. Folic Acid-Conjugated Graphene Oxide Loaded with Photosensitizers for Targeting Photodynamic Therapy. *Theranostics* **2011,** *1*, 240-250.

234. Bai, M.; Bornhop, D. J. Recent Advances in Receptor-Targeted Fluorescent Probes for in Vivo Cancer Imaging. *Current medicinal chemistry* **2012,** *19*, 4742-58.

235. Ma, X.; Sreejith, S.; Zhao, Y. Spacer Intercalated Disassembly and Photodynamic Activity of Zinc Phthalocyanine inside Nanochannels of Mesoporous Silica Nanoparticles. *ACS Applied Materials & Interfaces* **2013,** *5*, 12860-12868.

236. Huh, D.; Torisawa, Y.-s.; Hamilton, G. A.; Kim, H. J.; Ingber, D. E. Microengineered Physiological Biomimicry: Organs-on-Chips. *Lab on a Chip* **2012,** *12*, 2156-2164.

237. Grosberg, A.; Alford, P. W.; McCain, M. L.; Parker, K. K. Ensembles of Engineered Cardiac Tissues for Physiological and Pharmacological Study: Heart on a Chip. *Lab on a Chip* **2011,** *11*, 4165-4173.

238. Zhang, W.; Shi, Y.; Chen, Y.; Ye, J.; Sha, X.; Fang, X. Multifunctional Pluronic P123/F127 Mixed Polymeric Micelles Loaded with Paclitaxel for the Treatment of Multidrug Resistant Tumors. *Biomaterials* **2011,** *32*, 2894-2906.

239. Parijat Borah; Sivaramapanicker Sreejith; Palapuravan Anees; Nishanth Venugopal Menon; Yuejun Kang; Ayyappanpillai Ajayaghosh; Zhao, Y. Near-Ir Squaraine Dye-Loaded Gated Periodic Mesoporous Silica for Photo-Oxidation of Phenol in Continuous-Flow Device Dye-Loaded Pmo for Photo-Oxidation. *Science Advances* **2015**.

240. Shin, Y.; Han, S.; Jeon, J. S.; Yamamoto, K.; Zervantonakis, I. K.; Sudo, R.; Kamm, R. D.; Chung, S. Microfluidic Assay for Simultaneous Culture of Multiple Cell Types on Surfaces or within Hydrogels. *Nature Protocols* **2012,** *7*, 1247-1259.